

© 2013

Huanyu Jin

ALL RIGHTS RESERVED

**INHIBITION OF LUNG TUMORIGENESIS AND CANCER CELL GROWTH BY  
EGCG AND OTHER CHEMOPREVENTIVE AGENTS**

by

HUANYU JIN

A dissertation submitted to the  
Graduate School-New Brunswick  
Rutgers, The State University of New Jersey

and

The Graduate School of Biomedical Sciences  
University of Medicine and Dentistry of New Jersey

In partial fulfillment of the requirements

For the degree of

Doctor of Philosophy

Graduate Program in Cellular and Molecular Pharmacology

Written under the direction of

Professor Chung S. Yang

And approved by

---

---

---

---

New Brunswick, New Jersey

October, 2013

## **ABSTRACT OF THE DISSERTATION**

Inhibition of Lung Tumorigenesis and Cancer Cell Growth by EGCG and Other

Chemopreventive Agents

by HUANYU JIN

Dissertation Director:

Professor Chung S. Yang

Lung cancer is the leading cause of cancer death in the United States and the most commonly diagnosed cancer worldwide and smoking is a key risk factor of lung cancer. The purpose of this thesis study is to characterize the mechanisms of 4-(methylnitrosamino)-1-(3-pyridyl)-1-butanone (NNK)-induced lung tumorigenesis in A/J mice and the inhibitory activities of (-)-epigallocatechin-3-gallate (EGCG) and other chemopreventive agents including tocopherols, myo-inositol and atorvastatin.

DNA methyltransferase 1 (DNMT1), a key enzyme mediating DNA methylation, is known to be activated in cancers, including the mouse lung tumors induced by NNK. However, it is not known how NNK treatment affects the DNMT1 expression. We found that administration of NNK to A/J mice caused elevation of DNMT1 in bronchial epithelial cells at days 1-14. DNMT1 elevation at days 1 and 3 was accompanied by an increase in  $\gamma$ -H2AX and phospho-AKT (p-AKT), which has been shown to stabilize DNMT1 at the

protein level by inhibiting the ubiquitination of DNMT1. Induction of O<sup>6</sup>-methylguanine, cyclooxygenase-2 (COX-2), superoxide dismutase (SOD) and catalase by NNK treatment was also observed at days 1-14. DNMT1 expression decreased to lower levels at weeks 5-20 in lung tissues, but was highly elevated in lung tumors at week 20. In concordance with DNMT1 elevation, promoter hypermethylation of tumor suppressor genes *Cdh13*, *Prdm2* and *Runx3* was observed in lung tissues at day 3 and in lung tumors at week 20. EGCG (0.4% in diet) treatment attenuated the induction of DNMT1, p-AKT and  $\gamma$ -H2AX at days 1 and 3 and inhibited lung tumorigenesis.

EGCG,  $\gamma$ -tocopherol-rich mixture of tocopherols ( $\gamma$ -TmT) and myo-inositol significantly reduced tumor multiplicity and tumor size in the NNK model. The EGCG-generated reactive oxygen species (ROS) caused cell growth inhibition and induction of apoptosis and oxidative DNA damage *in vitro*. Apoptosis and oxidative DNA damage were also induced in lung tumors by EGCG treatment at the tumor stage. Short-term  $\gamma$ -TmT treatment at the tumor stage induced antioxidant enzymes SOD and glutathione peroxidase. Myo-inositol treatment significantly reduced the level of p-c-Jun in lung tumors.

## ACKNOWLEDGEMENTS

I wish to express my sincere gratitude to those who have made this thesis possible. First, I would like to express my greatest gratitude to my thesis advisor, Dr. Chung S. Yang, for his continuous support, encouragement and guidance. I treasure the precious experience through my work in his lab and his way of scientific thinking really sets a good model for me.

I am also grateful to the members of my thesis committee: Dr. Allan Conney, Dr. Nanjoo Suh, and Dr. George Wagner, for their valuable advice, guidance and encouragement throughout the progress of writing the thesis.

I want to thank my colleagues in Dr. Yang's lab: Dr. Shuiping Tu, Dr. Hong Wang, Mr. Jayson Chen, Mrs. Anna Liu, and Mr. Mao-jun Lee for their generous help and constructive suggestions. I also want to thank previous members of Dr. Yang's lab: Dr. Guangxun Li, Dr. Gary Lu, Dr. Zhihong Yang, Dr. Hang Xiao and Mrs. Yuhai Sun for their contribution to my thesis.

I would like to thank the administrative staff in the Department of Chemical Biology: Mrs. Dorothy Wong, Mrs. Deborah Stalling, Mrs. Erica DiPaola, Mrs. Bobbie Busch and Mrs. Annette Dionisio for their assistance in the administrative issues I encountered.

I also want to thank all the faculty members and colleagues in our department for their help and inspiration in my research. I am very proud to have conducted my thesis work in this friendly and collaborative environment that fosters the growth of each member in the department.

Finally, I give my deepest gratitude to my family. They are my source of motivation and the biggest support when I encountered difficulties during my graduate studies.

# TABLE OF CONTENTS

ABSTRACT.....	ii
ACKNOWLEDGEMENTS.....	iv
TABLE OF CONTENTS.....	v
LIST OF TABLES.....	xi
LIST OF ILLUSTRATIONS.....	xii
LIST OF ABBREVIATIONS.....	xv
I. INTRODUCTION.....	1
A. Cancer.....	1
B. Lung Cancer.....	2
B.1. Lung Carcinogenesis: Natural History, Classification, Pathogenesis and Epidemiology.....	2
B.2. Etiology of Lung Cancer.....	4
B.2.a. Smoking and Lung Cancer.....	5
B.2.b. Genetics and Lung Cancer.....	6
B.2.b.i. Oncogenes.....	6
B.2.b.ii. Tumor Suppressor Genes.....	8
B.2.c. Epigenetics and Lung Cancer.....	9
B.2.c.i. DNA Methyltransferases and Lung Cancer.....	10
B.2.c.ii. Aberrant DNA Methylation in Lung Cancer.....	11
C. Animal Models for the Studies of Lung Cancer.....	12
C.1. Animal Models of Lung Tumorigenesis.....	12
C.2. NNK-induced Lung Tumorigenesis Model.....	13
D. Dietary Constituents and Atorvastatin as Chemopreventive Agents.....	15
D.1. Dietary Constituents as Chemopreventive Agents.....	15

D.1.a. EGCG as a Chemopreventive Agent.....	15
D.1.b. Tocopherols as Chemopreventive Agents.....	19
D.1.c. Myo-inositol as a Chemopreventive Agent.....	22
D.2. Atorvastatin as a Chemopreventive Agent.....	23
II. GOALS AND SPECIFIC AIMS.....	26
III. RATIONALE AND RESEARCH DESIGN.....	28
A. Molecular Alterations in Lung Tissues Following NNK Administration and during the Progression of NNK-induced Lung Tumorigenesis and the Inhibitory Effect of EGCG ( <i>Specific Aim 1</i> ).....	28
A.1. NNK-induced Lung Tumorigenesis Model in Lung Cancer Studies.....	28
A.2. Research Design for Part A.....	28
A.2.a. Experiment 1: Molecular Alterations in Lung Tissues of A/J Mice Following NNK Administration and the Inhibitory Effect of EGCG.....	29
A.2.b. Experiment 2: Molecular Alterations in Lung Tissues of A/J Mice Following NNK Administration and the Inhibitory Effect of EGCG, $\delta$ -Tocopherol and Myo-inositol.....	30
A.2.c. Experiment 3: Molecular Alterations in Lung Tissues of A/J Mice during the Progression of NNK-induced Lung Tumorigenesis.....	31
B. Inhibitory Actions of EGCG, Atorvastatin, Tocopherols and Myo-inositol, Alone or In Combination, on NNK-induced Lung Tumorigenesis and Allografts Tumor Growth ( <i>Specific Aims 2 and 3</i> ).....	32
B.1. Research Design for Part B.....	32
B.1.a. Experiment 1: Inhibition of NNK-induced Lung Tumorigenesis by EGCG, Myo-inositol, $\gamma$ -TmT and Atorvastatin, Alone or In Combination.....	32

B.1.b. Experiment 2: Inhibition of NNK-induced Lung Tumorigenesis by EGCG, Myo-inositol and $\gamma$ -TmT, Alone or In Combination.....	34
B.1.c. Experiment 3: Effects of Short-term $\gamma$ -TmT and EGCG Treatment on NNK-induced Lung Tumors.....	36
B.1.d. Experiment 4: Effects of Short-term EGCG Treatment in NNK-induced Lung Tumors.....	37
B.1.e. Experiment 5: Inhibitory Actions of EGCG, $\delta$ -Tocopherol and Myo-inositol, Alone or in Combination, on the Growth of Allograft Tumors.....	38
IV. MATERIALS AND METHODS.....	40
A. Chemopreventive Agents and Research Diet.....	40
B. Animal Studies.....	40
C. Immunohistochemistry.....	43
D. Western Blot Analysis.....	44
E. DNA Methylation Analysis.....	46
F. Hydrogen Peroxide Assay.....	47
G. Cell Culture and Cell Viability Assay.....	48
H. Cell Cytosolic and Cytoplasm Membrane Fraction Preparation.....	49
I. Sphere Formation Assay.....	50
J. Enzyme-lined Immunosorbent Assay (ELISA) for mouse IL-6.....	50
K. Statistical Analysis.....	51
V. RESULTS.....	52

A. NNK-induced DNMT1 Elevation and Related Molecular Alterations in Lung Tissues Following NNK Administration and during the Progression of NNK-induced Lung Tumorigenesis and the Inhibitory Effect of EGCG.....	52
A.1. Effect of NNK Treatment on Animal Conditions.....	52
A.2. Progression of NNK-induced Lung Tumorigenesis.....	52
A.3. Induction of DNMT1 in the Lung by NNK Treatment and the Inhibitory Effect of EGCG.....	53
A.4. NNK-induced DNMT1 Elevation through AKT Phosphorylation and the Inhibitory Effect of EGCG.....	55
A.5. Induction of $\gamma$ -H2AX, O <sup>6</sup> -methylguanine and Cleaved Caspase-3 in the Lung by NNK Treatment and the Inhibitory Effects of EGCG.....	56
A.6. Changes in DNMT1 Protein Levels during the Progression of NNK-induced Lung Tumorigenesis and the Inhibitory Effect of EGCG.....	58
A.7. Induction of DNMT1 in Human Lung Cancer, Mouse Epithelial and Alveolar Cells.....	60
A.8. Increase of Gene-specific Promoter Hypermethylation in NNK-induced Lung Tumors and NNK-treated Lung Tissues.....	60
A.9. Increase of Global DNA Methylation in NNK-treated Lung Tissues.....	62
A.10. Induction of COX-2 in the Lung by NNK Treatment.....	62
A.11. Induction of SOD and Catalase in the Lung by NNK Treatment.....	63
B. Possible Mechanisms of Inhibition by EGCG in NNK-induced Lung Tumorigenesis and Lung Cancer Cell Growth.....	64
B.1. Hydrogen Peroxide Formation by EGCG Auto-oxidation.....	64
B.2. Inhibitory Effects of EGCG on Lung Cancer Cell Growth in the Presence or Absence of SOD and Catalase.....	65
B.3. Induction of Cleaved Caspase-3 and Changes in the Levels of Apoptosis-related Bcl-2 Family Proteins by EGCG in Lung Cancer Cells.....	67

B.4. Induction of $\gamma$ -H2AX by EGCG in Lung Cancer Cells in the Presence or Absence of SOD and Catalase.....	68
B.5. Induction of Cleaved Caspase-3 and $\gamma$ -H2AX, and Inhibition of p-c-Jun in NNK-induced Lung Tumors by Short-term EGCG Treatment at the Tumor Stage.....	68
B.6. EGCG Interrupts the Support of Cancer Cells from Stromal Microenvironment (Myofibroblasts).....	69
C. Inhibitory Effects of EGCG, Tocopherols, Myo-inositol and Atorvastatin, Alone or in Combination, on NNK-induced Lung Tumorigenesis and the Growth of Allograft Tumors and Lung Cancer Cells.....	70
C.1. Effects of Chemopreventive Agents on Animal Conditions.....	71
C.2. Inhibition of NNK-induced Lung Tumorigenesis by EGCG, $\gamma$ -TmT, Myo-inositol and Atorvastatin, Alone or in Combination.....	72
C.3. Inhibitory Effects of EGCG, $\delta$ -Tocopherol and Myo-inositol, Alone or in Combination, on CL-13 Mouse Lung Cancer Cell Allografts.....	74
C.4. Induction of Antioxidant Enzymes by Short-term $\gamma$ -TmT in NNK-induced Lung Tumors.....	74
C.5. Inhibition of p-c-Jun by Myo-inositol in NNK-induced Lung Tumors.....	76
C.6. Synergistic Inhibition of Lung Cancer Cell Growth by a Combination of EGCG and Atorvastatin.....	77
C.7. Effects of EGCG (or PPE, at EGCG equivalent concentration), Atorvastatin and Their Combination on the Levels of Apoptosis and Apoptosis-related Bcl-2 Family Proteins in Lung Cancer Cells.....	78
C.8. Counteraction of Atorvastatin-induced Cell Growth Inhibitor by Key Intermediates of Cholesterol Synthesis Pathway.....	80
C.9. Synergistic Inhibition of Lung Cancer Cell Growth by a Combination of Atorvastatin and $\gamma$ -TmT.....	81

C.10. Inhibition of Lung Cancer Cell Growth by a Combination of EGCG and Myo-inositol.....	82
VI. DISCUSSION AND FUTURE DIRECTION.....	84
A. Elevation of DNMT1 through AKT Phosphorylation and Increase of Gene-specific Promoter Hypermethylation in NNK-treated Lung Tissues and NNK-induced Lung Tumors.....	84
B. Induction of Oxidative Stress, Oxidative DNA Damage and Antioxidant Enzymes in Lung Tissues Following NNK Administration.....	88
C. Inhibitory Effects of EGCG on NNK-induced DNMT1 Elevation, AKT Phosphorylation and Oxidative DNA Damage in NNK-treated Lung Tissues.....	89
D. Anti-oxidative and Pro-oxidative Activities of EGCG in the Inhibition of Lung Tumorigenesis.....	92
E. Discrepancies between Animal and Cell Line Studies for EGCG.....	93
F. Inhibition of NNK-induced Lung Tumorigenesis and p-c-Jun in Lung Tumors by Myo-inositol.....	96
G. Supportive Role of Myofibroblast for Cancer.....	97
TABLES.....	101
FIGURES.....	104
REFERENCES.....	137

## LIST OF TABLES

<b>Table 1.</b> Progression of NNK-induced lung tumorigenesis.....	101
<b>Table 2.</b> Inhibition of NNK-induced lung tumorigenesis by EGCG, $\gamma$ -TmT, myo-inositol and atorvastatin, alone or in combination.....	102
<b>Table 3.</b> Inhibition of NNK-induced lung tumorigenesis by EGCG, $\gamma$ -TmT and myo-inositol treatment, alone or in combination.....	103

## LIST OF ILLUSTRATIONS

<b>Figure 1.</b> Chemical structures of EGCG, atorvastatin, tocopherols and myo-inositol.....	104
<b>Figure 2.</b> Experimental designs.....	105
<b>Figure 3.</b> NNK-induced elevation of DNMT1 in lung tissues of NNK-treated mice and the inhibitory effect of EGCG.....	106
<b>Figure 4.</b> NNK-induced elevation of p-AKT in lung tissues of NNK-treated mice and the inhibitory effect of EGCG.....	107
<b>Figure 5.</b> NNK-induced elevation of $\gamma$ -H2AX and O <sup>6</sup> -methylguanine in lung tissues of NNK-treated mice and the inhibitory effect of EGCG.....	108
<b>Figure 6.</b> Increased DNMT1 expression during the progression of NNK-induced lung tumorigenesis and the inhibitory effect of EGCG.....	109
<b>Figure 7.</b> NNK-induced elevation of DNMT1 in H1299, C22 and T7 cells.....	110
<b>Figure 8.</b> Increased gene-specific promoter hypermethylation and global DNA methylation in NNK-induced lung tumors and lung tissues of NNK-treated mice.....	111
<b>Figure 9.</b> NNK-induced elevation of COX-2 in bronchial epithelial cells of NNK-treated mice.....	112
<b>Figure 10.</b> NNK-induced elevation of SOD in bronchial epithelial cells of NNK-treated mice.....	113
<b>Figure 11.</b> NNK-induced elevation of catalase in bronchial epithelial cells of NNK-treated mice.....	114
<b>Figure 12.</b> Proposed mechanism for EGCG auto-oxidation.....	115

<b>Figure 13.</b> Hydrogen peroxide formation by EGCG auto-oxidation in RPMI-1640 culture medium.....	116
<b>Figure 14.</b> Cell growth inhibition by EGCG in the absence or presence of SOD and catalase.....	117
<b>Figure 15.</b> Cell growth inhibition by EGCG in the first 2 h or the following 22 h.....	118
<b>Figure 16.</b> Induction of cleaved caspase-3 and changes in the levels of apoptosis-related Bcl-2 family proteins by EGCG in H1299 lung cancer cells.....	119
<b>Figure 17.</b> Induction of $\gamma$ -H2AX by EGCG in CL-13 mouse lung cancer cells in the presence or absence of SOD and catalase.....	120
<b>Figure 18.</b> Effects of short-term EGCG treatment at the tumor stage on the levels of cleaved caspase-3, $\gamma$ -H2AX and p-c-Jun in NNK-induced lung tumors.....	121
<b>Figure 19.</b> EGCG interrupts the support of cancer cells from stromal microenvironment (myofibroblasts).....	122
<b>Figure 20.</b> Body weight of A/J mice in the study of inhibition of NNK-induced lung tumorigenesis by EGCG, $\gamma$ -TmT, myo-inositol and atorvastatin, alone or in combination.....	123
<b>Figure 21.</b> Inhibitory effects of EGCG, $\delta$ -tocopherol and myo-inositol, alone or in combination, on the growth of CL-13 mouse lung cancer cell allografts.....	124
<b>Figure 22.</b> Effects of short-term $\gamma$ -TmT and EGCG treatment at the tumor stage on the levels of Nrf2 and antioxidant enzymes in NNK-induced lung tumors.....	125
<b>Figure 23.</b> Effects of myo-inositol on the level of p-c-Jun in NNK-induced lung tumors.....	126

<b>Figure 24.</b> Effects of EGCG, atorvastatin, or their combination on the growth of CL-13 mouse lung cancer cells.....	127
<b>Figure 25.</b> Effects of EGCG, atorvastatin, or their combination on the growth of H1299 human lung cancer cells.....	128
<b>Figure 26.</b> Induction of apoptosis and changes in the levels of apoptosis-related Bcl-2 family proteins by EGCG, atorvastatin, or their combination in H1299 lung cancer cells.....	129
<b>Figure 27.</b> Down-regulation of anti-apoptotic Bcl-2 family proteins by EGCG, atorvastatin, or their combination in H1299 lung cancer cells.....	130
<b>Figure 28.</b> Induction of pro-apoptotic Bcl-2 family proteins by EGCG, atorvastatin, or their combination in H1299 lung cancer cells.....	131
<b>Figure 29.</b> A diagram of the cholesterol synthesis pathway and the inhibition of HMG-CoA reductase by atorvastatin.....	132
<b>Figure 30.</b> Effects of mevlonate, farnesyl pyrophosphate and geranylgeranyl pyrophosphate on the growth inhibition of CL-13 mouse lung cancer cells induced by atorvastatin.....	133
<b>Figure 31.</b> Effects of atorvastatin, $\gamma$ -TmT, or their combination on the growth of CL-13 mouse lung cancer cells.....	134
<b>Figure 32.</b> Effects of EGCG, myo-inositol, or their combination on the growth of CL-13 mouse lung cancer cells.....	135
<b>Figure 33.</b> Proposed mechanism of NNK-induced lung tumorigenesis through DNMT1 elevation and tumor suppressor gene promoter hypermethylation and the possible inhibitory actions of EGCG.....	136

## LIST OF ABBREVIATIONS

COX-2	cyclooxygenase-2
EGCG	(-)-epigallocatechin-3-gallate
HMG-CoA	3-hydroxy-3-methylglutaryl-coenzyme A
IL-6	interleukin-6
i.p.	intraperitoneal
MTT	3-(4,5-dimethylthiazole-2-yl)-2,5-diphenyltetrazolium bromide
NNK	4-(methylnitrosamino)-1-(3-pyridyl)-1-butanone
Nrf2	Nuclear factor (erythroid-derived 2)-like 2
<i>P16<sup>INK4A</sup></i>	cyclin-dependent kinase inhibitor 2A
p-AKT	phospho-AKT
ROS	reactive oxygen species
SOD	superoxide dismutase
$\gamma$ -TmT	$\gamma$ -tocopherol-rich mixture of tocopherols

## I. INTRODUCTION

### A. Cancer

Cancer is the leading cause of death worldwide and the second leading cause of death in the United States, accounting for about 23% of all deaths in the United States [1]. Over 12 million cases of cancer were diagnosed worldwide and 7.5 million people died as a result of cancer in 2008 alone [2]. There are over 100 types of cancers consisting with multiple subtypes. However, the majority of cancers can be classified into several types, based on their specific tissue site of origin. One example of a small number of cancers that cannot be characterized is melanomas [3]. Carcinomas, originated from epithelial cells, are the most common types of cancer and account for about 80% of all cancers [3]. Carcinomas can be further categorized into squamous cell carcinomas or adenocarcinomas based on the fact that the cells of origin are part of the protective epithelial layer (squamous cell carcinomas), or have secretory characteristics (adenocarcinomas). However, in many cases, carcinomas are not purely originated from one type of cells, but originate from locations where both type of cells co-exist [3]. Following carcinomas, the next major type of cancer are the sarcomas. Examples of sarcomas include bone cancers, such as osteosarcomas, and muscle tissue based cancers, such as rhabdomyosarcomas [3].

Cancer is caused by both environmental and genetic factors. Common environmental factors include: tobacco smoking, diet, obesity, infections, alcohol and other factors [4]. Studies in both human and animal carcinogenesis models demonstrated that the development of cancer is a complex, multi-step process which involves both genetic and epigenetic alterations in oncogenes and tumor suppressor genes caused by

environmental factors such as carcinogens and tumor promoters [3, 5]. The most clearly documented multi-step process of human cancer is in the epithelia of the intestine, which starts with an abnormally high rate of cell proliferation, defined as hyperplasia. The morphology of the hyperplastic cell continues to deviate from normal cell and progress to dysplasia and then adenoma. Based on whether the abnormal cells have broken through the basement layers, the adenoma cells continue to progress into malignant carcinoma cells. Among those malignant carcinoma cells, depending on whether they have penetrated deeply into the stromal layers and muscle and whether they have migrated to anatomically distant sites in the body, they can be further categorized as metastatic carcinomas [5]. This progression of carcinogenesis usually proceeds over a period of decades and the key features of a cancer cell include enhanced cell proliferation, inhibited apoptosis, and increased angiogenesis [6].

## **B. Lung Cancer**

### **B.1. Lung Carcinogenesis: Natural History, Classification, Pathogenesis and Epidemiology**

Lung cancer is the leading cause of cancer death for both males and females in the United States [1]. Lung cancer is also the leading cause of cancer death for males and second leading cause of cancer death for females worldwide, accounting for about 1.4 million deaths annually as of 2008 and this number has been increasing [2]. In the United States, lung cancer is the most commonly diagnosed cancer and the leading cause of cancer mortality [7]. Once diagnosed, the 5-year prognosis of lung cancer is less than 10%, and the survival rate has been consistently low for the past three decades [8-10]. Clinical

presentation is usually late in lung cancer and the most common symptoms of lung cancer usually include: weakness, shortness of breath, chronic cough, hemoptysis, chest pain, anorexia, weight loss, bronchitis, and pneumonia [11-13].

The major types of primary lung cancer are carcinomas, which derive from epithelial cells of the trachea and bronchi. In 98% of lung cancer cases, the epithelial cells forming the bronchial airway of the lung are transformed into carcinomas [14]. Based on the size and appearance of the malignant cells, lung cancer can be categorized into two major classes: small-cell lung cancer and non-small-cell lung cancer. Non-small-cell lung cancer is the most prevalent type of lung cancer, representing 75 to 85% of all the lung cancer cases [8]. Non-small-cell lung cancer can be further categorized into three subgroups: squamous cell carcinoma, adenocarcinoma, and large cell carcinoma [15]. Small-cell lung cancer represents 15 to 25% of all the lung cancer cases and tumors are located in larger airways such as the primary or secondary bronchi [8]. Small-cell lung cancer is an aggressive form of lung cancer with a high replication rate and early metastasis [10]. Small-cell lung cancer cells are relatively smaller and have scant cytoplasm, poor defined cell borders, finely granular chromatin and inconspicuous nucleoli, compared to normal cells of the primary or secondary bronchi [16]. The prognosis of small-cell lung cancer is poor and only 3% of the diagnosed patients will survive over 3 years [17]. Small-cell carcinoma are found in the central bronchus while adenocarcinoma originate in peripheral lung, distal airways and alveoli of the lung [18].

Lung cancer was a very rare disease until the beginning of the 20<sup>th</sup> century. Since then, the occurrence of lung cancer has increased rapidly and now it accounts for 13% (1.6 million) of the total cases and 18% (1.4 million) of the deaths in 2008 [2]. In males, the

highest lung cancer incidence rates are recorded in Eastern and Southern Europe, North America and Eastern Asia, while the lowest incidence rates are in sub-Saharan Africa [2]. In females, the highest rates are found in North America, Northern Europe and Australia/New Zealand. Surprisingly, Chinese females have a relatively high incidence rate (21 cases per 100000 females), despite their low prevalence of tobacco smoking (< 4% adult smokers), possibly attributed to second-hand smoke and heavy cooking habits [2, 19-21]. In most countries, the incidence rates are greater in low socioeconomic class and this pattern largely attributes to the high prevalence of tobacco smoking in low socioeconomic class.

Lung cancer commonly occurs in the central part of the lung, especially in the main lobe or first segmental bronchus. The most extensively studied lung cancer type is squamous cell carcinoma because it happens in a most typical multiple-stage process. The changes start from normal bronchial epithelium, to squamous metaplasia, mild dysplasia, severe dysplasia and eventually squamous carcinoma, and it may take more than 20 years to develop. The cell origin of lung cancer is still unclear, but there are two major theories. One is the pluripotent stem cell theory, that is, all cell types evolve from one pluripotent stem cell lineage, the other is the small-cell theory, that is, all cell types evolve from a type of small-cell neoplasm which undergoes transformation [22, 23]. Although the origin of different types of lung cancer is still controversial, increasing evidence support that lung cancers arise from a common cancer stem cell [22-24].

## **B.2. Etiology of Lung Cancer**

### **B.2.a. Smoking and Lung Cancer**

There are several risk factors of lung cancer, including tobacco smoking [25, 26], radon [27], asbestos [28], virus infection [29, 30], particulate air pollutions [31, 32], and dietary factors [32], among which, the most predominant cause is long-term exposure to tobacco smoke [25]. It has been estimated that tobacco smoking accounts for approximately 90% of lung cancer cases in men and 80% in women [26, 33, 34]. The health risks of tobacco smoking are not limited to smokers. Exposure to second-hand smoke, or environmental tobacco smoke also significantly increases the risk of lung cancer in non-smokers [35, 36]. The risk of lung cancer increases with the increase in time a person smokes and with the number of packs of cigarettes smoked per day. There is no evidence to support the idea that substituting cigarettes by cigar, pipe or low tar cigarettes correlates with reduced risk of lung cancer. Cessation of smoking is an effective way to lower the risk of lung cancer for all ages and genders [36, 37].

Tobacco smoke has been shown to contain over 4000 chemicals, of which over 50 are known carcinogens including tobacco-specific nitrosamines [26]. In the unburned tobacco, at least 16 known carcinogens are found [38]. Tobacco smoking is also a risk factor for other types of cancers including cancers of the pancreas, kidneys, bladder, mouth, esophagus and cervix [39]. There are over 1 billion smokers worldwide with nearly 80% of them living in low- and mid-income countries. Globally, 5.5 trillion cigarettes are consumed annually with an increase rate of 3.4% [39]. There are over 5 million deaths annually from tobacco use and this number is projected to increase to 8 million by 2030 [39].

### **B.2.b. Genetics and Lung Cancer**

Genetic alterations are important contributing factors of lung tumorigenesis. Those genetic alterations include mutations, genome rearrangements, amplifications, deletions and genome instability. Although tobacco smoking accounts for approximately 90% of lung cancer cases in men and 80% in women [26, 33, 34], only 15% of smokers actually develop lung cancer [26, 36, 40]. The fact that 85% of smokers do not develop lung cancer suggests that there must be significant variations in genetic susceptibility that contribute to the low rate of lung cancer incidence in smokers [41, 42]. In addition, previous studies have identified that positive familial history is also a risk factor for lung cancer [43]. Those familial genetic factors include polymorphisms of cytochrome P450 genes, mutations of oncogenes and tumor suppressor genes, and deficiencies in DNA repair capacity [9, 42-44]. One example of those familial genetic factors is *RGS17* gene found on chromosome 6q23-25 [45]. Tumors of lung cancer patients were reported to express high levels of *RGS17* mRNA transcripts, as compared to normal lung tissues, suggesting a possible role in carcinogenesis [45]. Recently, Emerging evidence suggests that lung cancer development in both humans and rodents is associated with the activation of oncogenes and the inactivation of tumor suppressor genes [46, 47].

#### **B.2.b.i. Oncogenes**

Oncogenes were first identified in 1976 with the discovery of *SRC* [48]. Generally, cancer cells confer an increased nucleus size and hyperchromicity, due to the increased DNA content as well as abnormal chromatin structure. During carcinogenesis, oncogene might be constitutively activated by the following mechanisms: a mutation that will change the structure of its protein products causing either an increased activity or a loss of

regulation; an increase of gene expression; an increase of protein stability; a chromosomal translocation causing an increased gene expression in the wrong cell type and improper time. Several oncogenes are known to be activated or overexpressed in small-cell lung cancers including *MYC*, *ERB-B1*, *RAF*, *MYB* and *FMS*, and in non-small-cell lung cancers including *K-RAS*, *EGFR*, *HER-2/neu*, *MYC* and *RAF*.

The *RAS* proto-oncogene family consists of *K-RAS*, *H-RAS* and *N-RAS*, which encodes plasma membrane proteins involved in cellular signal transduction. The *RAS* proto-oncogene family is activated in certain types of lung cancers by point mutations, of which *K-RAS* is the most predominantly activated *RAS* gene in lung cancer, representing 90% of all the mutated *RAS* found. *K-RAS* is mostly mutated at codon 12 but occasionally at codons 13 and 61. Approximately 20-30% of lung adenocarcinomas and in total, 15-20% of all non-small-cell lung cancers involve *K-RAS* mutations. By contrast, *K-RAS* mutations are rare in small-cell lung cancers [6, 49]. The occurrence time of *RAS* mutations varies by the types of lung tumor. For example, in squamous cell carcinoma, *RAS* mutations are usually late events in cancer development, but in lung adenocarcinomas, it might occur rather early [49, 50]. In addition, subtype heterogeneity also exists, for instance, *K-RAS* mutations exist in parenchymal but not bronchial adenocarcinomas. There are several studies of the correlation between *K-RAS* mutations and tobacco smoking. It was shown that 90% of patients contain a G to T transversion in exon 12 caused by the formation of bulky DNA adducts induced by nitrosamines and polycyclic hydrocarbons from tobacco smoke, and the presence of *K-RAS* mutations in a patient's lung tumor correlates with the poor prognosis in non-small-cell lung cancers [24, 50, 51]. The significance of *K-RAS* mutations in lung carcinogenesis has been demonstrated by various

transgenic mouse models that express *K-RAS* in the lung [47, 52, 53]. Regardless of the method by which *K-RAS* is expressed, lesions develop once the mutant K-RAS is expressed.

### **B.2.b.ii. Tumor Suppressor Genes**

The function of proteins encoded by tumor suppressor genes involves regulation of cell cycle, inhibition of cell growth and survival, or increase of apoptosis. When tumor suppressor genes are inactivated, normal cell functions associated are disrupted and the disruptions in a variety of normal cell functions contribute to tumorigenesis process. The first tumor suppressor gene, *RBI*, was discovered in 1987 [54, 55]. Phosphorylated by cyclin D/Cdk-4 or -6, the inactivation of the *RBI* protein product, pRb, causes the activation of the E2F transcription factor, which is required for the upregulation of various genes required for S phase initiation [56]. The inactivation of *RBI* has been observed in many types of cancers, including lung, breast, prostate and esophageal cancers [57]. Other classical tumor suppressor genes inactivated in multiple cancers include *P53* [58-60] and cyclin-dependent kinase inhibitor 2A (*P16<sup>INK4A</sup>*) [61-63].

In lung cancer, several tumor suppressor genes have been determined to be inactivated by deletion, mutation or aberrant promoter methylation. For example, the loss of heterozygosity of *P53* gene is very frequent in both small-cell lung cancers and non-small-cell lung cancers, but *P16<sup>INK4A</sup>* mutations are only frequently found in non-small-cell lung cancers [5, 24, 49, 51, 63]. Deletion of several chromosomal regions selectively happens in many lung tumor tissues, indicating that there might be some unidentified tumor suppressor genes in the deleted locations. Several candidate tumor

suppressor genes have been proposed but most of others need further investigation [64, 65]. The *P53* gene locates on the short arm of chromosome 17 (17p13.1), which encodes a 53 kD nuclear protein functioning as a transcription factor. The functions of p53 include inducing cell cycle arrest at G1/S regulation point for DNA damage recognition, activating several genes encoding the components of DNA repair machinery, and initiating apoptosis if DNA damage is irreparable. *P53* mutation occurs in more than 75% of small-cell lung cancers, and 50% of non-small-cell lung cancers, and mostly, *P53* mutations are G to T transversion [5, 49]. *P16<sup>INK4A</sup>* encodes for p16<sup>INK4A</sup>, an inhibitor of retinoblastoma [65]. The *P16<sup>INK4A</sup>* gene is mostly inactivated in non-small-cell lung cancers by aberrant promoter methylation (25%), homozygous deletions (10-40%), or point mutations (10-40%) [5, 24, 49, 51].

### **B.2.c. Epigenetics and Lung Cancer**

DNA methylation is the addition of methyl groups to the DNA. It occurs mostly at the carbon-5 position of cytosine of CpG islands, producing 5-methylcytosine [66-68]. DNA methylation regulates gene expression in a variety of biological processes including cell maturation, differentiation and DNA repair [69-72]. The level of CpG dinucleotides within the genome is generally not high. However, high levels of CpG dinucleotides are frequently observed as long repetitive sequences called CpG islands, which are frequently methylated in the promoter region of genes. The changes of methylation status at CpG islands have also been frequently identified in different types of cancers including lung cancer [73-77].

### **B.2.c.i. DNA Methyltransferases and Lung Cancer**

The enzymes responsible for DNA hypermethylation are DNA methyltransferases (DNMTs), which use S-adenosyl methionine as the methyl donor. Three active DNMTs, DNMT1, DNMT3a, and DNMT3b, have been identified in humans. DNMT1 is believed to maintain DNA methylation since it primarily methylates hemi-methylated DNA on the nascent strand of DNA following DNA replication [78]. This mechanism ensures the methylation status of DNA is inherited in daughter cells. DNMT1 has been reported to be essential for maintaining DNA methylation patterns in cell proliferation, suggesting its important role in development [79]. Although classically believed to be a maintenance DNA methyltransferase, emerging evidence indicates that it also plays a critical role in *de novo* DNA methylation, which needs the coordination from DNMT3a [80]. The activation of DNMT1 has been reported in various cancers including lung cancer [28, 81-87]. DNMT3a and DNMT3b are considered *de novo* DNA methyltransferases, establishing new DNA methylation patterns [88].

In a recent study of lung cancer patients, DNMT1 was highly expressed and had a strong binding capacity to hypermethylated promoter region of tumor suppressor genes in lung tumors and this overexpression and region-specific binding is related to tobacco smoking [28]. Another study by the same group demonstrated that tobacco smoking can induce DNMT1 overexpression and nuclear accumulation in human lung cancer patients and 4-(methylnitrosamino)-1-(3-pyridyl)-1-butanone (NNK)-induced lung tumors, indicating the important role of DNMT1 in lung tumorigenesis in both humans and rodents [84]. The inhibition of DNMT1, which can reverse the hypermethylated status and reactivate the silenced tumor suppressor genes, has been demonstrated by studies using

5-aza-2'-deoxycytidine [89-91], and dietary polyphenols including (-)-epigallocatechin-3-gallate (EGCG) [92, 93].

### **B.2.c.ii. Aberrant DNA Methylation in Lung Cancer**

DNA hypermethylation is a crucial mechanism of silencing several genes that are involved in cell cycle regulation, DNA repair, and apoptosis [69, 94]. However, the overall 5-methylcytosine levels within a cancer cell are usually decreased and this global hypomethylation pattern is considered a hallmark of cancer [95]. Recently, increasing studies indicate that hypomethylation can also occur to specific genes [96-98]. An important mechanism for the silencing of tumor suppressor genes is through aberrant hypermethylation of CpG islands at the promoter region [99-101].

Silencing of genes through gene-specific DNA hypermethylation in cancer was first demonstrated in 1986 when calcitonin gene was hypermethylated in small-cell lung cancer [102]. This study was followed by several analyses demonstrating the hypermethylation of several tumor suppressor genes, including *RBI* in retinoblastoma [103, 104], *CDH13* in gastric cancer [105], and *P16<sup>INK4A</sup>* [106] and *RASSF1* [107-112] in multiple types of cancers. A recent study of human lung cancer patients also showed a strong positive correlation between *RASSF1* hypermethylation and tobacco smoking [112]. Those studies demonstrated that promoter hypermethylation of tumor suppressor genes is a critical process in tumorigenesis. *CDH13* is another gene demonstrated to be hypermethylated in multiple types of cancers including lung cancer [113, 114]. *DAPK1* was also reported to be hypermethylated in multiple types of cancers including colorectal, cervical and lung cancers [115-117]. The hypermethylation of *DAPK1* is associated with poor prognosis and

low survival rate, suggesting the methylation of *DAPK1* is important in lung tumorigenesis [118, 119].

## **C. Animal Models for the Studies of Lung Cancer**

### **C.1. Animal Models of Lung Tumorigenesis**

Extensive efforts and a variety of approaches have been used to create murine lung cancer models. Studies showed a variety of chemical carcinogens can induce pulmonary tumors in animals including tobacco smoke, tobacco-smoke constituents polyaromatic hydrocarbons and nitrosamines, urethane, and aflatoxin. [120]. Certain inbred strains of mice are particularly sensitive to chemical induction of lung tumor from tobacco-specific carcinogens of cigarette smoke and can generate spontaneous lung tumors, of which, the most sensitive strains are A/J and SWR [121, 122]. Other strains range from intermediate sensitive (BALB/c and O20), to partial resistant (CBA and C3H), and to almost fully resistant (DBA and C57BL/6) [92, 121]. It has been found that several oncogenes and tumor suppressor genes are present in the susceptible strains and responsible for the sensitivity of certain strains to chemical carcinogens. One example of those genes is the *K-RAS* proto-oncogene. Actually, the *k-Ras* gene is found in most of the susceptible mouse strains and is believed to be important to the increased sensitivity to chemical carcinogens [123]. *p16<sup>INK4A</sup>* has also been shown to present with a higher frequency in sensitive mouse strains at susceptibility locus on chromosome 4 [124]. Both *k-Ras* and *p16<sup>INK4A</sup>* mutations have been demonstrated in human small-cell lung cancers and non-small-cell lung cancers,

suggesting that chemical carcinogen-induced lung cancer model could be useful for human lung cancer research [8].

## **C.2. NNK-induced Lung Tumorigenesis Model**

The tobacco-specific carcinogen NNK is a nicotine-derived nitrosamine ketone. NNK is present in both unburned tobacco and tobacco smoke. Tobacco-specific nitrosamines and polycyclic aromatic hydrocarbons are two classes of carcinogens present in tobacco smoke and NNK is a thoroughly studied example of carcinogenic nitrosamines. The carcinogenetic activity of NNK is achieved only after its metabolism activation by cytochrome P450s. NNK induces multiple organ tumors when given by oral administration or intraperitoneal (i.p.) injection, and has been one of the most used models for studies of lung cancer prevention. Studies demonstrated that there is a correlation between NNK induced DNA-adducts and tumor development. Acute DNA adducts such as O<sup>6</sup>-methylguanine, 7-methylguanine, O<sup>4</sup>-methylthymine, pyridyloxobutyl adducts and 4-hydroxyl-(3-pyridyl)-1-butanone adducts were observed within 24 h of NNK injection. The accepted theory of the mechanism of NNK-induced lung tumors is that NNK causes acute DNA adduct formation and oxidative stress, which will induce DNA mispairs and damage and gene mutation, and these changes will drive mutations in oncogenes and tumor suppressor genes. The activation of oncogenes such as *k-Ras* and silencing of tumor suppressor genes can lead to a series of downstream molecular changes and eventually induce lung tumors. Previous studies mostly focused on the mutation of tumor suppressor genes and oncogenes [125, 126], but recently several studies point to the epigenetic

changes, especially changes of DNMT levels caused by NNK or other tobacco-smoke carcinogens [84, 127-129].

The origin of NNK induced lung tumor is still controversial, but most results suggest that NNK-induced lung tumors are from bronchial epithelial clara cells or from type II alveolar cells [130-133]. NNK-induced lung tumors in A/J mice involve progression from normal to hyperplasia, to adenoma, and finally to adenocarcinoma. Two doses of NNK (100 mg/kg body weight and 50 mg/kg body weight, i.p.) can induce lung adenoma in 16-20 weeks and adenocarcinoma in 28-52 weeks [120, 134-136]. Metastasis is rare in this model and the interaction with stromal cells is weak. Therefore, the diagnosis for benign, pre-malignant, and malignant tumors is based on the presence of large pleomorphic cells with vesicular nuclei, prominent nucleoli, undifferentiated cytoplasm, and frequent mitosis. This model has been broadly used in characterizing chemopreventive activities of different agents and its molecular mechanisms (45).

NNK exposure has been reported to increase DNMT1 expression and to cause hypermethylation of multiple tumor suppressor genes in rodent lung and liver tumors, including *p16<sup>INK4A</sup>*, *Dapk1*, *Rarb*, and *Runx3* [100, 137-141]. In human studies, several tumor suppressor genes including *MGMT*, *P16<sup>INK4A</sup>*, *CDH13*, *PAX5*, *RARB*, *RASSF1*, *RUNX*, and *DAPK* have been identified to be hypermethylated in lung cancer patients, especially in smokers [115, 118, 142-144]. However, most of those human and animal studies were at the tumor stage and did not have information of DNMTs and the epigenetic changes in the initiation stage of lung tumorigenesis.

## **D. Dietary Constituents and Atorvastatin as Chemopreventive Agents**

### **D.1. Dietary Constituents as Chemopreventive Agents**

#### **D.1.a. EGCG as a Chemopreventive Agent**

Prevention of lung cancer by dietary constituents could be a safe, feasible and economical approach. Several dietary constituents and beverages have been reported to have cancer preventive or anti-cancer activities. Tea, derived from the dried leaves of *Camellia sinensis* plant, is a commonly consumed beverage worldwide and its cancer preventive activities have been investigated extensively [134]. Tea is a major source of dietary flavonoids (polyphenols) for many populations around the world especially Asian countries. There are three major forms of tea: green tea, black tea and oolong tea, distinguished by the methods of their production and chemical composition. Green tea, which represents 20% of world tea consumption, contains significant amounts of characteristic polyphenols known as catechins. Major catechins present in green tea include EGCG, (-)-epicatechin-3-gallate, (-)-epigallocatechin, and (-)-epicatechin. Tea catechins are characterized by the dihydroxyl or trihydroxyl substitutions on the B ring and the m-5,7-dihydroxyl substitutions on the A ring [145].

Among these catechins, EGCG is most abundant and biologically active in green tea [146]. Extensive laboratory and epidemiological studies have suggested that green tea polyphenols, especially EGCG, have preventive activities against chronic diseases including heart disease, diabetes, neurodegenerative disease and cancer [134, 147-150].

EGCG and other tea constituents have been shown to inhibit tumorigenesis in different organs including lung, skin, esophagus, liver, stomach, colon, oral cavity,

pancreas, bladder, small intestine, mammary glands and prostate in various animal models [134]. The inhibitory effects of EGCG or green tea constituents have been explored previously in NNK-induced lung tumorigenesis model in A/J mice by our laboratory and others and the inhibitory activities of EGCG or green tea have been proved to be effective when administered during the initiation, promotion, or progression stages of lung tumorigenesis [131, 133, 151-154]. In one study, treatment of A/J mice with green or black tea extract for 60 weeks inhibited the spontaneous formation of lung tumors and rhabdomyosarcomas [151]. In another study, treatment with polyphenon E or caffeine at week-20 after a single dose of NNK at the adenoma stage reduced the progression of lung adenomas to adenocarcinomas, possibly through the induction of apoptosis and the inhibition of cell proliferation and phosphorylation of c-Jun and ERK1/2 [131]. This result suggests that tea polyphenols can exert inhibitory actions against lung tumorigenesis at the progression stage. In a study using EGCG and atorvastatin as chemopreventive agents starting one week after the second dose of two weekly doses of NNK injections, we demonstrated that the synergistic inhibition of NNK-induced lung tumorigenesis by the combination of EGCG and atorvastatin were through the induction of apoptosis and down-regulation of anti-apoptotic Bcl-2 family proteins Mcl-1 and Bcl-xL [133]. These results suggest that EGCG or green tea polyphenols may exert inhibitory effects at different stages of lung tumorigenesis. In a study in the *Apc*<sup>Min/+</sup> mouse model of intestinal tumorigenesis by our laboratory, EGCG was shown to increase the level of E cadherin and decrease the levels of phospho-AKT (p-AKT), ERK1/2 and  $\beta$ -catenin [155]. However, high doses of EGCG or green tea polyphenols are required for the cancer preventive effect in some studies, possibly due to the relatively low bioavailability of EGCG. The cancer

preventive effects of EGCG and green tea constituents have been demonstrated in animal models [134, 156-158].

Many mechanisms have been proposed for the cancer preventive activities of EGCG and other green tea constituents. One of them is the anti-oxidative effect. EGCG is a well-known antioxidant from dietary sources and the anti-oxidative properties of EGCG can be attributed to the polyphenolic structure of EGCG: trihydroxyl structures on the B and D rings and m-5,7-dihydroxyl structure on the A ring. This polyphenolic structure allows electron delocalization, enabling EGCG to quench free radicals including superoxide [134]. Reactive oxygen species (ROS) have been shown to be critical in carcinogenesis and green tea constituents have been demonstrated to react with ROS including superoxide and hydrogen peroxide [145, 159, 160]. Green tea constituents are also strong chelators of metal ions and the chelation of free metal ions prevents the formation of ROS from the auto-oxidation of many compounds [134]. In humans, decreased level of 8-hydroxy-deoxyguanosine, an oxidative DNA damage marker, in the urinary of smokers by the administration of green tea was observed in two studies, suggesting that green tea constituents can reduce the level of oxidative stress in smokers [161].

On the other hand, EGCG also possesses pro-oxidative properties as the trihydroxyl and dihydroxyl structures of EGCG also increase the susceptibility to auto-oxidation under alkaline or neutral pH [134]. Our laboratory has demonstrated that in cell culture conditions, EGCG is readily auto-oxidized producing ROS including superoxide and hydrogen peroxide and this process is accompanied by the formation of EGCG semiquinone radicals, EGCG quinines and EGCG dimers [162, 163]. These ROS produced

during the auto-oxidation of EGCG were mostly abolished by the addition of superoxide dismutase (SOD) and catalase [163, 164]. In addition, intracellular ROS generation by EGCG treatment in lung cancer cells has also been demonstrated by our laboratory as measured by the oxidation of intracellular 2,7-dichlorodihydrofluorescein diacetate, suggesting that the EGCG incorporated into the cells generates ROS and oxidative stress-induced damages intracellularly [132]. In animal tissues, we previously demonstrated that EGCG could inhibit the growth of H1299 human lung cancer cell xenografts and this inhibition is accompanied with the increase of oxidative DNA damage markers  $\gamma$ -H2AX and 8-hydroxy-deoxyguanosine, as well as apoptosis [132]. However, due to the presence of antioxidant and detoxifying enzymes, the level of ROS is usually much lower than in cell culture conditions [165]. One important reason for the discrepancies between the results from cell culture studies and from studies in humans and animals is the low bioavailability of EGCG in humans and animals [161, 166]. In humans, the peak plasma levels of tea polyphenols are usually in the range of 0.2-0.3  $\mu$ M, following oral administration of the equivalent of two or three cups of green tea [161]. Even with high pharmacological doses of EGCG through oral administration, peak plasma levels of EGCG are only 2-9  $\mu$ M in mice and 7.5  $\mu$ M in humans, respectively [161]. However, in most cell line studies, the effective EGCG concentrations are in the range of 20-100  $\mu$ M.

The polyphenolic structure of EGCG enables it to be a very good donor molecule for hydrogen bonding to proteins and nucleic acids. EGCG binds strongly to many biomolecules and their binding may play key roles in the cancer preventive activities of EGCG. A good example has been demonstrated previously by our laboratory [167]. We found that the formation of five hydrogen bonds between EGCG and the active site of

DNMT1 is the key in the inhibition of DNMT1 activity and reactivation of methylation-silenced tumor suppressor genes. Another recent study demonstrated the binding of EGCG to both the WW and PPlase domains of peptidyl-prolyl *cis/trans* isomerase inhibited its activity [168]. This enzyme has been shown to be required for the activation of AP-1, NFkB,  $\beta$ -catenine and other signaling pathways.

### **D.1.b. Tocopherols as Chemopreventive Agents**

Vitamin E is a group of dietary natural compounds that share a chromanol ring and an aliphatic side chain. Based on the degree of saturation of the side chain, vitamin E can be divided into two subgroups: tocopherols and tocotrienols. Tocopherols have a saturated 16-carbon side-chain while tocotrienols have an unsaturated 16-carbon side-chain containing double bonds at positions 3', 7' and 11' [169-171]. Both tocopherols and tocotrienols consist 4 members denoted as  $\alpha$ -,  $\beta$ -,  $\gamma$ - and  $\delta$ -tocopherols or tocotrienols, respectively, based on the number and position of methyl groups on the chromanol ring [169].  $\alpha$ -Tocopherol is trimethylated at positions 5, 7 and 8;  $\beta$ -tocopherol is dimethylated at positions 5 and 8;  $\gamma$ -tocopherol is dimethylated at positions 7 and 8; and  $\delta$ -tocopherol is monomethylated at position 8 (Figure 1C). Tocopherols cannot be synthesized in humans and animals so they need to be obtained from dietary sources. The major dietary sources of tocopherols are vegetable oils including oils from soybean, corn, cottonseeds and nuts [172]. Among tocopherols,  $\gamma$ -tocopherol is the major form from diet.

Tocopherols are well-known dietary antioxidants. They function as chain-breaking antioxidants protecting cellular membranes from lipid-derived free radical damage and the anti-oxidative properties of tocopherols are mainly from the phenolic hydrogens in the

chromanol ring [173-176]. The anti-oxidative property of tocopherols in preventing different types of diseases including cardiovascular disease, atherosclerosis, neurodegenerative disease and cancer has been extensively explored in several clinical trials [177-181].  $\alpha$ -Tocopherol was thought to be the strongest form of tocopherols as an antioxidant as demonstrated in several *in vitro* studies. However, other studies indicate that  $\gamma$ -tocopherol possesses similar or even stronger anti-oxidative properties than  $\alpha$ -tocopherol [182]. In addition to serving as direct antioxidants scavenging free radicals, tocopherols can also serve as indirect antioxidants by inducing the expression of Nuclear factor (erythroid-derived 2)-like 2 (Nrf2) and related antioxidant enzymes. Nrf2 is a transcription factor that serves as a sensor of chemical-induced oxidative stress. In response to oxidative stress or stimuli, Nrf2 is released from Kelch-like-ECH-associated protein 1 and translocates into nucleus from cytoplasm, dimerizes with small Maf proteins, and binds to the anti-oxidant-responsive element, inducing the expression of gene expression of antioxidant enzymes including SOD, glutathione peroxidase, heme oxygenase-1 and catalase [183-185].

Besides anti-oxidative properties, the mechanisms of cancer preventive activities of different forms of tocopherols have been investigated extensively [186-190].  $\alpha$ -Tocopherol is the most active form over others among different forms of tocopherols as the chromanol ring of  $\alpha$ -tocopherol is trimethylated. Furthermore, it is the most abundant form of tocopherol found in the blood and tissues. Therefore, it received most attention and its cancer preventive activities have been studied extensively [191]. However, recent large-scale intervention studies in humans with high doses of  $\alpha$ -tocopherol have been unsuccessful [177, 192, 193].  $\gamma$ -tocopherol has been shown to possess stronger

anti-inflammatory and cancer preventive activities as compared to  $\alpha$ -tocopherol by previous studies [189, 194-196].  $\gamma$ -Tocopherol-rich mixture of tocopherols ( $\gamma$ -TmT), easily obtained as a by-product of vegetable oil containing 57%  $\gamma$ -tocopherol, 24%  $\delta$ -tocopherol, 13%  $\alpha$ -tocopherol, and 0.5%  $\beta$ -tocopherol, has been used in several chemopreventive studies recently by our laboratory and collaborators showing inhibition of lung, colon, prostate and mammary carcinogenesis in animal models [190, 197-201]. In one study, we demonstrated the inhibition of both NNK-induced lung tumorigenesis and H1299 lung cancer cell xenograft tumors by  $\gamma$ -TmT treatment, through the inhibition of oxidative stress and induction of apoptosis [190].

As for humans, several studies have demonstrated the positive relationship between lower nutritional levels of tocopherols and increased risk of different types of cancers [191, 202-204]. The cancer preventive activities of tocopherols on lung cancer have been demonstrated in both case-control and cohort, and interventions studies. There are four case-control studies [205-208] and three cohort studies [209-211] on the relationship between dietary or blood levels of tocopherols and lung cancer risk since 1986. Among them, three case-control studies [206-208] and two cohort studies [144, 210] showed inverse relationship between dietary intake of tocopherols and lung cancer risk. Interestingly, in the two cohort studies with positive findings, the preventive effects of tocopherols were found in current smokers, suggesting that the protective effects of tocopherols might be on smoking-induced molecular changes in the lung [144, 210].

### **D.1.c. Myo-inositol as a Chemopreventive Agent**

Inositols are a group of nine isomeric forms of cyclohexanehexol and abundantly available in various dietary sources. Inositols are chemically very stable polar molecules possessing versatile properties and are important building blocks of all eukaryotic membrane phosphoinositides [212]. Myo-inositol (cis-1,2,3,5-trans-4,6-cyclohexanehexol) is an isomer of glucose and the most common form of inositols found from dietary sources. The primary source of myo-inositol is inositol hexaphosphate, which is hydrolyzed in the gastrointestinal tract to free myo-inositol by phytase [213].

Myo-inositol is well-known for its extremely low toxicity in the field of chemoprevention. Dietary myo-inositol has been shown to inhibit NNK- and benzo(a)pyrene-induced lung tumorigenesis in a number of studies [214-221]. The inhibitory effect of myo-inositol against carcinogen-induced lung tumorigenesis has been demonstrated in all stages of tumorigenesis. In one study, continuous treatment with 0.3% myo-inositol in the diet starting one week before the benzo(a)pyrene administration inhibited the formation of pulmonary tumor by 53% [216]. In another study, inhibition of lung tumor multiplicity was observed when myo-inositol was given in the post-initiation phase (one week after the last dose of eight weekly doses of benzo(a)pyrene until the end of the 27-week experiment) [219]. In the same study, the inhibitory effect of myo-inositol short-term treatment (one week treatment prior to, during, and one week after benzo(a)pyrene administration) was also observed on lung tumor multiplicity [219]. In humans, myo-inositol has been investigated in the treatment of psychiatric disorders [222-227]. In the area of cancer, myo-inositol has been shown to inhibit AKT and ERK1/2 phosphorylation in bronchial lesions of the lung in heavy smokers [228]. Furthermore, a

phase I clinical study was conducted in 2006 and showed that a dose of 18 g/day for up to 3 months was well tolerated by humans and significant regression of dysplastic lesions [213]. Studies on the anti-cancer activities using inositol phosphates have also been conducted. It was found that the inhibition of AP-1 (c-Jun/c-Fos dimer) activation by inositol phosphates was through the inhibition of PI3K/AKT pathway, and this inhibition was required for their anti-cancer activities [229, 230]. Cell line studies have also been carried out using human small airway and bronchial epithelial cells and endothelial cells in vitro to clarify the mechanism of actions of myo-inositol [228, 231, 232]. PI3K/AKT pathway is involved in cell growth, survival and proliferation and the inhibition of basal levels of AKT activity and nicotine-induced activation of AKT by myo-inositol was associated with the inhibition of cell proliferation in human bronchial epithelial cells [228]. The level of p-AKT was also assessed in NNK- and benzo(a)pyrene-induced lung tissues in A/J mice but only modest inhibition by myo-inositol was observed [219, 221]. However, the analysis was done using whole lung lysates and the changes of p-AKT in specific cell types may not be discovered.

## **D.2. Atorvastatin as a Chemopreventive Agent**

Atorvastatin (commercial name Lipitor) belongs to the statin family, a class of 3-hydroxy-3-methylglutaryl coenzyme A (HMG-CoA) reductase inhibitors used to reduce cholesterol and low density lipoproteins. Statins were first discovered in the 1970s by Akira Endo [233]. The outstanding efficacy in the prevention of cardiovascular disease and the relative safety of statins have resulted in its widespread use. Many cell line and animal studies have shown that statins serve as chemopreventive drugs in various cancers including lung cancer [133, 234-236]. HMG-CoA reductase is the major rate-limiting

enzyme of the cholesterol synthesis pathway. The inhibition of HMG-CoA reductase by statins prevents the conversion of HMG-CoA to mevalonate, and the synthesis of mevalonate downstream products such as farnesyl pyrophosphate and geranylgeranyl pyrophosphate [237-239]. The isoprenylation of small G proteins such as RhoA and k-Ras, requires farnesyl pyrophosphate and geranylgeranyl pyrophosphate and their isoprenylation is required for the translocation from cytosol to plasma membrane, where they become functionally active [237, 240-242]. Many of the downstream products of the cholesterol synthesis pathway are necessary for critical cellular functions including membrane integrity, protein synthesis and cell cycle progression [239, 243, 244]. Disruption of those cellular functions in neoplastic cells by statins could result in the inhibition of cell growth and induction of apoptosis, in which RhoA translocation was involved [243-246].

For human lung cancer, the results from several studies seem inconclusive. There are four case-control studies evaluating the association between statin use and lung cancer risk showing that statin is not effective in reducing lung cancer risk [235, 247-249]. The disappointing results might be due to the relatively small number of cases used in these four studies as the results from another case-control study with almost 2000 lung cancer cases showed a 45% reduction in lung cancer risk among statin users when compared to non-users [250]. The results from cohort studies are also not conclusive as two studies showed no association between statin use and the risk of lung cancer [251, 252] but the other two studies demonstrated reduction in the risk of lung cancer among statin users as compared to non-users [253, 254]. In conclusion, human studies on the relationship

between statin use and lung cancer risk is not conclusive and the chemopreventive effect in humans remains to be established.

## II. GOALS AND SPECIFIC AIMS

### Goals

The main goal of this thesis research was to study the mechanisms of NNK-induced lung tumorigenesis and the inhibitory activities of EGCG. Another goal of this thesis research was to study the inhibitory activities of EGCG, tocopherols, myo-inositol and atorvastatin, alone or in combination, and to elucidate the possible mechanisms of inhibition involved in the NNK-induced lung tumorigenesis. The NNK-induced lung cancer model has been a very commonly used model for chemoprevention studies [120]. Our previous studies have demonstrated the inhibitory activities of EGCG, tocopherols, myo-inositol and atorvastatin in NNK-induced lung cancer model [131, 255-257]. However, those studies focused on the molecular alterations mainly at the tumor stage and did not have information of epigenetic changes. Recently, emerging evidence suggests that lung cancer development in both humans and rodents is associated with the inactivation of tumor suppressor genes [63, 258]. An important mechanism for the silencing of tumor suppressor genes is through aberrant hypermethylation of CpG islands at the promoter region of DNA [99-101]. Therefore, we hypothesized that the induction of DNMT1 and the silencing of tumor suppressor genes through promoter hypermethylation in bronchial epithelial cells of NNK-treated lungs contribute to the initiation and progression of NNK-induced lung tumorigenesis, and EGCG confers inhibitory actions against NNK-induced lung tumorigenesis through the suppression of NNK-induced DNMT1 elevation and promoter hypermethylation of tumor suppressor genes. Furthermore, we hypothesized that EGCG, tocopherols, myo-inositol and atorvastatin, alone or in

combination, confer inhibitory actions against NNK-induced lung tumorigenesis and multiple mechanisms are involved.

### **Specific Aims**

1. To Characterize the Molecular Alterations in Lung Tissues Following NNK Administration and during the Progression of NNK-induced Lung Tumorigenesis and the Inhibitory Effect of EGCG

2. To Investigate the Possible Mechanisms of Inhibition by EGCG in NNK-induced Lung Tumorigenesis and Lung Cancer Cell Growth

3. To Determine the Inhibitory Actions of EGCG, Tocopherols, Myo-inositol and Atorvastatin, Alone or in Combination, on NNK-induced Lung Tumorigenesis and the Growth of Allograft Tumors and Lung Cancer Cells

### III. RATIONALE AND RESEARCH DESIGN

#### **A. Molecular Alterations in Lung Tissues Following NNK Administration and during the Progression of NNK-induced Lung Tumorigenesis and the Inhibitory Effect of EGCG (*Specific Aim 1*)**

##### **A.1. NNK-induced Lung Tumorigenesis Model in Lung Cancer Studies**

Two doses of NNK administered by i.p. injection (100 mg/kg body weight and 50 mg/kg body weight) can induce lung adenoma in 16-20 weeks and adenocarcinoma in 28-52 weeks [120, 134-136]. The NNK-induced lung cancer model has been widely used to study the mechanisms of smoking-related lung cancers and the inhibitory actions of different chemopreventive agents since developed. Molecular alterations including *K-RAS* mutation, *c-MYC* overexpression and reduction of *Rb* tumor suppressor gene in NNK-induced lung tumors has been demonstrated previously [125, 126]. However, molecular alterations such as changes in the level of DNMT1 and gene-specific promoter methylation in lung tissues following NNK administration has not been demonstrated yet. The information obtained from this thesis study will be important in providing a basis for developing new chemopreventive studies of lung cancer focusing on the chemopreventive effects of previously validated chemopreventive agents in the first few weeks following NNK administration.

##### **A.2. Research Design for Part A**

### **A.2.a. Experiment 1: Molecular Alterations in Lung Tissues of A/J Mice Following NNK Administration and the Inhibitory Effect of EGCG**

Female A/J mice were randomized based on body weight and divided into seven groups as follows:

Group 1: Zero-day saline control mice fed with AIN-93M diet (n = 5)

Group 2: One-day NNK-treated mice fed with AIN-93M diet (n = 5)

Group 3: One-day NNK-treated mice receiving 0.5% EGCG in AIN-93M diet (n = 5)

Group 4: Three-day NNK-treated mice fed with AIN-93M diet (n = 5)

Group 5: Three-day NNK-treated mice receiving 0.5% EGCG in AIN-93M diet (n = 5)

Group 6: Fourteen-day NNK-treated mice fed with AIN-93M diet (n = 5)

Group 7: Fourteen-day NNK-treated mice receiving 0.5% EGCG in AIN-93M diet (n = 5)

Four-week old female A/J mice were purchased from the Jackson Laboratory (Bar Harbor, ME). The animals were maintained at room temperature ( $20 \pm 2$  °C) with a relative humidity of  $50 \pm 10\%$  and with an alternating 12 h light/dark cycle. The animals were acclimated in our animal facility for one week and then fed with either AIN-93M diet or AIN-93M diet containing 0.5% EGCG, starting one week before the one dose NNK i.p. injection (100 mg/kg body weight). One, three and fourteen days after the NNK administration, 5 mice from each NNK group were euthanized and sacrificed. The lungs of each animal were removed, inflated and then either fixed in 10% buffered formalin or frozen at  $-80^{\circ}\text{C}$  directly. Body weight, food consumption, fluid intake and general health status were monitored. Blood was taken by cardiac puncture and centrifuged for 15 min at

3000 g for the preparation of serum. The liver and spleen were also removed and their weights were measured.

### **A.2.b. Experiment 2: Molecular Alterations in Lung Tissues of A/J Mice Following NNK Administration and the Inhibitory Effect of EGCG, $\delta$ -Tocopherol and Myo-inositol**

Female A/J mice were randomized based on body weight and divided into eight groups as follows:

Group 1: Zero-day saline control mice fed with AIN-93M diet (n = 8)

Group 2: One-day NNK-treated mice fed with AIN-93M diet (n = 8)

Group 3: Three-day NNK-treated mice fed with AIN-93M diet (n = 8)

Group 4: Three-day NNK-treated mice receiving 0.5% EGCG in AIN-93M diet (n = 8)

Group 5: Three-day NNK-treated mice receiving 0.3%  $\delta$ -tocopherol in AIN-93M diet (n = 8)

Group 6: Three-day NNK-treated mice receiving 2% myo-inositol in drinking fluid (n = 8)

Group 7: Seven-day NNK-treated mice fed with AIN-93M diet (n = 8)

Group 8: Fourteen-day NNK-treated mice fed with AIN-93M diet (n = 8)

Four-week old female A/J mice were purchased from the Jackson Laboratory (Bar Harbor, ME). The animals were maintained at room temperature ( $20 \pm 2$  °C) with a relative humidity of  $50 \pm 10\%$  and with an alternating 12 h light/dark cycle. The animals were acclimated in our animal facility for one week and then treated with 0.5% EGCG or 0.3%

$\delta$ -tocopherol in AIN-93M diet, or 2% myo-inositol in drinking fluid, starting one week before the one dose NNK i.p. injection (100 mg/kg body weight). One, three, seven and fourteen days after the NNK administration, animals were euthanized and sacrificed. The lungs of each animal were removed, then either fixed in 10% buffered formalin, frozen at  $-80^{\circ}\text{C}$  directly, or stored in RNAlater solution (Qiagen, Valencia, CA). Body weight, food consumption, and general health status were monitored. Blood was taken by cardiac puncture and centrifuged for 15 min at 3000 g for the preparation of serum. The liver and spleen were also removed and their weights were measured.

### **A.2.c. Experiment 3: Molecular Alterations in Lung Tissues of A/J Mice during the Progression of NNK-induced Lung Tumorigenesis**

Female A/J mice were randomized based on body weight and divided into eight groups as follows:

Group 1: Five-week saline control mice fed with AIN-93M diet (n = 2)

Group 2: Five-week NNK-treated mice fed with AIN-93M diet (n = 8)

Group 3: Ten-week saline control mice fed with AIN-93M diet (n = 2)

Group 4: Ten-week NNK-treated mice fed with AIN-93M diet (n = 8)

Group 5: Fifteen-week saline control mice fed with AIN-93M diet (n = 2)

Group 6: Fifteen-week NNK-treated mice fed with AIN-93M diet (n = 8)

Group 7: Twenty-week saline control mice fed with AIN-93M diet (n = 2)

Group 8: Twenty-week NNK-treated mice fed with AIN-93M diet (n = 8)

Four-week old female A/J mice were purchased from the Jackson Laboratory (Bar Harbor, ME). The animals were maintained at room temperature ( $20 \pm 2$  °C) with a relative humidity of  $50 \pm 10\%$  and with an alternating 12 h light/dark cycle. The animals were acclimated in our animal facility for two weeks and then treated with two weekly doses of NNK (100 and 75 mg/kg body weight, i.p., respectively). Body weight, food consumption, fluid intake and general health status were monitored weekly. Animals were euthanized and sacrificed at weeks 4, 9, 14 and 19 after NNK treatment. The lungs of each animal were removed, and two lobes were inflated and fixed in 10% buffered formalin. One lobe was put in RNAlater solution (Qiagen), one lobe in HistoPrep solution (Qiagen), and one lobe in eppendorf tube, respectively, and then frozen at  $-80^{\circ}\text{C}$ . Visible tumors ( $>0.1$  mm in diameter), if observed, in the lungs were counted and the sizes were measured under a dissecting microscope. Blood was taken by cardiac puncture and centrifuged for 15 min at 3000 g for the preparation of serum. The liver and spleen were also removed and their weights were measured.

**B. Inhibitory Actions of EGCG, Atorvastatin, Tocopherols and Myo-inositol, Alone or In Combination, on NNK-induced Lung Tumorigenesis and Allografts Tumor Growth (*Specific Aims 2 and 3*)**

**B.1. Research Design for Part B**

**B.1.a. Experiment 1: Inhibition of NNK-induced Lung Tumorigenesis by EGCG, Myo-inositol,  $\gamma$ -TmT and Atorvastatin, Alone or In Combination**

Female A/J mice were randomized based on body weight and divided into nine groups as follows:

Group 1: Saline control mice fed with AIN-93M diet (n = 10)

Group 2: NNK-treated mice fed with AIN-93M diet (n = 30)

Group 3: NNK-treated mice receiving 0.4% EGCG in AIN-93M diet (n = 30)

Group 4: NNK-treated mice receiving 0.3%  $\gamma$ -TmT in AIN-93M diet (n = 30)

Group 5: NNK-treated mice receiving 0.2% EGCG and 0.15%  $\gamma$ -TmT in AIN-93M diet (n = 30)

Group 6: NNK-treated mice receiving 2% myo-inositol in drinking fluid (n = 30)

Group 7: NNK-treated mice receiving 0.2% EGCG in AIN-93M diet and 1% myo-inositol in drinking fluid (n = 30)

Group 8: NNK-treated mice receiving 400 ppm atorvastatin in AIN-93M diet (n = 30)

Group 9: NNK-treated mice receiving 200 ppm atorvastatin in AIN-93M diet and 1% myo-inositol in drinking fluid (n = 30)

Four-week old female A/J mice were purchased from the Jackson Laboratory (Bar Harbor, ME). The animals were maintained at room temperature ( $20 \pm 2$  °C) with a relative humidity of  $50 \pm 10\%$  and with an alternating 12 h light/dark cycle. The animals were acclimated in our animal facility for one week and then fed with AIN-93M diet or AIN-93M diet supplemented with 0.4% EGCG, 0.3%  $\gamma$ -TmT, 0.2% EGCG plus 0.15%  $\gamma$ -TmT, 2% myo-inositol, 0.2% EGCG plus 1% myo-inositol, 400 ppm atorvastatin, or 200 ppm atorvastatin plus 1% myo-inositol, respectively, until the end of the experiment

(week-20). One week after changing to chemopreventive diet, animals were treated with two weekly doses of NNK (100 and 75 mg/kg body weight, i.p., respectively). Body weight, food consumption, and general health status were monitored weekly. The animals were euthanized and sacrificed at week 20. The lungs of each animal were removed, then either fixed in 10% buffered formalin or frozen at -80°C directly. Visible tumors (>0.1 mm in diameter), if observed, in the lungs were counted and the sizes were measured under a dissecting microscope. Blood was taken by cardiac puncture and centrifuged for 15 min at 3000 g for the preparation of serum. The liver and spleen were also removed and their weights were measured.

#### **B.1.b. Experiment 2: Inhibition of NNK-induced Lung Tumorigenesis by EGCG, Myo-inositol and $\gamma$ -TmT, Alone or In Combination**

Female A/J mice were randomized based on body weight and divided into ten groups as follows:

Group 1: Saline control mice fed with AIN-93M diet (n = 10)

Group 2: NNK-treated mice fed with AIN-93M diet (n = 30)

Group 3: NNK-treated mice receiving 0.4% EGCG in AIN-93M diet (n = 30)

Group 4: NNK-treated mice receiving 0.3%  $\gamma$ -TmT in AIN-93M diet (n = 30)

Group 5: NNK-treated mice receiving 0.2% EGCG and 0.15%  $\gamma$ -TmT in AIN-93M diet (n = 30)

Group 6: NNK-treated mice receiving 0.25% myo-inositol in drinking fluid (n = 30)

Group 7: NNK-treated mice receiving 0.5% myo-inositol in drinking fluid (n = 30)

Group 8: NNK-treated mice receiving 1% myo-inositol in drinking fluid (n = 30)

Group 9: NNK-treated mice receiving 0.2% EGCG in AIN-93M diet and 0.25% myo-inositol in drinking fluid (n = 30)

Group 10: NNK-treated mice receiving 0.2% EGCG in AIN-93M diet and 0.5% myo-inositol in drinking fluid (n = 30)

Four-week old female A/J mice were purchased from the Jackson Laboratory (Bar Harbor, ME). The animals were maintained at room temperature ( $20 \pm 2$  °C) with a relative humidity of  $50 \pm 10\%$  and with an alternating 12 h light/dark cycle. The animals were acclimated in our animal facility for one week and then fed with AIN-93M diet or AIN-93M diet supplemented with 0.4% EGCG, 0.3%  $\gamma$ -TmT, 0.2% EGCG plus 0.15%  $\gamma$ -TmT, 0.25% myo-inositol, 0.5% myo-inositol, 1% myo-inositol, 0.2% EGCG plus 0.25% myo-inositol, or 0.2% EGCG plus 0.5% myo-inositol, respectively, until the end of the experiment (week-20). One week after changing to the chemopreventive diet, animals were treated with two weekly doses of NNK (100 and 75 mg/kg body weight, i.p., respectively). Body weight, food consumption, and general health status were monitored weekly. The animals were euthanized and sacrificed at week 20. The lungs of each animal were removed, then either fixed in 10% buffered formalin or frozen at  $-80^{\circ}\text{C}$  directly. Visible tumors ( $>0.1$  mm in diameter), if observed, in the lungs were counted and the sizes were measured under a dissecting microscope. Blood was taken by cardiac puncture and centrifuged for 15 min at 3000 g for the preparation of serum. The liver and spleen were also removed and their weights were measured.

### **B.1.c. Experiment 3: Effects of Short-term $\gamma$ -TmT and EGCG Treatment on NNK-induced Lung Tumors**

Six-week old female A/J mice were treated with two weekly doses of NNK (100 and 75 mg/kg body weight, i.p., respectively). Nineteen weeks from the first dose of NNK administration (week-20), mice were randomized based on body weight and divided into four groups as follows:

Group 1: Week-20 saline control mice fed with AIN-93M diet (n = 5)

Group 2: Week-20 NNK-treated mice fed with AIN-93M diet (n = 5)

Group 3: Week-20 NNK-treated control mice receiving 0.3%  $\gamma$ -TmT in AIN-93M diet for seven days (n = 5)

Group 4: Week-20 NNK-treated mice receiving 0.4% EGCG in AIN-93M diet for seven days (n = 5)

Four-week old female A/J mice were purchased from the Jackson Laboratory (Bar Harbor, ME). The animals were maintained at room temperature ( $20 \pm 2$  °C) with a relative humidity of  $50 \pm 10\%$  and with an alternating 12 h light/dark cycle. The animals were acclimated in our animal facility for two weeks and then treated with two weekly doses of NNK (100 and 75 mg/kg body weight, i.p., respectively). The animals were fed with AIN-93M diet until nineteen weeks after the first dose of NNK administration (Week-20). Mice were then fed with control diet or diet supplemented with 0.3%  $\gamma$ -TmT or 0.4% EGCG for 7 days. The animals were euthanized and sacrificed at week 20. Body weight, food consumption, and general health status were monitored weekly. The lungs of each

animal were removed, inflated and then either fixed in 10% buffered formalin or frozen at  $-80^{\circ}\text{C}$  directly. Visible tumors ( $>0.1$  mm in diameter), if observed, in the lungs were counted and the sizes were measured under a dissecting microscope. Blood was taken by cardiac puncture and centrifuged for 15 min at 3000g for the preparation of serum. The liver and spleen were also removed and their weights were measured.

#### **B.1.d. Experiment 4: Effects of Short-term EGCG Treatment in NNK-induced Lung Tumors**

Six-week old female A/J mice were treated with two weekly doses of NNK (100 and 75 mg/kg body weight, i.p., respectively). Nineteen weeks from the first dose of NNK administration (week-20), mice were randomized based on body weight and divided into four groups as follows:

Group 1: Week-20 saline control mice fed with AIN-93M diet (n = 5)

Group 2: Week-20 NNK-treated mice fed with AIN-93M diet (n = 5)

Group 3: Week-20 NNK-treated mice receiving two days of EGCG by daily i.p. injection (30 mg/kg body weight) (n = 5)

Group 4: Week-20 NNK-treated control mice receiving five days of EGCG by daily i.p. injection (30 mg/kg body weight) (n = 5)

Four-week old female A/J mice were purchased from the Jackson Laboratory (Bar Harbor, ME). The animals were maintained at room temperature ( $20 \pm 2^{\circ}\text{C}$ ) with a relative humidity of  $50 \pm 10\%$  and with an alternating 12 h light/dark cycle. The animals were

acclimated in our animal facility for two weeks and then treated with two weekly doses of NNK (100 and 75 mg/kg body weight, i.p., respectively). The animals were fed with AIN-93M diet until nineteen weeks after the first dose of NNK administration (Week-20). Mice were then treated with EGCG by daily i.p. injection (30 mg/kg body weight) for 2 and 5 days. The animals were euthanized and sacrificed at week 20. Body weight, food consumption, and general health status were monitored weekly. The lungs of each animal were removed, inflated and then either fixed in 10% buffered formalin or frozen at -80°C directly. Visible tumors (>0.1 mm in diameter), if observed, in the lungs were counted and the sizes were measured under a dissecting microscope. Blood was taken by cardiac puncture and centrifuged for 15 min at 3000g for the preparation of serum. The liver and spleen were also removed and their weights were measured.

**B.1.e. Experiment 5: Inhibitory Actions of EGCG,  $\delta$ -Tocopherol and Myo-inositol, Alone or in Combination, on the Growth of Allograft Tumors**

Six-week old female A/J mice were inoculated subcutaneously with CL-13 mouse lung cancer cells ( $1 \times 10^6$ ) and divided into five groups as follows:

Group 1: A/J mice fed with AIN-93M diet (n = 12)

Group 2: A/J mice receiving 0.5% EGCG in AIN-93M diet (n = 11)

Group 3: A/J mice receiving 0.3%  $\delta$ -tocopherol in AIN-93M diet (n = 19)

Group 4: A/J mice receiving 2% myo-inositol in drinking fluid (n = 17)

Group 5: A/J mice receiving 0.17%  $\delta$ -tocopherol in AIN-93M diet and 1% myo-inositol in drinking fluid (n = 20)

Four-week old female A/J mice were purchased from the Jackson Laboratory (Bar Harbor, ME). The animals were maintained at room temperature ( $20 \pm 2$  °C) with a relative humidity of  $50 \pm 10\%$  and with an alternating 12 h light/dark cycle. The animals were acclimated in our animal facility for one week and then given AIN-93M diet or AIN-93M diet supplemented with 0.5% EGCG, 0.3%  $\delta$ -tocopherol, 2% myo-inositol, and 0.17%  $\delta$ -tocopherol plus 1% myo-inositol respectively, until the end of the experiment (day-49). One week after changing to chemopreventive diet, animals were inoculated with CL-13 cells ( $1 \times 10^6$  cells in 100  $\mu$ L PBS) on both rear flanks (day 0). Body weight and food consumption were monitored weekly. Tumor size were measured twice per week by a caliper and calculated using the formula  $V = (L \times W^2)/2$ , where  $V$  is the tumor volume,  $L$  is the longest and  $W$  is the shortest tumor dimension. The animals were sacrificed by CO<sub>2</sub> asphyxiation when the average tumor volume in the control group reached approximately 1.0 cm<sup>3</sup> (day-49). Tumors were dissected and tumor weights were measured. Half of the tumor was fixed in 10% buffered formalin for immunohistochemistry and the other half was frozen at -80 °C for biochemical analysis. The liver, lung, kidney and serum samples were collected.

## IV. MATERIALS AND METHODS

### A. Chemopreventive Agents and Research Diet

EGCG was obtained as a gift from Dr. Yukihiko Hara of Mitsui Norin Co., Ltd. (Tokyo, Japan). Atorvastatin was a gift from LKT Laboratories (St. Paul, MN).  $\gamma$ -TmT was obtained from Cognis Corporation (Cincinnati, OH) and contained 57%  $\gamma$ -tocopherol, 24%  $\delta$ -tocopherol, 13%  $\alpha$ -tocopherol, and 0.5%  $\beta$ -tocopherol.  $\delta$ -Tocopherol was purified from  $\gamma$ -TmT in our laboratory. Myo-inositol was purchased from Sigma-Aldrich (St. Louis, MO). All diets including AIN-93M rodent diet and AIN-93M rodent diet supplemented with different compounds were made at Research Diets, Inc. (New Brunswick, NJ) and maintained at 4°C. The diets were separated into sealed bags after they were flushed with nitrogen gas to prevent oxidation of the diet while they were stored at 4 °C. The food cups were replenished with fresh pellets twice weekly.

### B. Animal Studies

Female A/J mice (4-week old) were purchased from the Jackson Laboratory (Bar Harbor, ME). NNK was purchased from Chemsyn Science Laboratories (Lenexa, KS). After a one-week acclimation period, the animals were randomized based on body weight and fed the AIN-93M diet, AIN-93M diet supplemented with different chemopreventive agents, including EGCG, atorvastatin and tocopherols, , or AIN-93M control diet plus myo-inositol in drinking fluid. The mice were maintained at room temperature ( $20 \pm 2$  °C) with a relative humidity of  $50 \pm 10\%$  and with an alternating 12 h light/dark cycle. All animals were kept in non-sterile rooms of the animal facility in the Department of

Chemical Biology at Rutgers, The State University of New Jersey (Piscataway, NJ) and all animal studies complied with the animal protocol (Protocol No. 91-024) approved by the Animal Care and Facilities Committee of Rutgers, the State University of New Jersey. Body weight, food consumption, and general health status were monitored weekly.

In the short-term experiment investigating the molecular alterations in lung tissues following NNK administration, the mice were treated with a single dose of NNK (100 mg/kg body weight, i.p.) or saline on day 0 and euthanized and sacrificed at days 1, 3, 7 and 14 afterwards. The lungs of each animal were removed, then either fixed in 10% buffered formalin, frozen at  $-80^{\circ}\text{C}$  directly, or stored in RNAlater solution (Qiagen, Valencia, CA). For the EGCG treated group, EGCG (0.5% in diet) was administrated starting one week before NNK treatment.

To study the progression of NNK-induced lung tumorigenesis, the mice were given two weekly doses of NNK (100 and 75 mg/kg body weight, i.p., respectively) or saline. Animals were euthanized and sacrificed at weeks 4, 9, 14 and 19 after the first dose of NNK treatment. Visible tumors ( $>0.1$  mm in diameter), if observed, in the lungs were counted and the sizes were measured under a dissecting microscope. Tumor volume ( $\text{mm}^3$ ) was measured using the formula  $V = 4/3 \pi r^3$ , where  $V$  is tumor volume and  $r$  is the radius of the tumor determined by the mean values of the longest and shortest diameters. The lungs of each animal were removed, then either fixed in 10% buffered formalin, frozen at  $-80^{\circ}\text{C}$  directly, or stored in RNAlater solution (Qiagen) or HistoPrep solution (Qiagen). Blood was collected by cardiac puncture and centrifuged for 15 min at 3000 g for the preparation of serum. Liver and spleen were also removed, weighed and examined for any abnormalities and then fixed in 10% buffered formalin. The frozen tissues were stored at

-80°C, and the formalin-fixed tissues were processed, embedded in paraffin, sectioned and mounted onto glass slides for analysis.

In the study of inhibitory effects of chemopreventive agents, animals were fed the AIN-93M control diet or AIN-93M diet supplemented with EGCG, atorvastatin, tocopherols and myo-inositol (in drinking fluid), alone or in combination. One week after feeding with control diet or diet supplemented with chemopreventive agents, the mice were given two weekly doses of NNK (100 and 75 mg/kg body weight, i.p., respectively) or saline. The mice were euthanized and sacrificed 19 weeks after the first dose of NNK treatment. Visible tumors (>0.1 mm in diameter), if observed, in the lungs were counted and the sizes were measured under a dissecting microscope. The lungs of each animal were removed, then either fixed in 10% buffered formalin or frozen at -80°C directly. Blood was collected by cardiac puncture and centrifuged for 15 min at 3000 g for the preparation of serum. Liver and spleen were also removed, weighed and examined for any abnormalities and then fixed in 10% buffered formalin. The frozen tissues were stored at -80°C, and the formalin-fixed tissues were processed, embedded in paraffin, sectioned and mounted onto glass slides for analysis.

To study the mechanisms of different chemopreventive agents, animals fed with AIN-93M control diet were given two weekly doses of NNK (100 and 75 mg/kg body weight, i.p., respectively) or saline. In one set of experiment, nineteen weeks after the first dose of NNK treatment (week-20), animals were i.p. injected daily with saline for 5 days or with EGCG (30 mg/kg body weight) for 2 and 5 days. In another set of experiment, nineteen weeks after NNK treatment, animals were fed AIN-93M control diet or AIN-93M diet supplemented with 0.4% EGCG or 0.3%  $\gamma$ -TmT for 7 days and then sacrificed. In both

experiments, the lungs of each animal were removed, then either fixed in 10% buffered formalin or frozen at  $-80^{\circ}\text{C}$  directly. Blood was collected by cardiac puncture and centrifuged for 15 min at 3000 g for the preparation of serum. Liver and spleen were also removed, weighed and examined for any abnormalities and then fixed in 10% buffered formalin. The frozen tissues were stored at  $-80^{\circ}\text{C}$ , and the formalin-fixed tissues were processed, embedded in paraffin, sectioned and mounted onto glass slides for analysis.

In the CL-13 mouse lung cancer cell allograft study, animals were fed the AIN-93M control diet, AIN-93M diet supplemented with 0.5% EGCG, 0.3%  $\delta$ -tocopherol and 1% myo-inositol (in drinking fluid) plus 0.17%  $\delta$ -tocopherol in the diet, or AIN-93M control diet plus 2% myo-inositol in drinking fluid. After one week of feeding with experimental diet, each mouse was inoculated subcutaneous with CL-13 cells ( $1 \times 10^6$  cells in 100  $\mu\text{L}$  PBS) on both rear flanks. Body weight and food consumption were determined weekly. Tumor size were measured twice per week by a caliper and calculated using the formula  $V = (L \times W^2)/2$ , where  $V$  is the tumor volume,  $L$  is the longest and  $W$  is the shortest tumor dimension. The animals were sacrificed by  $\text{CO}_2$  asphyxiation when the average tumor volume in the control group reached approximately  $1.0 \text{ cm}^3$  (day-49). Tumors were dissected and tumor weights were measured. Half of the tumor was fixed in 10% buffered formalin for immunohistochemistry analysis and the other half was snap frozen for biochemical analysis. The liver, lung, kidney and serum samples were collected.

### **C. Immunohistochemistry**

Immunohistochemistry was performed on lung tissue sections using specific antibodies to detect the localization and to quantify the levels of the positive staining.

Deparaffinized sections were unmasked in antigen-unmasking solution (DAKO, Copenhagen, Denmark) in a microwave oven for antigen retrieval. Endogenous peroxidase was quenched with 3% H<sub>2</sub>O<sub>2</sub>. Non-specific bindings were blocked by 3% serum for 1 h at room temperature. The slides were stained with the primary antibody overnight at 4°C, biotin-conjugated secondary antibody (1:200) for 45 min at room temperature, and avidin-biotin peroxidase complex (1:100) for 45 min at room temperature. Diaminobenzidine (Sigma-Aldrich) was used as a chromogen. Negative controls were processed in the absence of the primary antibody. Antibodies against DNMT1 (1:200; Abcam, Cambridge, MA), p-AKT (1:200; Cell Signaling, Danvers, MA),  $\gamma$ -H2AX (1:400; Cell Signaling), O<sup>6</sup>-methylguanine (1:200; Cell Signaling), COX-2 (1:400; Cayman Chemicals, Ann Arbor, MI), SOD (1:400; Cell Signaling), catalase (1:500; Abcam), cleaved caspase-3 (1:200; Cell Signaling), p-c-Jun (1:200; Cell Signaling), Nrf2 (1:500; Abcam), glutathione peroxidase (1:200; Cell Signaling) and heme oxygenase-1 (1:200; Cell Signaling) were used for the analyses. Negative controls were processed in the absence of the primary antibody. For each slide, 5 representative  $\times 200$  power photomicrographs were taken and these images were quantified for positive-stained cells and total number of cells using the ImagePro Plus Image Processing System (Media Cybernetics, Silver Spring, MD).

#### **D. Western Blot Analysis**

For animal tissues, Lung tissue and tumor extracts were prepared using Omni Bead Ruptor 24 (Omni International, Kennesaw, GA) in T-Per tissue extraction buffer (Pierce, Rockford, IL) supplemented with phosphatase inhibitors (1:100, Sigma-Aldrich) and

protease inhibitor cocktails (1:100, Sigma-Aldrich). For lung cancer cell lines, following the treatments with different chemopreventive agents, cells were lysed in RIPA lysis buffer (Boston BioProducts, Ashland, MA) supplemented with phosphatase inhibitors (1:100, Sigma-Aldrich) and protease inhibitor cocktails (1:100, Sigma-Aldrich) and scraped from cell culture dishes. Tissue extracts and cell lysates were centrifuged at 14,000 rpm for 10 min. The protein concentration was determined by BCA reagent kit (Pierce, Rockford, IL). Tissue extracts and cell lysates were denatured at 95°C for 5 min in Laemmli sample buffer and the protein samples were then loaded into SDS-PAGE gels and run under 80 V for 2-3 h. The proteins in the gels were then electro-transferred onto pure nitrocellulose membrane (Bio-Rad, Hercules, CA) under 25 V overnight or 100V for 90 min. The proteins on the membranes were subsequently blocked with Commercial Li-Cor Blocking Buffer (Li-Cor Biotechnologies, Lincoln, NE) for 1 h at room temperature. The membranes were blotted with primary antibodies overnight at 4°C, respectively. After washing with TBS-T for 3 times, the membranes were blotted with the fluorescence-conjugated secondary antibodies IRdye 800 or IRdye 680 (Li-Cor Biosciences) for 1 h at room temperature. The bands were detected by Odyssey® Infrared Imaging System (Li-Cor Biosciences). The primary antibodies against DNMT1, Nrf2 and catalase were from Abcam (Cambridge, MA); p-AKT, AKT,  $\gamma$ -H2AX, cleaved caspase-3, cleaved PARP, Mcl-1, Bcl-xL, Bcl-2, Bax, Bim, Bok, p-JNK, p-p38, Na<sup>+</sup>/K<sup>+</sup> ATPase, SOD, glutathione peroxidase, heme oxygenase-1 were from Cell Signaling (Danvers, MA); RhoA and k-Ras were from Santa Cruz Biotechnology (Santa Cruz, CA); and  $\beta$ -actin was from Sigma-Aldrich (St. Louis, MO).

## **E. DNA Methylation Analysis**

Genomic DNA was extracted from NNK-induced lung tumors and its matching normal-appearing lung tissue from 2 mice using AllPrep DNA/RNA Mini Kit (Qiagen). These DNA samples (2 tumors and 2 matching controls) were used for the methylation-sensitive, methylation-dependent and double restriction digestions using EpiTect Methyl DNA Restriction Kit (Qiagen) according to the manufacturer's protocol. The digested products were then used for qPCR to analyze the DNA methylation of 24 mouse lung cancer signature genes in the Mouse Lung Cancer DNA Methylation PCR Array (Qiagen). The real-time PCR was run on ABI 7900 HT Fast Real Time PCR system (Life Technologies, Beverly, MA) according to the manufacturer recommended protocol using POWER SYBR Green PCR Master Mix (Life Technologies). The methylation status of the 24 signature genes was determined by analyzing the qPCR result with Data Analysis templates available on Qiagen/SABioscience website.

To quantify the level of DNA methylation in our NNK-treated lung tissues and NNK-induced tumors, a modified methylation-sensitive, restriction enzyme-based quantitative PCR method was used [259, 260]. In brief, genomic DNA was extracted from NNK-induced lung tumors or from lung tissues at days 0, 1, 3 and 14 after NNK treatment and subjected to digestion by methylation-sensitive HpaII and methylation-insensitive Isoschizomer MspI (New England Biolabs, Beverly, MA). Typically, 0.125  $\mu$ g of DNA was incubated with 10 units of restriction enzyme in a 30  $\mu$ l final reaction volume for 6 h according to the manufacturer's suggested conditions. Real-time PCR reactions were carried out in the ABI 7900 system using POWER SYBR Green PCR Master Mix and specific primer set that brackets 2-4 HpaII/MspI recognition sites for each gene [Cdh13:



At different time points (0, 0.5, 1.5, 3, 8 and 16 h) after EGCG was put in, RPMI-1640 culture media were taken and immediately analyzed for the amount of hydrogen peroxide formed using an Amplex Red Hydrogen Peroxide assay kit (Molecular Probes, Eugene, OR).

### **G. Cell Culture and Cell Viability Assay**

Mouse lung adenocarcinoma cell line CL-13 was generously provided by Dr. Steven A. Belinsky (Lovelace Respiratory Research Institute, Albuquerque, NM). Conditionally immortalized mouse clara cell line C22 and immortal differentiated mouse type II alveolar cell line T7 were provided by Dr. Hong Wang (Rutgers, The State University of New Jersey, Piscataway, NJ). Human non-small-cell lung cancer-derived cell line H1299, human lung carcinoma-derived cell line A549 and human lung cancer-derived cell line H460 were purchased from American Type Culture Collection (ATCC, Manassas, VA). CL-13 cells, H1299 cells and A549 cells were maintained in RPMI-1640 medium (Mediatech Inc., Herndon, VA) supplemented with 10% fetal bovin serum. H460 cells, C22 cells and T7 cells were maintained in DMEM medium (Mediatech Inc.) supplemented with 10% fetal bovin serum. All cell lines were maintained in 5% CO<sub>2</sub> humidified atmosphere at 37°C. Cells used for treatment experiments were at 70-80% confluence that was achieved usually 24-48 h after plating. For chemopreventive agents treatment, EGCG and myo-inositol were dissolved in double-deionized sterilized water and atorvastatin and  $\gamma$ -TmT were dissolved in dimethyl sulfoxide. The final concentration of dimethyl sulfoxide in all experiments was less than or equal to 0.2%.

In the studies investigating the ROS effect of EGCG, the cells were incubated with different concentrations of EGCG in the fresh serum-free RPMI-1640 or DMEM medium in the presence or absence of SOD (5 unit/mL) and catalase (30 unit/mL) for 24 or 48 h at 37°C. In the combinational treatment studies investigating the possible synergistic effect between different chemopreventive agents (EGCG, atorvastatin,  $\gamma$ -TmT or myo-inositol, alone or in combination), SOD (5 unit/mL) and catalase (30 unit/mL) were always added into the culture media whenever EGCG is included in the treatment. Cells were seeded into 96-well plates at 1000-2500 cells/well and allowed to attach overnight. Following chemopreventive agents treatment for 24 or 48 h, the medium was replaced with fresh medium containing 0.5 mg/mL 3-(4,5-dimethylthiazole-2-yl)-2,5-diphenyltetrazolium bromide (MTT, Sigma-Aldrich) and incubated with the cells at 37°C for 2 h, and the formazan dye formed is solubilized by dimethyl sulfoxide. After gentle mixing, the absorbance was monitored at 550 nm using a plate reader (TECAN, Phoenix Research Products, Candler, NC). The comparison between the treated and control groups was expressed as the percentage of viable cells.

#### **H. Cell Cytosolic and Cytoplasm Membrane Fraction Preparation**

After cell harvest, cells were resuspended in membrane preparation buffer (10 mM Tris-HCl, pH 7.5, 1 mM EDTA, 1 mM EGTA, 0.1 mM dithiothreitol supplemented with phosphatase inhibitors and protease inhibitor cocktails). Cells were sonicated on ice for 5 sec each time for 4 times, and then centrifuged at 4 °C, 25,000 g for 1 h. The supernatant was collected as the cytosolic fraction. The pellet was washed once with membrane preparation buffer, solubilized with RIPA lysis buffer (Boston BioProducts) containing

phosphatase inhibitors and protease inhibitor cocktails and put on ice for 30 min after thorough mixing. The dissolved membrane protein remained in the supernatant were collected after centrifugation at 4 C, 10,000 g for 10 min.

### **I. Sphere Formation Assay**

Bone marrow-derived myofibroblasts were generated from gastric dysplastic tissues of IL-1 $\beta$  transgenic mice [262]. Bay 11-7082, an NF $\kappa$ B inhibitor, and JSI-124, a STAT3 inhibitor, were purchased from Sigma-Aldrich. Stem cell medium was a modified RPMI-1640 medium supplemented with basic fibroblast growth factor (bFGF; 10 ng/mL), epidermal growth factor (EGF; 20 ng/mL) and 0.1% bovine serum album [263]. A549 human lung cancer cells ( $1 \times 10^4$ /well) were cultured alone or co-cultured together with bone marrow-derived myofibroblasts ( $2 \times 10^4$ /well) in 2 mL of stem cell medium in a 6-well plate for 2 weeks. Spheres were recognized as cell colonies showing a 3-dimensional structure and blurred cell margin. The ratio of the sphere was calculated as the percentage of sphere number to the total colony number.

### **J. Enzyme-lined Immunosorbent Assay (ELISA) for mouse IL-6**

H1299 xenograft-derived cancer-associated fibroblasts were fibroblasts isolated by our laboratory from xenografts of H1299 cells subcutaneously injected on rear flanks of the athymic nude mice. H1299 human lung cancer cells ( $1 \times 10^5$ /well) were cultured alone or co-cultured together with bone marrow-derived myofibroblasts ( $1 \times 10^5$ /well) or H1299 xenograft-derived cancer-associated fibroblasts ( $1 \times 10^5$ /well) in 2 mL of RMPI 1640 medium supplemented with 10% fetal bovine serum in a 6-well plate for 48 hours.

The culture media were then collected for ELISA. Mouse interleukin-6 (IL-6) was quantified using mouse quantitative ELISA kits according to the manufacturer's instructions (R&D System, Minneapolis, MN).

### **K. Statistical Analysis**

Two-tailed Student's *t*-test was used for simple comparisons between two groups. Statistical significance was indicated by \* ( $P < 0.05$ ) and † ( $P < 0.01$ ). One-way analysis of variance (ANOVA) followed by Turkey's post-hoc test was used for comparisons among multiple groups. The interaction between different chemopreventive agents in cell culture studies was analyzed by the method of Chou and Talalay using CompuSyn program [264]. The combination index was used to determine whether the interaction was synergistic, additive, or antagonistic as well as the degree of synergism and antagonism. All data was presented as mean  $\pm$  SD or mean  $\pm$  SE.

## V. RESULTS

### **A. NNK-induced DNMT1 Elevation and Related Molecular Alterations in Lung Tissues Following NNK Administration and during the Progression of NNK-induced Lung Tumorigenesis and the Inhibitory Effect of EGCG**

#### **A.1. Effect of NNK Treatment on Animal Conditions**

In the 14-day short-term NNK treatment experiment, female A/J mice were fed with AIN-93M rodent diet or AIN-93M rodent diet supplemented with 0.5% (-)-epigallocatechin-3-gallate (EGCG) one week before a single dose of NNK treatment by intraperitoneal (i.p.) injection (100 mg/kg body weight) (Figure 2A). All mice from the NNK treatment groups survived the NNK treatment until the respective termination time points of each group. No significant body weight difference was found between NNK-treated and saline control group at day 1 after NNK administration. However, body weights between NNK-treated and saline control groups at days 3, 7 and 14 after NNK administration were significantly reduced by 0.7, 2.0 and 2.1 g, respectively ( $P < 0.05$ ). No significant difference in body weight was found between mice fed with the control diet or the diet supplemented with EGCG. No significant differences in food and fluid consumption were found between NNK-treated and saline control groups as well as between EGCG and control diet groups.

To study the progression of NNK-induced lung tumorigenesis, the mice were given two weekly doses of NNK (100 and 75 mg/kg body weight, i.p., respectively) (Figure 2B). There were 8 mice in each NNK-treated group and 2 mice in each saline control group. One mouse from the saline control group died before the termination of the experiment,

which did not appear to be related to saline treatment. During the 20-week experimental period, no significant differences were found between NNK-treated and saline control groups in body weight, food consumption and fluid intake. No signs of toxicity or differences in liver weight were found in any NNK- or saline-treated mice.

### **A.2. Progression of NNK-induced Lung Tumorigenesis**

Lung tumors occurred starting from week 10 after NNK treatment, with a tumor incidence of 12.5% (1/8; Table 1). The incidence of lung tumor increased to 100% at weeks 15 (8/8) and 20 (8/8). In control mice that received saline, no tumor was found. The tumors were diagnosed as lung adenomas based on our previous criteria [265]. Lung adenomas were in a solid, papillary or mixed growth pattern and were generally composed of well-differentiated cells. The total number of tumors/mouse was 2 at week 10, but increased to  $12.0 \pm 0.76$  and  $15.9 \pm 1.36$  at weeks 15 and 20, respectively. Along the progression of NNK-induced lung tumorigenesis, tumor size was also increased as the total tumor volume/mouse increased from 0.58 at week 10 to  $2.27 \pm 0.31$  and  $3.42 \pm 0.39$  mm<sup>3</sup>/mouse at weeks 15 and 20, respectively (Table 1).

### **A.3. Induction of DNMT1 in the Lung by NNK Treatment and the Inhibitory Effect of EGCG**

In order to study the effect of NNK on the DNMT1 protein level in lung tissues following NNK administration, female A/J mice were treated with one dose of NNK (100 mg/kg body weight, i.p.). Mice were sacrificed at days 1, 3, 7 and 14 after the NNK treatment, and the DNMT1 protein level was determined by immunohistochemistry using

an anti-DNMT1 antibody (1:200). Strong positive nuclear and cytoplasmic staining was observed in bronchial epithelial cells of the mouse lung in all NNK-treated groups at days 1, 3 and 14 after NNK treatment (Figure 3A). Quantification of DNMT1-positive cells showed that the protein levels of DNMT1 were elevated significantly in bronchial epithelial cells at days 1, 3 and 14 after NNK treatment. The percentage of cells with positive nuclear staining for DNMT1 increased to 77.9%, 88.7% and 71.3%, respectively, from 4.4% (that was found in saline control samples) ( $P < 0.01$ ; Figure 3B). The elevated levels of DNMT1 in lung tissues at days 1, 3, 7 and 14 were also verified by Western blot analysis, showing increases by 11-, 14-, 9- and 7-fold, respectively, compared to the saline control group ( $P < 0.05$ ; Figure 3C and 3D).

The possible inhibitory effect of EGCG on NNK-induced DNMT1 elevation was also studied by immunohistochemistry. Compared to the NNK-treated groups, significantly fewer positive nuclear staining and much less intensive cytoplasmic staining was observed in bronchial epithelial cells of the mouse lung in all EGCG-treated groups (Figure 3A). Quantification of the DNMT1-positive cells showed that the elevation of DNMT1 proteins at days 1, 3 and 14 was significantly attenuated by dietary EGCG treatment (by 70.0%, 54.5% and 25.0%, respectively,  $P < 0.05$ ; Figure 3B).

We also examined the DNMT1 protein level in alveolar cells of the mouse lung by immunohistochemistry. However, no change was observed between any NNK-treated group and the saline control group, or between any EGCG-treated group and NNK-treated group. The protein levels of the other two members of the DNMT family, DNMT3a and DNMT3b, were also examined by immunohistochemistry with anti-DNMT3a (1:200) and

DNMT3b (1:200) antibodies, respectively. However, no positive staining in bronchial epithelial or alveolar cells of the mouse lung was observed in any group.

#### **A.4. NNK-induced DNMT1 Elevation through AKT Phosphorylation and the Inhibitory Effect of EGCG**

The activation/phosphorylation of AKT has been reported to stabilize DNMT1 at the protein level by inhibiting the ubiquitination of DNMT1 [266]. Since increased phospho-AKT (p-AKT) has been observed previously in both NNK-treated lung cancer cells and NNK-induced mouse lung tumors [84], we reasoned that our presently observed DNMT1 elevation in lung tissues at such an early stage was also resulted from the activation of AKT. We examined the p-AKT level by immunohistochemistry with anti-p-AKT antibody (1:200). Indeed, quantification of the cytosolic p-AKT staining intensity showed that the p-AKT levels in bronchial epithelial cells of NNK-treated mice were significantly higher at days 1 and 3 after NNK treatment; the percentage of the total area that stained for p-AKT increased to 67.5% and 44.8%, respectively, from 11.4% (saline control group,  $P < 0.05$ ; Figure 4B). The level of p-AKT also appeared to be induced by NNK at day 14, but the change was not statistically significant based on the analysis by two-tailed Student's *t*-test. The induction of p-AKT in lung tissues at days 1, 3 and 14 was also verified by Western blot analysis showing increases by 6-, 8- and 4-fold, respectively ( $P < 0.05$ ; Figure 4C and 4D); whereas, the total AKT protein level was not changed by NNK treatment (Figure 4C).

The possible inhibitory effect of EGCG on NNK-induced AKT phosphorylation was also studied by immunohistochemistry. A significantly reduced p-AKT staining intensity

was observed in bronchial epithelial cells of the mouse lung in EGCG-treated groups at days 1 and 3 after NNK treatment, compared to the NNK-treated groups at the same time points (Figure 4A). The percentage of the total area that stained for p-AKT at days 1 and 3 after NNK treatment were markedly reduced by EGCG (by 71.9% and 49.8%, respectively,  $P < 0.01$ ; Figure 4B). The level of p-AKT in alveolar cells of the mouse lung was also assessed by immunohistochemistry. However, no change was observed between any NNK-treated group and the saline control group, or between any EGCG-treated group and NNK-treated group.

In order to determine whether the elevated level of DNMT1 resulted from an increase in the transcription of DNMT1, we determined the mRNA levels of DNMT1 by qPCR (Figure 3E). No significant change on DNMT1 mRNA level was found at days 0, 1 and 3, suggesting that the up-regulation of DNMT1 is not at the mRNA level (Figure 3F). It is highly likely that the elevation of DNMT1 is through DNMT1 protein stabilization induced by p-AKT.

#### **A.5. Induction of $\gamma$ -H2AX, O<sup>6</sup>-methylguanine and Cleaved Caspase-3 in the Lung by NNK Treatment and the Inhibitory Effects of EGCG**

To assess the DNA damage induced by NNK, we determined the formation of  $\gamma$ -H2AX foci, an early event of DNA double-strand breaks, by immunohistochemistry with anti- $\gamma$ -H2AX antibody (1:200). Strong positive nuclear staining was observed in bronchial epithelial cells of the mouse lung in all NNK-treated groups at days 1, 3 and 14 after NNK treatment (Figure 5A). By contrast, no positive nuclear or cytoplasmic staining was observed in the saline control groups (Figure 5A). NNK treatment was found to markedly induce  $\gamma$ -H2AX formation in bronchial epithelial cells by the quantification of

$\gamma$ -H2AX-positive cells; the percentage of cells with positive nuclear staining for  $\gamma$ -H2AX increased to 79.3%, 42.8% and 12.3% on days 1, 3 and 14, respectively, from 0% (saline control group,  $P < 0.01$ ; Figure 5B). This immunohistochemistry result was also found to be consistent with a 4-fold increase of  $\gamma$ -H2AX protein level in lung tissues at days 1 and 3, compared to the saline control group ( $P < 0.05$ ), by Western blot analysis (Figure 5E and 5F).

The possible inhibitory effect of EGCG on NNK-induced  $\gamma$ -H2AX formation was also studied by immunohistochemistry. Markedly fewer positive nuclear staining was observed in bronchial epithelial cells of the mouse lung in all EGCG-treated groups, compared to NNK-treated groups at the same time points (Figure 5A). Quantification of the  $\gamma$ -H2AX-positive cells showed that the induction of  $\gamma$ -H2AX was significantly inhibited by EGCG at days 1, 3 and 14, showing reductions by 91.3%, 68.5% and 74.0%, respectively ( $P < 0.01$ ; Figure 5B).

O<sup>6</sup>-methylguanine, generated by carbenium ion or carbocation formed through the metabolic activation of NNK, has been shown to be critical in the initiation of NNK-induced lung tumorigenesis [267]. Measured by immunohistochemistry with an antibody against O<sup>6</sup>-methylguanine (1:200), higher levels of O<sup>6</sup>-methylguanine were detected in bronchial epithelial cells at days 1, 3 and 14 after NNK treatment (Figure 5C). The percentage of cells with positive nuclear staining for O<sup>6</sup>-methylguanine increased to 86.4%, 88.3% and 43.3%, respectively, from 3.5% (the saline controls,  $P < 0.01$ ; Figure 5D). However, in the samples from mice fed EGCG, the NNK-induced O<sup>6</sup>-methylguanine formation was only slightly decreased by EGCG, if any (not statistically significant). This result suggests that EGCG does not significantly affect the metabolic activation of NNK

and the inhibitory effects of EGCG on the induction of DNMT1 and p-AKT by NNK are due to other mechanisms.

To determine the possible induction of apoptosis by NNK, we examined cleaved caspase-3 level by Western blot analysis with anti-cleaved caspase-3 antibody (1:1000, Figure 5E). We found that cleaved caspase-3 was elevated in lung tissues by 9-fold at days 1 and 3 ( $P < 0.01$ ), and by 6-fold at days 7 ( $P = 0.08$ ) and 14 ( $P < 0.01$ ) (Figure 5F). Together with the  $\gamma$ -H2AX induction result, NNK treatment induces cell death possibly due to NNK-induced oxidative stress.

#### **A.6. Changes in DNMT1 Protein Levels during the Progression of NNK-induced Lung Tumorigenesis and the Inhibitory Effect of EGCG**

An up-regulation of DNMT1 has been reported in NNK-treated lung cancer cells and NNK-induced mouse lung tumors previously [84]. Our results demonstrated the elevation of DNMT1 in the first two weeks after NNK treatment (Figure 3). However, the levels of DNMT1 during the progression of NNK-induced lung tumorigenesis were not known. In order to determine whether the NNK-induced changes in DNMT1, p-AKT, and other proteins persist over time, we analyzed lung samples at weeks 5, 10, 15 and 20 after NNK treatment.

By investigating the levels of DNMT1 in lung tissues at weeks 5, 10, 15 and 20 after NNK treatment using both immunohistochemistry and Western blot analysis, we found that DNMT1 in bronchial epithelial cells at weeks 5 to 20 were elevated but lower than those observed in the first two weeks after NNK treatment (Figure 6A). The percentages of cells with positive nuclear staining for DNMT1 were 20-30% during weeks 5 to 20, which

is markedly higher than the 1.9% found in the saline controls at the same time points (Figure 6B). The percentage of DNMT1-positive cells in bronchial epithelial cells at week 20 was significantly decreased in the EGCG-treated group as compared to week-20 NNK control group (Figure 6B). Western blot analysis also confirmed that the levels of DNMT1 in NNK-treated groups at weeks 5 to 20 were much lower than the level on day 3, but still remained 3- to 7-fold higher than saline controls ( $P < 0.05$ ; Figure 6C and 6D). The induction of p-AKT,  $\gamma$ -H2AX and cleaved caspase-3 in lung tissues at weeks 5 to 20 dropped markedly from the day 3 level with p-AKT and cleaved caspase-3 remained at about 200% of the saline controls and  $\gamma$ -H2AX reduced to the level of the saline controls as determined by Western blot analysis (Figure 6C and 6D).

With the observed up-regulation of DNMT1 during the progression of NNK-induced lung tumorigenesis, we further determined whether similar events occurred in NNK-induced lung tumors harvested at week 20. In NNK-induced lung tumors, the level of DNMT1 was much higher than the level in lung tissues of saline-treated control mice (by 16-fold,  $P < 0.01$ ), and equivalent to the level in lung tissues at day 3 after NNK treatment (Figure 6C and 6D). The levels of p-AKT,  $\gamma$ -H2AX and cleaved caspase-3 were also significantly higher in NNK-induced lung tumors (6- to 7-fold higher than lung tissues of control mice,  $P < 0.05$ ) and similar to the levels found in day 3 samples (Figure 6C and 6D).

Together, the DNMT1 at weeks 5 to 20 were lower than that at days 1 to 14 after NNK administration, suggesting the possibility that this higher levels of DNMT1 during the progression of NNK-induced lung tumorigenesis (weeks 5 to 20) may represent the residue DNMT1 induced by NNK at the earlier stage.

### **A.7. Induction of DNMT1 in Human Lung Cancer, Mouse Epithelial and Alveolar Cells**

The elevation of DNMT1 was observed in bronchial epithelial cells within 2 weeks following NNK administration (Figure 3) and along the progression of NNK-induced lung tumorigenesis (5-20 weeks; Figure 6A and 6B). In addition, the elevation of DNMT1 was also observed in NNK-induced lung tumors (Figure 6C and 6D). To determine whether the elevation of DNMT1 by NNK treatment occurs in lung cancer cells and in immortalized bronchial epithelial or alveolar cells, we examined the levels of DNMT1 in H1299 human lung cancer cells, C22 mouse clara cells (a type of bronchial epithelial cells) and T7 mouse type II alveolar cells (a type of alveolar cells) by Western blot analysis (Figure 7). Treatment with different concentrations of NNK (1, 10, 100 and 500  $\mu$ M) increased the levels of DNMT1 in both H1299 and C22 cells dose-dependently. However, only marginal increase was observed in T7 cells, suggesting that H1299 and C22 cells are more responsive to NNK treatment as compared to T7 cells (Figure 7). This result is consistent with our findings in animals that the elevation of DNMT1 at days 1 to 14 following NNK administration and along the progression of lung tumorigenesis (weeks 5-20) was only observed in bronchial epithelial cells but not in alveolar cells.

### **A.8. Increase of Gene-specific Promoter Hypermethylation in NNK-induced Lung Tumors and NNK-treated Lung Tissues**

Promoter hypermethylation of several genes in NNK-induced lung tumors has been previously reported [100, 137-141]. In this study, we investigated whether gene-specific

promoter hypermethylation occurred in our NNK-induced lung tumors harvested at week 20. We used the mouse lung cancer EpiTect Methyl PCR array to measure 24 different tumor suppressor genes whose promoter CpG islands hypermethylation has been reported in a variety of human lung cancers. Out of the 24 different tumor suppressor genes we analyzed, the promoter methylation of *Cdh13*, *Rassf1* and *Prdm2* was significantly increased (by 200%, 200% and 150%, respectively;  $P < 0.05$ ) in lung tumor samples compared to the adjacent normal lung tissues (Figure 8A). No hypermethylation was detected in the lung samples from saline control group.

Further investigation using methylation-sensitive, restriction enzyme-based quantitative PCR confirmed the hypermethylation of *Cdh13* and *Prdm2* promoters (Figure 8B, *Rassf1* was not investigated). Besides that, a significant increase in promoter methylation of *Runx3* was also detected in lung tumor samples. While promoter hypermethylation of *Cdh13*, *Rassf1* and *Runx3* has been reported [139], *Prdm2* promoter hypermethylation is new in NNK-induced lung tumors.

To determine whether promoter hypermethylation of genes occurred in the first two weeks after NNK treatment, samples from days 1, 3 and 14 were analyzed using methylation-sensitive, restriction enzyme-based quantitative PCR. The results indicate there was a slight, non-significant change in promoter methylation of *Cdh13* and *Runx3* at day 1 after NNK treatment, compared to the control group (increased by 30% and 10%, respectively; Figure 8C). Interestingly, a significant increase in methylation was observed for *Cdh13* (6.4-fold), *Prdm2* (7.9-fold) and *Runx3* (3.6-fold) on day 3 (Figure 8C). On day 14, the level of methylation has decreased to approximately the baseline level of the control group. Similar results were observed in a repeated experiment, and the results indicate that

there was gene promoter hypermethylation associated with the induction of DNMT1 at day 3 after NNK treatment.

### **A.9. Increase of Global DNA Methylation in NNK-treated Lung Tissues**

With the observed increase in gene-specific hypermethylation in both NNK-induced lung tumors and NNK-treated lung tissues, we further determined the global DNA methylation level in NNK-treated lung tissues at days 1 and 3 after NNK treatment, using ultra-performance liquid chromatography-ion trap tandem mass spectrometry analysis as described previously [261]. The molar ratio of 5mdC/2dG in lung tissues, which reflects the global DNA methylation status, was significantly increased from  $7.63 \pm 0.16$  (day 0 saline-treated mice) to  $7.91 \pm 0.35$  (day 1,  $P = 0.14$ ) and  $7.91 \pm 0.17$  (day 3,  $P < 0.05$ ) from NNK-treated mice (Figure 8D). This increase of global DNA methylation coincides with the elevation of DNMT1 at day 3 after NNK treatment, suggesting that the elevated DNMT1 may have resulted in an increase of global DNA methylation.

### **A.10. Induction of COX-2 in the Lung by NNK Treatment**

Cyclooxygenase-2 (COX-2), a membrane-bound enzyme that catalyzes the formation of prostaglandins including prostaglandin E<sub>2</sub>, plays a key role in carcinogenesis and is overexpressed in various types of cancers including lung cancer [268], colon cancer [268, 269], breast cancer [270], and gastric cancer [271]. However, the level of COX-2 following carcinogen treatment in animal models has not been demonstrated previously. In this study, the level of COX-2 was determined by immunohistochemistry with anti-COX-2 antibody (1:400; Figure 9A). Quantification of the SOD staining intensity on microsome

and endoplasmic reticulum membranes showed that the levels of COX-2 in bronchial epithelial cells of NNK-treated mice were significantly higher at days 1, 3, 7 and 14 after NNK treatment; the percentage of the total area that stained for COX-2 increased to 58.4%, 58.6%, 55.2% and 49.2%, respectively, from 32.0% (saline control mice,  $P < 0.01$ ; Figure 9B).

#### **A.11. Induction of SOD and Catalase in the Lung by NNK Treatment**

The levels of antioxidant enzymes SOD and catalase were determined by immunohistochemistry with anti-SOD (1:400; Figure 10) and anti-catalase (1:500; Figure 11) antibodies. Quantification of the cytosolic SOD staining intensity showed that the levels of SOD in bronchial epithelial cells of NNK-treated mice were significantly higher at days 1, 3, 7 and 14 after NNK treatment; the percentage of the total area that stained for SOD increased to 46.2%, 63.3%, 48.1% and 45.3%, respectively, from 22.7% (saline control mice,  $P < 0.01$ ; Figure 10B).

Quantification of the peroxisomal staining intensity of catalase showed that the catalase levels in bronchial epithelial cells of NNK-treated mice were significantly higher at days 1, 3, 7 and 14 after NNK treatment; the percentage of the total area that stained for catalase increased to 73.2% ( $P < 0.01$ ), 78.6% ( $P < 0.01$ ), 54.2% ( $P < 0.05$ ) and 43.9% ( $P < 0.05$ ), respectively, from 26.3% (that was found in saline control samples; Figure 11B). The level of catalase tended to decrease by time during the 14-day experimental period as catalase level at day 14 was statistically different from days 1 and 3 ( $P < 0.05$ ), analyzed by one-way ANOVA followed by Turkey's post-hoc test. This result suggests that NNK

treatment can stimulate bronchial epithelial cells to express antioxidant enzymes combating the NNK-induced oxidative stress possibly from NNK metabolic activation.

## **B. Possible Mechanisms of Inhibition by EGCG in NNK-induced Lung Tumorigenesis and Lung Cancer Cell Growth**

### **B.1. Hydrogen Peroxide Formation by EGCG Auto-oxidation**

EGCG is known to be unstable in cell culture conditions. Our laboratory has demonstrated that EGCG is readily auto-oxidized in cell culture medium to produce superoxide, hydrogen peroxide, and perhaps other reactive oxygen species (ROS) [272, 273] (Figure 12). SOD and catalase were shown to stabilize EGCG in cell culture conditions and abolish the formation of hydrogen peroxide by EGCG auto-oxidation [274, 275]. In this study, we assessed the hydrogen peroxide formation by EGCG auto-oxidation in the presence or absence of SOD and catalase in cell culture medium. A significant level of hydrogen peroxide was formed immediately (0.5 h) after EGCG was put in RPMI-1640 culture medium and the formation of hydrogen peroxide mostly occurred within 2 h after EGCG was put in the cell culture medium (Figure 13). A continued increase of hydrogen peroxide formation was observed after the initial 2 h (for as long as 16 h). However, the rate of increase dropped dramatically after the initial 2 h. A dose-dependent increase in the formation of hydrogen peroxide by EGCG auto-oxidation was observed. The presence of SOD (5 unit/mL) and catalase (30 unit/mL) in cell culture medium completely abolished the formation of hydrogen peroxide (Figure 13).

## **B.2. Inhibitory Effects of EGCG on Lung Cancer Cell Growth in the Presence or Absence of SOD and Catalase**

In this study, we assessed the cell growth inhibitory effects of EGCG in the presence or absence of SOD and catalase by 3-(4,5-dimethylthiazole-2-yl)-2,5-diphenyltetrazolium bromide (MTT) assay in 4 different human and lung cancer cell lines, including CL-13 mouse lung cancer cells, and H1299, H460 and A549 human lung cancer cells. H1299 cells were treated with different concentrations of EGCG in serum-free medium for 24 h. As shown in Figure 14A and 14C, the numbers of viable H1299 cells were dose-dependently decreased by EGCG in the absence of SOD and catalase, showing an estimated  $IC_{50}$  of 21  $\mu$ M. The presence of SOD (5 unit/mL) and catalase (30 unit/mL) markedly attenuated the inhibitory effect of EGCG. Similar studies were also conducted with CL-13, H460 and A549 lung cancer cells. Among the 4 cell lines tested, CL-13 cells appeared to be the most susceptible to EGCG treatment with an estimated  $IC_{50}$  of 17  $\mu$ M (Figure 14B), which were followed by H1299 cells (estimated  $IC_{50}$  of 20  $\mu$ M; Figure 14C) and then H460 cells (estimated  $IC_{50}$  of 27  $\mu$ M; Figure 14D). The least responsive to EGCG treatment are A549 cells, showing an estimated  $IC_{50}$  of 42  $\mu$ M (Figure 14E). By adding SOD and catalase, the inhibitory activity of EGCG was also markedly attenuated in CL-13 cells. On the other hand, the attenuation effects of SOD and catalase on EGCG-induced cell growth inhibition were less pronounced in H460 and A549 cells, suggesting that EGCG-generated ROS may play a less important role in reducing the number of viable cells in H460 and A549 cells as compared to CL-13 and H1299 cells.

Since EGCG auto-oxidation mostly occurs within 2 h of exposure, we further investigated whether the cell growth inhibition of EGCG is mainly due to the cell killing

effects of ROS (hydrogen peroxide and superoxide) generated within the first 2 h or the following 22 h. We performed MTT assay in CL-13 and H1299 cells with a design shown in Figure 15A. As shown in Figure 15B, a 50% cell growth inhibition of that produced by a complete 24 h EGCG treatment (50  $\mu$ M) was observed when cells were treated with 50  $\mu$ M of EGCG for 2 h followed by 22 h incubation with fresh medium supplemented with SOD and catalase, suggesting that the ROS generated by EGCG over the first 2 h contributes about half of the cell killing effect of a complete 24 h EGCG treatment. On the other hand, treatment with 50  $\mu$ M of EGCG for 2 h followed by 22 h incubation with fresh medium caused a 95% cell growth inhibition of that produced by a complete 24 h EGCG treatment (50  $\mu$ M) in CL-13 cells, suggesting that either ROS generated by EGCG that is incorporated into the cells or mechanisms other than EGCG-generated ROS contribute the other half of the cell killing effect of a complete 24 h EGCG treatment.

Treatment with 50  $\mu$ M of EGCG supplemented with SOD and catalase for 2 h followed by the incubation of cells with fresh medium for 22 h caused a 70% cell growth inhibition of that produced by a complete 24 h EGCG treatment (50  $\mu$ M) in CL-13 cells. This cell growth inhibition is about 20% more as compared to that produced by 2 h EGCG treatment followed by 22 h incubation with fresh medium supplemented with SOD and catalase (50% inhibition). In another experiment, an 85% cell growth inhibition of that produced by a complete 24 h EGCG treatment (50  $\mu$ M) was observed when cells were treated with fresh media for 2 h followed by the incubation of cells with EGCG conditional media (2h) for 22 h. Both results suggest that even though the majority of the ROS is generated by EGCG within the first 2 h, ROS generated after the first 2 h still contribute about 20-35% of the cell killing effect of a complete 24 h EGCG treatment. In addition, the

above results are consistent with the results from our hydrogen peroxide formation assay (Figure 13) where the estimated hydrogen peroxide formed after the first 2 h contributed about 27% of the total hydrogen peroxide formed in a complete 24 h duration. In all experiments where SOD and catalase were completely supplemented during the 24 h experimental period, the cell killing effects of EGCG were all significantly attenuated. This result is also consistent with our findings in the hydrogen formation assay (Figure 13) where no hydrogen peroxide was formed from EGCG auto-oxidation when supplemented with SOD and catalase. Similar results were observed in H1299 cells (Figure 15C).

### **B.3. Induction of Cleaved Caspase-3 and Changes in the Levels of Apoptosis-related Bcl-2 Family Proteins by EGCG in Lung Cancer Cells**

In order to determine the time-dependent effects of EGCG on apoptosis and apoptosis-related Bcl-2 family proteins, H1299 cells were treated with 40  $\mu$ M of EGCG in the presence of SOD and catalase for 1, 2, 4, 6, 12, 24 and 48 h (Figure 16). Cleaved caspase-3 expression was not observed until 24 and 48 h after EGCG treatment, suggesting that EGCG induces apoptosis starting from 24 h after treatment to the cells. Time-dependent increases of Bax, Bim and Bok were observed by EGCG treatment starting from about 4-6 h after treatment to the cells. We also determined the anti-apoptotic Bcl-2 family proteins Mcl-1, Bcl-xL and Bcl-2 in a time-dependent experiment but EGCG treatment only had minimal effects on the levels of Mcl-1, Bcl-xL and Bcl-2. This result indicates that the EGCG induces apoptosis possibly through the up-regulation of pro-apoptotic Bcl-2 family proteins.

#### **B.4. Induction of $\gamma$ -H2AX by EGCG in Lung Cancer Cells in the Presence or Absence of SOD and Catalase**

In order to study the involvement of DNA damage in EGCG-induced cell growth inhibition in lung cancer cells, the levels of  $\gamma$ -H2AX were measured at 3, 12 and 24 h after EGCG treatment in the presence or absence of SOD and catalase in CL-13 cells by Western blot analysis (1:1000; Figure 17). When cells were incubated with 5 or 30  $\mu$ M of EGCG, a time-dependent and dose-dependent induction of  $\gamma$ -H2AX was observed. The induction of  $\gamma$ -H2AX was observed starting from 12 h time point and a higher level of  $\gamma$ -H2AX was observed for 24 h time point. SOD and catalase supplement only slightly reduced the formation of  $\gamma$ -H2AX at both 12 and 24 h after EGCG treatment, suggesting that the induction of  $\gamma$ -H2AX by EGCG treatment involves other mechanisms in addition to ROS effects generated by EGCG auto-oxidation.

#### **B.5. Induction of Cleaved Caspase-3 and $\gamma$ -H2AX, and Inhibition of p-c-Jun in NNK-induced Lung Tumors by Short-term EGCG Treatment at the Tumor Stage**

In order to study the mechanism of inhibition by EGCG in NNK-induced lung tumorigenesis, mice were treated with EGCG (30 mg/kg body weight daily i.p. injection for 5 days or 0.4% in the diet for 7 days) at the tumor stage (week-20). The levels of cleaved caspase-3,  $\gamma$ -H2AX and p-c-Jun were determined by immunohistochemistry using anti-cleaved caspase-3 (1:200), anti- $\gamma$ -H2AX (1:400) and anti-p-c-Jun (1:200) antibodies (Figure 18). Quantification of cleaved caspase-3-positive cells showed that the level of cleaved caspase-3 was significantly increased by EGCG treatment in NNK-induced lung tumors from EGCG-treated mice as compared to NNK control mice (Figure 18A). The percentage of cells with positive nuclear staining for cleaved caspase-3 was increased by

3.6-fold for EGCG-treated group as compared with NNK control group ( $P < 0.05$ ; Figure 18B). Quantification of  $\gamma$ -H2AX-positive cells showed that short-term EGCG treatment at the tumor stage markedly increased the level of  $\gamma$ -H2AX formation in NNK-induced lung tumors from EGCG-treated mice as compared to NNK control mice (Figure 18C). The percentage of cells with positive nuclear staining for  $\gamma$ -H2AX showed a 100% increase in EGCG-treated group as compared with NNK control group ( $P < 0.05$ ; Figure 18D). Quantification of p-c-Jun-positive cells showed that the level of p-c-Jun was significantly decreased by EGCG treatment in NNK-induced lung tumors from EGCG-treated mice as compared to NNK control mice (Figure 18E). The percentage of cells with positive nuclear staining for p-c-Jun was decreased by 62% in EGCG-treated group as compared with NNK control group ( $P < 0.05$ ; Figure 18F).

#### **B.6. EGCG Interrupts the Support of Cancer Cells from Stromal Microenvironment (Myofibroblasts)**

In order to study the interaction between cancer cells and its stromal microenvironment, A549 human lung cancer cells were cultured alone or co-cultured together with bone marrow-derived myofibroblasts in stem cell medium for 2 weeks. The light photomicrographs showed that under co-culturing condition, A549 cells form spheres with a 3-dimensional structure and blurred cell margin (Figure 19A). By contrast, when cultured alone, A549 cells are evenly distributed on the surface of cell culture dishes and spheres with 3-dimensional structure was not observed.

As shown in Figure 19B, Enzyme-linked Immunosorbent Assay (ELISA) results demonstrated that the mouse interleukin-6 (IL-6) levels in culture media were detected when mouse-originated bone marrow-derived myofibroblasts or H1299 xenograft-derived cancer-associated fibroblasts were present in the cell culture system, alone or co-cultured with human-originated A549 cells. In addition, co-culturing with A549 cells significantly increased the secretion of mouse IL-6 by bone marrow-derived myofibroblasts or H1299 xenograft-derived cancer-associated fibroblasts (by 12.2- or 3.6-fold, respectively,  $P < 0.01$ ; Figure 19B). This induction of mouse IL-6 secretion by bone marrow-derived myofibroblasts when co-cultured with A549 cells was dose-dependently inhibited by 25  $\mu\text{M}$  (by 34%,  $P < 0.05$ ) and 50  $\mu\text{M}$  (by 67%,  $P < 0.01$ ) of EGCG treatment in the absence of SOD and catalase (Figure 19C). In addition, supplement with SOD and catalase significantly attenuated this inhibitory effect of EGCG at both 25 and 50  $\mu\text{M}$  concentrations ( $P < 0.05$ ).

Similar dose-dependent inhibition of mouse IL-6 secretion was observed when cell culture media were supplemented with Bay 11-7082 (NF $\kappa$ B inhibitor, 2.5 and 5  $\mu\text{M}$ ), showing inhibitions of 52% and 71%, respectively ( $P < 0.05$  for the lower dose and  $P < 0.01$  for the higher dose; Figure 19D). The addition of JSI-124 (STAT3 inhibitor, 1 and 2  $\mu\text{M}$ ) to the cell culture media also inhibited mouse IL-6 secretion, showing inhibitions of 39% and 79%, respectively ( $P < 0.05$  for the lower dose and  $P < 0.01$  for the higher dose; Figure 19D).

## **C. Inhibitory Effects of EGCG, Tocopherols, Myo-inositol and Atorvastatin, Alone or in Combination, on NNK-induced Lung Tumorigenesis and the Growth of Allograft Tumors and Lung Cancer Cells**

### **C.1. Effects of Chemopreventive Agents on Animal Conditions**

One week before the first dose of two weekly NNK injections (100 and 75 mg/kg body weight, i.p., respectively), EGCG,  $\gamma$ -TmT, myo-inositol and atorvastatin, alone or in combination, were given to mice in the diet or in drinking fluid as described in Research Design Part (B.2.a and B.2.b.). The body weights of experimental animals were monitored weekly until the end of the experiment and shown in Figure 20. Final body weights of experimental animals at the end of the experiments were summarized in Table 2 and 3. There are 30 mice in each NNK-treated group and 10 mice in the saline control group. One mouse in the NNK control group and one mouse from atorvastatin-treated group died shortly after the first or second dose of NNK injection due to NNK toxicity. One mouse in the  $\gamma$ -TmT-treated group also died before the termination of the experiment, but not appeared to be related to  $\gamma$ -TmT treatment.

The NNK treatment caused a decrease in food consumption (by 16%, dropped from 2.5 to 2.1 g per mouse per day) and fluid intake (by 20%, dropped from 3.5 to 2.8 mL per mouse per day), which recovered one week after the second dose of NNK administration. During the rest of the 20-week experimental period, no significant differences in food or fluid consumption were found among groups. No difference in body weight was found between any NNK-treated group and the saline control group and between any chemopreventive agent-treated group and NNK-treated control group as analyzed by one-way ANOVA followed by Turkey's post-hoc test (Table 2 and 3). The body weights of

the mice in the EGCG-treated group were found different from all other chemopreventive agents-treated groups except for EGCG plus  $\gamma$ -TmT group in one experiment (Table 2). However, this body weight difference between EGCG-treated group and other chemopreventive agents-treated groups was not observed in another experiment (Table 3), suggesting that EGCG treatment may not be the key contributing to the observed body weight difference. No signs of toxicity or differences in liver weight were found among any groups were found as analyzed by one-way ANOVA followed by Turkey's post-hoc test.

In the CL-13 mouse lung cancer cell allografts experiment, five groups of mice were used. No significant differences in food consumption, fluid intake and body weight gain were observed for treatment groups as compared to the control diet group or among different treatment groups as analyzed by one-way ANOVA followed by Turkey's post-hoc test.

## **C.2. Inhibition of NNK-induced Lung Tumorigenesis by EGCG, $\gamma$ -TmT, Myo-inositol and Atorvastatin, Alone or in Combination**

Data on lung tumor incidence (%), total number of tumors/mouse and total tumor volume/mouse ( $\text{mm}^3$ ) is summarized in Table 2 and Table 3. Almost all (96%) NNK-treated mice developed lung tumors at the end of the 20-week experiment and the only chemopreventive agent that showed inhibitory effect on tumor incidence was myo-inositol (alone or in combination with EGCG or atorvastatin). No tumors were found in the saline control group. The tumors were diagnosed as lung adenomas based on our

previous criteria [276]. Lung adenomas were in a solid, papillary or mixed growth pattern and were generally composed of well-differentiated cells.

Interestingly, the total number of tumors/mouse was most significantly reduced by different concentrations (0.25%, 0.5%, 1% and 2%) of myo-inositol treatment, showing 68%, 73%, 82% and 80% inhibition, respectively ( $P < 0.01$ ). EGCG and  $\gamma$ -TmT treatment also significantly reduced the total number of tumors/mouse by about 18-21% and 14-18%, respectively ( $P < 0.05$ ). However, the inhibitory actions of EGCG or  $\gamma$ -TmT in reducing the total number of tumors/mouse were not as strong as myo-inositol. No synergistic interactions were found between myo-inositol and EGCG or atorvastatin, or between EGCG and  $\gamma$ -TmT, as analyzed by CompuSyn program.

Myo-inositol treatment at different concentrations (0.25%, 0.5%, 1% and 2%) also showed the strongest effects in reducing the total tumor volume/mouse (by 80%, 83%, 86% and 80%, respectively,  $P < 0.01$ ). EGCG treatment significantly reduced the total tumor volume/mouse by about 27-40% ( $P < 0.05$ ). However, the inhibitory effect of EGCG in reducing the total number of tumors/mouse was not as strong as myo-inositol.  $\gamma$ -TmT treatment also reduced the total tumor volume/mouse. However, the results were statistical significant in one experiment (Table 3) but not in another one (Table 2). Atorvastatin failed to inhibit NNK-induced lung tumorigenesis as no significant differences were found for both the total number of tumors/mouse and total tumor volume/mouse as compared to NNK-treated control group. In addition, we did not observe any synergy for the combination treatment between myo-inositol and EGCG or atorvastatin, or between EGCG and  $\gamma$ -TmT, based on the analysis using CompuSyn program.

### **C.3. Inhibitory Effects of EGCG, $\delta$ -Tocopherol and Myo-inositol, Alone or in Combination, on CL-13 Mouse Lung Cancer Cell Allografts**

The possible inhibitory effects of EGCG,  $\delta$ -tocopherol and myo-inositol, alone or in combination, on the growth of CL-13 mouse lung cancer allograft tumors were studied. EGCG,  $\delta$ -tocopherol, myo-inositol or  $\delta$ -tocopherol plus myo-inositol were given to A/J mice in the diet or in drinking fluid one week before the cancer cell implantation until the end of the experiment. Tumor size was monitored twice/week until the end of the experiment. Forty nine days after the cancer cell inoculation, mice were sacrificed and tumor weights were determined. As shown in Figure 21A, inhibitory effects were observed for all treatment groups during the 49-day experimental period. At the end of the experiment, the final tumor weights were significantly reduced in 0.5% EGCG, 0.3%  $\delta$ -tocopherol and 2% myo-inositol treatment groups (by 66%, 65% and 59%, respectively,  $P < 0.05$ ) as compared to the control group (Figure 21B). Among treatment groups with single chemopreventive agent, EGCG treatment showed the best effect on the growth inhibition of CL-13 allografts. In addition, 0.17%  $\delta$ -tocopherol plus 1% myo-inositol treatment led to a much more significant growth inhibition by showing a 77% inhibition ( $P < 0.01$ ) as compared to the 0.3%  $\delta$ -tocopherol treatment group or the 2% myo-inositol treatment group. Statistical analysis using ANOVA test demonstrated no difference between any of the treatment groups, indicating that there is no synergistic interaction between  $\delta$ -tocopherol and myo-inositol.

### **C.4. Induction of Antioxidant Enzymes by Short-term $\gamma$ -TmT Treatment in NNK-induced Lung Tumors**

Nuclear factor (erythroid-derived 2)-like 2 (Nrf2) is a transcription factor that plays a key role in the transcriptional regulation of antioxidant and detoxification genes to inhibit inflammation and protect against oxidative stress [240-242, 277]. Thus, we determined the levels of Nrf2 and antioxidant enzymes in NNK-induced lung tumors as compared to normal lung tissues of saline-treated control mice and the possible effects of  $\gamma$ -TmT and EGCG.

In NNK-induced lung tumors, the level of Nrf2 was significantly higher than the level in lung tissues of mice in the control group determined by immunohistochemistry ( $P < 0.05$ ; Figure 22A). Similar induction of Nrf2 was also observed in NNK-induced lung tumors as compared to lung tissues of saline-treated mice by Western blot analysis (Figure 22B). The possible effects of  $\gamma$ -TmT and EGCG on the elevation of Nrf2 in NNK-induced lung tumors were also studied by immunohistochemistry and Western blot analysis. The results from both immunohistochemistry and Western blot showed that  $\gamma$ -TmT and EGCG treatment only slightly reduced the level of Nrf2, if any, in  $\gamma$ -TmT- or EGCG-treated tumors as compared to tumors from NNK-treated control mice.

The levels of antioxidant enzymes including SOD, glutathione peroxidase, heme oxygenase-1 and catalase were determined by both immunohistochemistry and Western blot analysis. In NNK-induced lung tumors, the level of SOD was significantly higher than the level in lung tissues of mice in the control group determined by immunohistochemistry ( $P < 0.05$ ; Figure 22A). Similar induction of SOD was observed in NNK-induced lung tumors as compared to lung tissues of saline-treated mice by Western blot analysis (Figure 22B). The levels of glutathione peroxidase and heme oxygenase-1 were also higher than the levels in lung tissues in the control group determined by both immunohistochemistry

and Western blot analysis. However, the difference is not statistically significant based on the analysis by two-tailed Student's *t*-test. No change on the level of catalase was observed in NNK-induced lung tumors as compared to lung tissues of saline-treated mice.

Tocopherols are well-known for their direct antioxidant functions [278]. However, they may also serve as indirect antioxidants by activating antioxidant enzymes [279, 280]. In this study, treatment with  $\gamma$ -TmT significantly increased the levels of SOD ( $P < 0.01$ ) and glutathione peroxidase ( $P < 0.05$ ) determined by immunohistochemistry (Figure 22A). Similar increases in the levels of SOD and glutathione peroxidase were also observed by Western blot analysis (Figure 22B). No change on the levels of heme oxygenase-1 and catalase was observed in  $\gamma$ -TmT treated tumors as compared to tumors from NNK-treated control mice. EGCG treatment had no effect on the levels of SOD, glutathione peroxidase, heme oxygenase-1 and catalase. This result is consistent with our recent findings that the antioxidant and anti-inflammatory activities of tocopherols are independent of Nrf2 in mice [281].

### **C.5. Inhibition of p-c-Jun by Myo-inositol in NNK-induced Lung Tumors**

The levels of p-c-Jun were determined by immunohistochemistry using an anti-p-c-Jun (1:200) antibody (Figure 23). Quantification of p-c-Jun-positive cells showed that the level of p-c-Jun was significantly decreased by myo-inositol treatment in NNK-induced lung tumors from myo-inositol-treated mice as compared to NNK control mice (Figure 23A). The percentage of cells with positive nuclear staining for p-c-Jun was decreased by 64% in myo-inositol-treated group as compared with NNK control group ( $P < 0.05$ ; Figure 23B).

### **C.6. Synergistic Inhibition of Lung Cancer Cell Growth by a Combination of EGCG and Atorvastatin**

To study the possible synergistic interaction between EGCG and atorvastatin, we examined the cell growth inhibition by the combination treatment of EGCG and atorvastatin in a concentration-dependent manner in CL-13 mouse lung cancer cells (Figure 24) and H1299 human lung cancer cells (Figure 25). The concentrations of EGCG used were 3, 6, 12, 24 and 36  $\mu\text{M}$  in CL-13 cells and 5, 10, 20, 30 and 40  $\mu\text{M}$  in H1299 cells. The concentrations of atorvastatin used were one twelfth those of the EGCG in CL-13 cells and one tenth those of EGCG in H1299 cells. The ratio of EGCG and atorvastatin were determined experimentally based on the relative potency of the compounds in these two cell lines.

After 24 and 48 h of treatment, viable cells were measured using MTT assay. As shown in Figure 24A, dose-dependent inhibition was observed for EGCG, atorvastatin and their combination treatment in CL-13 cells at 48 h after treatment. The combination index plot generated by CompuSyn program demonstrated that the 3 higher dose pairs tested generated combination indices lower than 1.0, suggesting a synergistic interaction between EGCG and atorvastatin in the growth inhibition of CL-13 cells (Figure 24B). In addition, a trend for lower combination indices as the doses of the combination got higher was predicted. The degree of synergism between EGCG and atorvastatin in the growth inhibition of CL-13 cells was determined as “synergism” (Combination Index = 0.39; Figure 24C) based on the criteria for synergism and antagonism from CompuSyn program (Figure 24D). Similar results were observed at 24 h after treatment.

In H1299 cells, dose-dependent inhibition was also observed for EGCG, atorvastatin and their combination treatment at 48 h after treatment (Figure 25A). As shown in Figure 25B, the combination index plot generated by CompuSyn program demonstrated that the 2 higher dose pairs tested generated combination indices lower than 1.0, suggesting a synergistic interaction between EGCG and atorvastatin in the growth inhibition of H1299 cells. Furthermore, a trend for lower combination indices as the doses of the combination got higher was predicted. As shown in Figure 25C, the degree of synergism between EGCG and atorvastatin in the growth inhibition of H1299 cells was determined as “synergism” (Combination Index = 0.41) based on the criteria for synergism and antagonism in CompuSyn program (Figure 25D). Similar results were observed at 24 h after treatment.

#### **C.7. Effects of EGCG (or Polyphenon E, at EGCG equivalent concentration), Atorvastatin and Their Combination on the Levels of Apoptosis and Apoptosis-related Bcl-2 Family Proteins in Lung Cancer Cells**

The effects of EGCG (or Polyphenon E, at EGCG equivalent concentration), atorvastatin and their combination on apoptosis and apoptosis-related Bcl-2 family proteins were studied in H1299 cells by Western blot analysis with antibodies against cleaved caspase-3, cleaved caspase-9, cleaved PARP, Mcl-1, Bcl-xL, Bcl-2, Bax, Bim and Bok. To assess the time-dependent effects, H1299 cells were treated with EGCG (40  $\mu$ M, in the presence of SOD and catalase), atorvastatin (4  $\mu$ M) or their combination (10:1 ratio) for 1, 2, 4, 6, 12, 24 and 48 h. As shown in Figure 26A, cleaved caspase-3 expression was not observed until 24 and 48 h after EGCG, atorvastatin or their combination treatment. The combination treatment significantly increased the cleaved caspase-3 levels at both 24

and 48 h after treatment, compared to EGCG or atorvastatin treatment alone. In another experiment, H1299 cells were treated with EGCG (40  $\mu$ M, in the presence of SOD and catalase), Polyphenon E (40  $\mu$ M EGCG equivalent), atorvastatin (4  $\mu$ M), or their combination for 24 and 48 h. Atorvastatin treatment increased the level of cleaved caspase-9 and decreased the level of caspase-9 at 48 h after treatment, but EGCG or Polyphenon E treatment alone showed no effect on the levels of cleaved caspase-9 and caspase-9. Furthermore, a much stronger band was detected by the combination treatment of atorvastatin plus EGCG or atorvastatin plus Polyphenon E as compared to atorvastatin treatment alone (Figure 26B). Cleaved PARP, another marker for apoptosis, was also assessed. No significant increase was observed for cleaved PARP by atorvastatin, EGCG or Polyphenon E treatment alone at 24 and 48 h after treatment. However, a significant induction was observed by the combination treatment of atorvastatin plus EGCG or atorvastatin plus Polyphenon E at 48 h after treatment. The results on the levels of three apoptosis markers indicate a strong synergistic interaction between atorvastatin and EGCG (Polyphenon E) in apoptosis induction.

The levels of anti-apoptotic Bcl-2 family proteins Mcl-1, Bcl-xL and Bcl-2 were determined in 2 experiments. As shown in Figure 26B, the combination treatment of atorvastatin plus EGCG or atorvastatin plus Polyphenon E synergistically decreased the level of Mcl-1 at 48 h after treatment in H1299 cells as compared to atorvastatin, EGCG or Polyphenon E treatment alone. In the time-dependent study in H1299 cells, we confirmed that a strong synergistic interaction between atorvastatin and EGCG on decreasing the level of Mcl-1 was observed at both 24 and 48 h after treatment (Figure 27A). Similar synergistic interaction between atorvastatin and EGCG (Polyphenon E) in reducing the

levels of Bcl-xL and Bcl-2 were observed at 48 h after treatment in both experiments (Figure 26B, 27B and 27C). However, the synergistic interaction on the levels of Bcl-xL and Bcl-2 was much less as compared to that on Mcl-1, suggesting that Mcl-1 may be the key regulator in the induction of apoptosis caused by the combination treatment of atorvastatin and EGCG (Polyphenon E).

The levels of pro-apoptotic Bcl-2 family proteins Bax, Bim and Bok were also determined (Figure 28). Time-dependent increases of Bax (Figure 28A), Bim (Figure 28B) and Bok (Figure 28C) were observed by atorvastatin, EGCG and their combination treatment. However, synergistic interaction between atorvastatin and EGCG was only observed for Bok at 24 and 48 h after treatment (Figure 28C). In another experiment, synergistic interaction between atorvastatin and EGCG (Polyphenon E) was observed for Bax at 24 and 48 h after treatment (Figure 26B).

### **C.8. Counteraction of Atorvastatin-induced Cell Growth Inhibition by Key Intermediates of Cholesterol Synthesis Pathway**

Atorvastatin is known to inhibit HMG-CoA reductase and block the synthesis of mevalonate and subsequently, the synthesis of several isoprenoids, including farnesyl pyrophosphate and geranylgeranyl pyrophosphate (Figure 29) [237, 238]. We hypothesize that the growth inhibitory effect of atorvastatin, alone or in combination with EGCG, is mainly through the blockage of cholesterol synthesis pathway and its downstream signaling such as the isoprenylation of small G proteins RhoA and k-Ras. Therefore, we investigated whether the addition of different intermediates in the cholesterol synthesis

pathway, including mevalonate, farnesyl pyrophosphate and geranylgeranyl pyrophosphate, would counteract the growth inhibition by atorvastatin (Figure 30).

As measured by MTT assay, the addition of mevalonate and geranylgeranyl pyrophosphate eliminated the majority of the growth inhibitory effect of atorvastatin on CL-13 cells. The supplement of farnesyl pyrophosphate also partially attenuated the growth inhibitory effect of atorvastatin. However, the attenuation by farnesyl pyrophosphate is much less than mevalonate or geranylgeranyl pyrophosphate. This result suggests that geranylgeranyl pyrophosphate is important for cell growth; the addition of geranylgeranyl pyrophosphate eliminated most of the cell growth inhibition by atorvastatin and the addition of mevalonate restored the levels of both farnesyl pyrophosphate and geranylgeranyl pyrophosphate under atorvastatin treatment. However, the addition of farnesyl pyrophosphate could not restore geranylgeranyl pyrophosphate level because this restoration would require isopentenyl pyrophosphate, which was not available after mevalonate depletion caused by atorvastatin treatment (Figure 29). The partial attenuation of cell growth inhibition by the supplement of farnesyl pyrophosphate under atorvastatin treatment suggests that farnesyl pyrophosphate also contributes to cell growth.

### **C.9. Synergistic Inhibition of Lung Cancer Cell Growth by a Combination of Atorvastatin and $\gamma$ -TmT**

To study the possible synergistic interaction between atorvastatin and tocopherols, we examined the cell growth inhibition by the combination treatment of atorvastatin and  $\gamma$ -TmT at the ratio of 1:25 in CL-13 cells (Figure 31). After 24 and 48 h of treatment, viable cells were measured by MTT assay. Dose-dependent inhibition was observed for atorvastatin,  $\gamma$ -TmT and their combination treatment (Figure 31A). The combination index

plot generated by CompuSyn program showed that the 2 higher dose pairs tested resulted in combination indices lower than 1.0, suggesting a synergistic interaction between atorvastatin and  $\gamma$ -TmT in the growth inhibition of CL-13 cells (Figure 31B). Furthermore, a trend for lower combination indices as the doses of the combination got higher was predicted. As shown in Figure 31C, the degree of synergism between atorvastatin and  $\gamma$ -TmT in the growth inhibition of CL-13 cells was determined as “synergism” (Combination Index = 0.63; Figure 31C) based on the criteria for synergism and antagonism from CompuSyn program (Figure 31D). Similar results were observed at 24 h after treatment.

#### **C.10. Inhibition of Lung Cancer Cell Growth by a Combination of EGCG and Myo-inositol**

To study the possible synergistic interaction between EGCG and myo-inositol, we examined the cell growth inhibition by the combination treatment of EGCG and myo-inositol (1:1000 ratio) in a concentration-dependent manner in CL-13 cells (Figure 32). As shown in Figure 32A, dose-dependent inhibition was only observed for EGCG and the combination treatment. Surprisingly, no cell killing effect was observed for myo-inositol treatment even though the highest concentration of myo-inositol used reached 50 mM. This result is consistent with previous reports on the low toxicity of myo-inositol. The combination index plot generated by CompuSyn program demonstrated that all five dose pairs tested generated combination indices higher than or close to 1.0, suggesting that there is no synergistic interaction between EGCG and myo-inositol in the growth inhibition of CL-13 cells (Figure 32B). This is confirmed by the result of degree of

synergism generated by CompuSyn program, indicating a “moderate antagonism” between EGCG and myo-inositol in the growth inhibition of CL-13 cells (Combination Index = 1.29; Figure 32C).

## VI. DISCUSSION AND FUTURE DIRECTION

### **A. Elevation of DNMT1 through AKT Phosphorylation and Increase of Gene-specific Promoter Hypermethylation in NNK-treated Lung Tissues and NNK-induced Lung Tumors**

In the present study, we demonstrated the elevation of DNMT1 in bronchial epithelial cells of A/J mice at days 1 and 3 following NNK administration. To our knowledge, this is the first demonstration of the induction of DNMT1 by NNK in the first few days after administration, which may be related to NNK-induced oxidative stress and activation/phosphorylation of AKT. While the elevated level of DNMT1 decreased at weeks 5 to 20, the level was still significantly higher than the control group. In the lung tumors, the levels of both DNMT1 and p-AKT were highly elevated and comparable to those at day 3 following NNK administration.

Our results that DNMT1 mRNA levels were not significantly affected at days 1 and 3 suggest that the elevation of DNMT1 protein level was not due to increased transcription. We hypothesize that NNK treatment induces the phosphorylation of AKT to form p-AKT, which mediates DNMT1 protein stabilization, similar to recent reports in cell lines [84, 266]. Our result on the increase of p-AKT level in bronchial epithelial cells at days 1 and 3 after NNK treatment is consistent with the reported PI3K/AKT activation in bronchial epithelial cells and non-small-cell lung cancer cells by NNK treatment *in vitro* [283, 284], and the activation of PI3K/AKT pathway in normal and premalignant bronchial epithelial cells of smokers with airway lesions [285]. Another possible mechanism of NNK-induced

DNMT1 protein stabilization is through disrupting APC-mediated DNMT1 degradation as was demonstrated in breast and colon cancer cells [286].

The elevation of DNMT1 may be involved in the hypermethylation of genes such as *Cdh13*, *Prdm2*, *Rassf1* and *Runx3*. *CDH13* encodes H-cadherin, a membrane-bound member of the cadherin superfamily. *CDH13* has been found hypermethylated in many types of cancers. It was first identified silenced through promoter hypermethylation in human lung cancer in 1998 [287]. Subsequent findings further confirmed its hypermethylation in human lung cancer [288-292]. In animals, the hypermethylation of *Cdh13* has been shown to be associated with tumorigenicity of athymic nude mice xenograft tumors [293] and invasiveness of chemical-induced lung tumors [294]. We demonstrated herein, the promoter hypermethylation of *Cdh13* in NNK-induced lung tumors (Figure 8A and 8B), and in NNK-treated lung tissues at day 3 after a single dose of NNK administration (Figure 8C) by two different methods (EpiTect Methyl PCR array and Methylation-Sensitive, Restriction Enzyme-based quantitative PCR).

*PRDM2* is a tumor suppressor gene encoding a member of the histone/protein-methyltransferase superfamily which was involved in chromatin-mediated gene expression in cancer [295]. *PRDM2* functions as a tumor suppressor mainly through its methyltransferase activity [296]. In animals, it has been shown that knockout of *PRDM2* increased tumor susceptibility [297]. In humans, hypermethylation of *PRDM2* has been demonstrated in gastric, prostate, breast and thyroid cancers [298-301]. However, the only study relating lung cancer and the inactivation of *PRDM2* is a cell line study and the methylation status of *PRDM2* was not investigated [302]. The present study is the first demonstration showing the promoter hypermethylation of *Prdm2* in lung cancer animal

model and may serve as the start point for future studies investigating the involvement and mechanisms of *PRDM2* in human lung cancer.

*RASSF1* is a tumor suppressor gene encoding seven Ras-associated putative tumor suppressors through alternative splicing of its eight exons, designated RASSF1A-G. The inactivation of *RASSF1* through methylation was first described in human lung cancer in 2000 [303]. Since then, several studies have demonstrated the silencing of *RASSF1* through promoter hypermethylation in human lung cancer [304-307]. The functions of RASSF1 include regulation of apoptosis and cell growth, and overexpression of RASSF1 results in cell cycle arrest which is associated with dramatic changes in the expression of genes including cyclin D [308, 309]. The regulation of apoptosis by RASSF1 involves its binding to Bax-associated Modulator of Apoptosis 1 and subsequent initiation of caspase-dependent apoptosis when RASSF1 is overexpressed [310].

RUNX3, belonging to the Runt family of transcription factors, regulates cell growth, differentiation and apoptosis through the modulation of transforming growth factor- $\beta$  signaling [311]. *RUNX3* is a tumor suppressor gene and its tumor suppressive role has been demonstrated in gastric cancer [312]. The promoter hypermethylation of *RUNX3* in NNK-induced lung tumors has been demonstrated previously [313]. However, whether this occurs in lung tissues following NNK administration is unknown. In the present study, we confirmed the promoter hypermethylation of *RUNX3* in NNK-induced lung tumors (Figure 8B) and further demonstrated the methylation of *RUNX3* in lung tissues at day 3 after NNK treatment (Figure 8C).

Aberrant promoter hypermethylation of tumor suppressor genes occurs frequently in different types of cancers in humans and animals [115, 142-144]. The importance of

DNMT1 in cancer has been demonstrated in several recent publications [81-87, 314-321]. Furthermore, increased levels of DNMT1 and hypermethylation of multiple tumor suppressor genes have been reported in NNK-induced mouse lung tumors [100, 137-141]. Consistent with previous reports, our study detected the elevation of DNMT1 and gene promoter hypermethylation of tumor suppressor genes *Cdh13*, *Rassf1* and *Runx3* in NNK-induced lung tumors. In addition, we made the new finding that *Prdm2* is also hypermethylated in the lung tumors. Interestingly, we also observed the hypermethylation of *Cdh13*, *Prdm2* and *Runx3* at day 3 after NNK treatment, correlating with the elevation of DNMT1. To our knowledge, this is the first demonstration of the gene-specific promoter hypermethylation in lung tissues by NNK treatment in the first few days after administration. The close association between DNMT1 induction, gene promoter hypermethylation, and lung cancer suggests that the NNK-induced early stage DNMT1 elevation may play a crucial role in lung tumorigenesis, and this remains to be further investigated in future studies.

It would be interesting to test whether the gene hypermethylation status persists during the progression of NNK-induced lung tumorigenesis. Future studies on the promoter methylation status of *Cdh13*, *Prdm2*, *Rassf1*, *Runx3* and other key lung cancer related tumor suppressor genes using lung samples of NNK-treated mice terminated at weeks 5 to 20 may provide us information to clarify the epigenetic mechanism of NNK-induced lung tumorigenesis. Further more, it would be even more interesting to determine the possible inhibitory effects of EGCG and other dietary chemopreventive agents on the methylation status of tumor suppressor genes in lung tissues at weeks 5 to 20 in our future studies.

## **B. Induction of Oxidative Stress, Oxidative DNA Damage and Antioxidant Enzymes in Lung Tissues Following NNK Administration**

For NNK to exert its carcinogenic effect, it must be activated metabolically. There are three major routes of NNK metabolic activation: carbonyl reduction, pyridine N-oxidation and  $\alpha$ -hydroxylation [120]. During the metabolic activation of NNK, ROS were shown to be generated by our laboratory in 1995 [322]. The presently observed induction of oxidative DNA damage marker  $\gamma$ -H2AX at days 1 and 3 following NNK treatment may result from NNK-induced oxidative stress (Figure 5A and 5B). Time- and dose-dependent induction of  $\gamma$ -H2AX by tobacco-smoke condensate have been previously shown in A549 lung cancer cells and human bronchial epithelial cells [323].  $\gamma$ -H2AX formation is an early molecular event of DNA double-strand breaks. It is commonly used as a marker for oxidative DNA damage and its formation usually indicates the existence of ROS that cause the damage. Our results on the parallel induction and pattern of changes of  $\gamma$ -H2AX and p-AKT in bronchial epithelial cells at days 1, 3 and 14 suggest that AKT is phosphorylated in response to NNK-induced oxidative stress. On the other hand, there could be a functional link between  $\gamma$ -H2AX and DNMT1; for example, it has been reported that the recruitment of DNMT1 to DNA damage sites is for the maintenance of DNA methylation pattern in the newly synthesized DNA during the repair process [324, 325].

In order to combat oxidative stress, cells can express antioxidant enzymes including SOD, glutathione peroxidase, heme oxygenase-1 and catalase to quench the excess ROS. In the present study, we observed the elevation of SOD and catalase at days 1 to 14 after NNK treatment (Figure 10 and 11). The elevation of antioxidant enzymes indicates that

oxidative stress may exist in bronchial epithelial cells of the mouse lung at days 1 to 14 following NNK administration, which may result from the metabolic activation of NNK. The expression of antioxidant enzymes is regulated by transcription factor Nrf2. Further studies on the level of Nrf2 in bronchial epithelial cells of the mouse lung following NNK administration will be needed to determine whether Nrf2 is involved in the elevation of antioxidant enzymes in lung tissues to combat NNK-induced oxidative stress.

### **C. Inhibitory Effects of EGCG on NNK-induced DNMT1 Elevation, AKT Phosphorylation and Oxidative DNA Damage in NNK-treated Lung Tissues**

As reviewed previously, many mechanisms have been proposed for the inhibitory actions of EGCG against carcinogenesis [134]. Our laboratory and others have demonstrated the inhibition of DNMT1 activity and the reactivation of methylation silenced genes by EGCG in esophageal, colon, prostate and other cells *in vitro* [326-328]. The present study is the first study demonstrating the inhibitory effect of dietary EGCG on NNK-induced elevation of DNMT1 *in vivo*. Dietary EGCG treatment also reduced the expression of DNMT1 in lung tissues at week 20 and this reduction of DNMT1 proteins is associated with the reduction in total number of tumors/mouse and total tumor volume/mouse at week 20. It is interesting to propose that the attenuation of DNMT1 and promoter hypermethylation of tumor suppressor genes by EGCG contributed to the inhibition of lung tumorigenesis. Therefore, future studies on the level of DNMT1 and promoter methylation status in lung samples from EGCG-treated mice terminated at weeks 5 to 20 is needed to link the inhibitory activities of EGCG in NNK-treated lung tissues following administration and in NNK-induced lung tumors.

The activation/phosphorylation of c-Jun has been consistently reported in non-small-cell carcinomas in human studies [329, 330]. The AP-1 (c-Jun/c-Fos dimer) activity has been reported to be inhibited by tea constituents in several cell line studies [331-334]. Furthermore, our laboratory has demonstrated that the level of p-c-Jun increased during the progression from adenoma to adenocarcinoma and the inhibition of p-c-Jun at both adenoma and adenocarcinoma stages by tea polyphenols [131]. The present study demonstrated that lower level of p-c-Jun was observed in NNK-induced lung tumors when mice received daily EGCG by i.p. injection for 5 days at the tumor stage (30 mg/kg body weight; Figure 18E and 18F). A previous study showed that c-Jun can regulate DNMT1 expression through binding to three c-Jun-dependent enhancers binding site of human *DNMT1* gene [335]. Therefore, it is possible that the inhibitory activity of EGCG on the levels of DNMT1 in lung tissues following NNK administration and in NNK-induced lung tumors could be through the inhibition of AP-1 (c-Jun/c-Fos dimer) activity. Further studies are needed to validate this hypothesis.

Accompanying the inhibition of DNMT1 elevation in bronchial epithelial cells following NNK administration was the decrease of p-AKT and  $\gamma$ -H2AX levels by EGCG, but the level of O<sup>6</sup>-methylguanine was not significantly inhibited. The formation of O<sup>6</sup>-methylguanine is a result of the metabolic activation of NNK. Our results suggest that the inhibitory action of EGCG against the elevation of DNMT1, p-AKT and  $\gamma$ -H2AX is not due to its inhibition of the metabolic activation of NNK, but may be due to the anti-oxidative activities of EGCG.

It has been previously demonstrated that excess ROS present are critical in carcinogenesis. Furthermore, green tea constituents were shown to react with ROS such as

superoxide and hydrogen peroxide [145, 159, 160]. In humans, the administration of green tea decreased the level of 8-hydroxy-deoxyguanosine, an oxidative DNA damage marker, in the urinary of smokers, suggesting that green tea constituents could reduce oxidative stress in smokers [161]. The anti-oxidative properties of EGCG may be due to its polyphenolic structure. The trihydroxyl structures on the B and D rings and m-5,7-dihydroxyl structure on the A ring allow electron delocalization, enabling EGCG to excess ROS [134]. When excess ROS exist, cells will induce antioxidant enzymes to quench the excess ROS. The present study demonstrated the elevation of antioxidant enzymes SOD and catalase in bronchial epithelial cells of the mouse lung at days 1 to 14 after NNK treatment (Figure 10 and 11). This elevation of antioxidant enzymes indirectly suggests that excess ROS exist in bronchial epithelial cells of NNK-treated mouse lung possibly due to NNK-induced oxidative stress during its metabolic activation. However, the possible inhibitory effect of EGCG on the levels of antioxidant enzymes has not been investigated. The anti-oxidative properties of EGCG makes it a good dietary constituent to combat NNK-induced oxidative stress and this could be an important area of future studies for the prevention of tobacco-smoke related lung cancer. Therefore, the effects of EGCG on NNK-induced elevation of antioxidant enzymes should be addressed in the future.

In summary, the present study demonstrated the NNK-induced elevation of DNMT1 protein levels in lung tissues of A/J mice at days 1 and 3 following NNK administration and during the progression of lung tumorigenesis. The induction of DNMT1 is likely due to its protein stabilization by the activation of AKT in response to NNK-induced oxidative stress. The inhibitory effects of EGCG in the induction of DNMT1, p-AKT and  $\gamma$ -H2AX levels could be due to its anti-oxidative activities. Promoter hypermethylation of some

tumor suppressor genes was observed in lung tissues at day 3 after NNK treatment and in lung tumors at week 20. Future studies are needed to clarify the functional importance of early stage induction of DNMT1 and gene hypermethylation in carcinogenesis.

#### **D. Anti-oxidative and Pro-oxidative Activities of EGCG in the Inhibition of Lung Tumorigenesis**

The inhibition of DNMT1 elevation, AKT phosphorylation and  $\gamma$ -H2AX formation by EGCG was possibly due to its anti-oxidative activity and it has been discussed in the last section. On the other hand, EGCG could also prevent lung cancer through its pro-oxidative activities. The pro-oxidative activities of EGCG can be explained by its biochemical properties. The trihydroxyl groups on the B and D rings and the m-5,7-dihydroxyl groups on the A ring play dual roles: in addition to quenching excess ROS through electron delocalization, they also serve as targets for oxidation under alkaline or neutral pH [134]. The present study demonstrated that EGCG induced ROS *in vitro* and oxidative DNA damage and apoptosis both *in vitro* and *in vivo*: We showed a dose-dependent formation of hydrogen peroxide by EGCG auto-oxidation in cell culture conditions (Figure 13). We also demonstrated the induction of oxidative DNA damage ( $\gamma$ -H2AX) and apoptosis (cleaved caspase-3) in both NNK-induced lung tumors by short-term EGCG treatment (Figure 18) and in cell culture conditions (Figure 16 and 17). In addition, the induction of apoptosis-related pro-apoptotic Bcl-2 family proteins by EGCG was demonstrated in cell cultures (Figure 16). As we previously demonstrated, the ROS generation by EGCG auto-oxidation is accompanied by the formation of EGCG semiquinone radicals, EGCG quinines and EGCG dimers [162, 163] and the proposed mechanism for EGCG

auto-oxidation is summarized in Figure 12. Furthermore, our laboratory has previously demonstrated that intracellular levels of ROS was induced by EGCG dose-dependently and the inhibition of H1299 human lung cancer cell xenografts by EGCG was associated with increased oxidative DNA damage ( $\gamma$ -H2AX and 8-hydroxy-deoxyguanosine) and apoptosis (cleaved caspase-3) in xenograft tumors [132]. In the present study, we demonstrated a similar type of action in NNK-induced lung cancer animal model. Together, these results suggest that EGCG may undergo intracellular auto-oxidation and this intracellular ROS effect of EGCG may contribute to the inhibition of lung tumorigenesis *in vivo*. However, how the pro-oxidative and anti-oxidative activities of EGCG work together and when will one functions over the other remain unknown and future studies to clarify its dual role in the prevention of lung tumorigenesis is needed.

#### **E. Discrepancies between Animal and Cell Line Studies for EGCG**

In the present study, the cell growth inhibition by EGCG in four different lung cancer cells were studied and dose-dependent inhibitions were observed for EGCG treatment in the absence of SOD and catalase. However, A549 and H460 cells are not very responsive to EGCG treatment as compared to CL-13 and H1299 cells. Based on the estimated  $IC_{50}$  of each cell line, the responsiveness to EGCG among the 4 cell lines tested can be ranked as: CL-13 > H1299 > H460 > A549 (estimated  $IC_{50}$  of 17, 20, 27 and 42  $\mu$ M, respectively; Figure 14). The addition of SOD and catalase significantly attenuated the cell growth inhibition by EGCG in both CL-13 and H1299 cells but the attenuation effects of SOD and catalase on EGCG-induced cell growth inhibition were less pronounced in H460 and A549 cells (Figure 14). This ranking of responsiveness to EGCG treatment and to the

protective action of SOD and catalase is found consistent with our previous findings on the basal expression levels of antioxidant enzymes heme oxygenase-1, thioredoxin and NAD(P)H quinone oxidoreductase 1, where the expression levels of all three antioxidant enzymes were lowest in CL-13 cells followed by H1299 and H460 cells and were highest in A549 cells [132]. However, the basal expression levels of Nrf2 in those 4 cell lines is not ranked in this order with CL-13 and A549 cells slightly higher than H1299 and H460 cells [132].

The discrepancies in the effective concentrations of EGCG *in vivo* and *in vitro* have been commonly observed previously. In our cell line studies, the effective EGCG concentrations are in the range of 15-50  $\mu\text{M}$  in the absence of SOD and catalase and will increase significantly if supplemented with SOD and catalase. However, the peak plasma level of EGCG in animals treated with dietary EGCG (0.5%) is about 0.5  $\mu\text{M}$  in male athymic nude mice in a H1299 xenograft model study [132]. Even with i.p. injection (30 mg/kg body weight), the peak plasma level of EGCG is only about 2.9  $\mu\text{M}$  [132]. The concentrations of EGCG in our long-term EGCG chemopreventive study (in the diet, 0.2% in combination treatment and 0.4% in single agent treatment) and short-term EGCG treatment at the tumor stage (30 mg/kg body weight daily i.p. injection for 5 days or 0.4% in the diet for 7 days) are similar to those used in the H1299 xenograft model study [132]. One important reason for the observed differences in the effective concentrations of EGCG in this study might be the low bioavailability of EGCG in humans and animals [161, 166]. Short exposure to EGCG in cell culture studies (1-48 h) versus 20-week long-term treatment may also be a possible reason for the discrepancy as prolonged treatment of

EGCG in cell culture conditions could dramatically reduce the effective concentration of EGCG [336, 337].

In many of the previous cell culture studies using EGCG, the effects of EGCG were mostly examined 24, 48 or 72 h after EGCG was added to the cell culture media. It is not known whether the action of EGCG was exerted in the first few hours or throughout the experimental period. In this study, we designed an experiment with different treatment conditions of EGCG (or fresh media in the presence or absence of SOD and catalase) for the first 2 h or the following 22 h in the presence or absence of SOD and catalase (Figure B4). Our results provide a more complete picture of the inhibitory actions of EGCG in lung cancer cell growth. We demonstrated that the cell killing effect of ROS generated by EGCG over the first 2 h contributes about half the effect of a complete 24 h EGCG treatment and either ROS generated by EGCG that is incorporated into the cells or mechanisms other than EGCG-generated ROS contributes the other half. Similar to the results of our hydrogen peroxide formation assay, our laboratory previously demonstrated that the rate of EGCG uptake by HT-29 colon cancer cells in cell culture conditions was extremely high in the first 15 min and this rate dropped dramatically afterwards [164]. In addition, the hydrogen peroxide formed inside the cells is believed to be decomposed through the action of antioxidant enzymes such as glutathione peroxidase, SOD and catalase [164]. Therefore, it is more likely that most of the cell killing effect after the first 2 h of EGCG treatment is through modulating cell signaling pathways such as binding to protein targets rather than the effect from EGCG-generated ROS inside the cells.

## **F. Inhibition of NNK-induced Lung Tumorigenesis and p-c-Jun in NNK-induced Lung Tumors by Myo-inositol**

Myo-inositol was shown to be a relatively safe dietary chemopreventive agent due to the proven low toxicity in both humans and animals. In a phase I clinical study conducted in 2006, a dose of 18 g/day for up to 3 months was well tolerated by humans [213]. The inhibition of NNK- and benzo(a)pyrene-induced lung tumorigenesis by myo-inositol has been reported in many studies and it was shown effective when given in different stages of tumorigenesis [214-221]. The present study demonstrated that among different chemopreventive agents used, myo-inositol showed the best inhibitory effects on tumor incidence (myo-inositol was the only agent showing inhibition on tumor incidence), total number of tumors/mouse and total tumor volume/mouse (Table 2 and 3). However, mechanism in the inhibition of carcinogen-induced lung tumorigenesis by myo-inositol is very limited. Therefore, mechanism studies are urgently needed for clarifying the inhibitory activities of myo-inositol. We demonstrated herein, the inhibition of NNK-induced lung tumorigenesis by myo-inositol is accompanied by the inhibition of p-c-Jun in NNK-induced lung tumors (Figure 23).

It has been reported previously that NNK treatment activates the PI3K/AKT pathway in bronchial epithelial cells and non-small-cell lung cancer cells in cell culture studies [283, 284]. The activation of PI3K/AKT pathway regulates cell proliferation and survival. Previous studies have demonstrated that the inhibition of AP-1 (c-Jun/c-Fos dimer) activation by inositol phosphates (hexaphosphate and pentakisphosphate) by inhibiting PI3K/AKT pathway is required for their anti-cancer activities [229, 230]. Furthermore, myo-inositol has been shown to inhibit AKT and ERK1/2 phosphorylation in

bronchial lesions of the lung in heavy smokers [228]. The same study also showed the inhibition of basal level as well as nicotine-induced AKT activities in human bronchial epithelial cells [228]. We demonstrated herein, the inhibition of p-c-Jun in NNK-induced lung tumors by myo-inositol, suggesting that AP-1 (c-Jun/c-Fos dimer) regulated cell growth and differentiation in the lung tumors are inhibited by myo-inositol in NNK-induced lung cancer model. In addition, we also demonstrated in this study, the activation/phosphorylation of AKT in bronchial epithelial cells of the mouse lung at days 1 and 3 following NNK administration (Figure 4) and in NNK-induced lung tumors (Figure 6C and 6D). Therefore, future studies on the levels of p-c-Jun and PI3K/AKT pathway components at different stages of NNK-induced lung tumorigenesis could be performed. Additionally, the level of p-c-Jun and PI3K/AKT pathway components in lung tissues of myo-inositol-treated mice following NNK administration and during the progression of lung tumorigenesis would be needed to clarify the mechanism of inhibition of NNK-induced lung tumors by myo-inositol.

### **G. Supportive Role of Myofibroblast for Cancer**

IL-6 is secreted from stromal cells including myofibroblasts and fibroblasts to enhance cancer initiation, promotion and progression [338]. Fibroblast, the precursor cell of myofibroblast, has been implicated to play an important role in cancer initiation and progression through the secretion of cytokines and chemokines including IL-6 [164, 338, 339]. Recent studies using genetically altered animal models of spontaneous lung cancer shows that IL-6 plays a critical role in lung tumorigenesis [264, 340]. Cigarette-smoke carcinogens are shown to induce chronic inflammation in the lung [263]. Chronic

inflammation, which induces sustained production of cytokines and chemokines and tissue damages, is an important factor contributing to the development of lung cancer [262]. In addition, one study showed that cigarette smoke could induce IL-6 secretion through the activation of STAT3 pathway in the mouse lung by subchronically exposed to mainstream tobacco smoke, suggesting a relation between smoking and induction of IL-6 secretion [339]. Another recent study demonstrated that benzo(a)pyrene diol epoxide, a cigarette-smoke carcinogen, can stimulate the secretion of IL-6 by human lung fibroblasts through the activation of NF $\kappa$ B pathway and fibroblast-secreted IL-6 activates STAT3 pathway in human bronchial cells and enhances benzo(a)pyrene diol epoxide-mediated transformation of the cells [340].

We demonstrated that myofibroblasts could enhance tumor cell growth in a gastric xenograft model (unpublished data). The co-injection of MKN45 or MKN28 gastric cancer cells with bone marrow-derived myofibroblasts significantly increased tumor incidence as compared to cancer cells injection alone. This enhancement in tumor initiation by bone marrow-derived myofibroblasts was through the IL-6/NF $\kappa$ B and TGF- $\beta$ 1/STAT3 signaling loop between myofibroblasts and cancer cells. The IL-6 secretion by bone marrow-derived myofibroblasts was mediated by NF $\kappa$ B pathway and the gastric cancer cell-derived TGF- $\beta$ 1 secretion was through STAT3 pathway (unpublished data). STAT3 activation has been shown to be essential for the initiation and progression of stomach [341, 342], colon [343, 344], and liver cancers [345, 346]. In the present study, our ELISA results showed that the secretion of mouse IL-6 was significantly inhibited by the addition of an NF $\kappa$ B inhibitor (Bay 11-7082) or a STAT3 inhibitor (JSI-124) in a dose-dependent manner in the H1299 lung cancer cell and bone marrow-derived myofibroblasts

co-culturing study (Figure 19D). This result suggests that the mechanism of interaction demonstrated in the gastric cancer cell xenograft model may also be the key in our lung cancer cell study.

In this study, we demonstrated the dose-dependent inhibitory effect of EGCG in the absence of SOD and catalase on the secretion of IL-6 by bone marrow-derived myofibroblasts (Figure 19C). In addition, the supplement of SOD and catalase significantly attenuated the inhibition of IL-6 secretion by bone marrow-derived myofibroblasts. Our results are consistent with a recent report showing that EGCG inhibited NF $\kappa$ B pathway and IL-6 mRNA expression induced by lipopolysaccharide in bone marrow-derived macrophages, a stromal cell type derived from bone marrow other than myofibroblast [279]. EGCG has also been shown to inhibit the production of other cytokines secreted by stromal cells. For example, EGCG was shown to inhibit IL-12 secretion induced by lipopolysaccharide in bone marrow-derived dendritic cells [280].

One thing of notice is that EGCG only showed inhibitory effect on IL-6 secretion by myofibroblasts, either co-cultured with lung cancer cells or cultured alone, when culture media were supplemented with 2% fetal bovine serum. In addition, the attenuation of this inhibitory effect of EGCG by the supplement of SOD and catalase indicates that the inhibition may be due to the ROS generated by EGCG auto-oxidation. This finding suggests that the inhibitory effect of EGCG may only be observed when myofibroblasts are under stress conditions and this effect may not be relevant in humans and animals. Therefore, future studies in animal models would be needed to rule out this possibility. In summary, our results demonstrated that the support from stromal microenvironment such as cytokines secreted by myofibroblast may play an important role in lung cancer cell

growth and EGCG may interrupt this support from myofibroblasts by targeting on both myofibroblasts and lung cancer cells.

**Table 1:** Progression of NNK-induced lung tumorigenesis\*

Group	Treatment	Duration (weeks)	Total number of mice	Tumor incidence	Total number of tumors/mouse	Total tumor volume/mouse (mm <sup>3</sup> )
1	Saline Control	5	2	0/2	0	0
2	NNK	5	8	0/8	0	0
3	Saline Control	10	2	0/2	0	0
4	NNK	10	8	1/8	2	0.58
5	Saline Control	15	2	0/2	0	0
6	NNK	15	8	8/8	12.0 ± 0.76 <sup>a</sup>	2.27 ± 0.31 <sup>a</sup>
7	Saline Control	20	1	0/1	0	0
8	NNK	20	8	8/8	15.9 ± 1.36 <sup>b</sup>	3.42 ± 0.39 <sup>b</sup>

\*Note: The mice were given two weekly doses of NNK (100 and 75 mg/kg body weight, i.p.) or saline and sacrificed at different time points. Under a dissecting microscope, visible tumors > 0.1 mm in diameter in the lungs were scored. Tumor volume (mm<sup>3</sup>) was measured using the formula  $V = 4/3 \pi r^3$ , where  $V$  is tumor volume and  $r$  is the radius of the tumor determined by the mean values of the longest and shortest diameters. Total tumor volume/mouse was calculated as the sum of the tumor volume of all tumors in one animal. Values shown in the table are means ± SE. Different superscripts indicate statistical significance by one-way ANOVA followed by Turkey's post-hoc test ( $P < 0.05$ ).

**Table 2:** Inhibition of NNK-induced lung tumorigenesis by EGCG,  $\gamma$ -TmT, myo-inositol and atorvastatin, alone or in combination\*

Group	Treatment	Total number of mice	Tumor incidence (%)	Total number of tumors/mouse	Total tumor volume/mouse (mm <sup>3</sup> )	Body weight (g)
1	Saline Control	10	0	0	0	22.4 ± 1.00 <sup>ab</sup>
2	NNK Control	29	100	22.9 ± 1.38 <sup>a</sup>	4.46 ± 0.35 <sup>a</sup>	22.7 ± 0.71 <sup>ab</sup>
3	NNK, 0.4% EGCG	30	100	18.2 ± 1.46 <sup>b</sup>	3.27 ± 0.32 <sup>b</sup>	23.9 ± 0.67 <sup>b</sup>
4	NNK, 0.3% $\gamma$ -TmT	30	100	18.7 ± 1.89 <sup>b</sup>	3.82 ± 0.39 <sup>ab</sup>	20.9 ± 0.49 <sup>a</sup>
5	NNK, 0.2% EGCG + 0.15% $\gamma$ -TmT	30	100	17.4 ± 1.23 <sup>b</sup>	3.35 ± 0.27 <sup>b</sup>	21.9 ± 0.58 <sup>ab</sup>
6	NNK, 2% Myo-inositol	30	90	4.5 ± 0.48 <sup>c</sup>	0.90 ± 0.12 <sup>c</sup>	21.3 ± 0.58 <sup>a</sup>
7	NNK, 0.2% EGCG + 1% Myo-inositol	30	93	3.6 ± 0.44 <sup>c</sup>	0.78 ± 0.10 <sup>c</sup>	21.2 ± 0.36 <sup>a</sup>
8	NNK, 400 ppm Atorvastatin	29	100	21.9 ± 1.56 <sup>a</sup>	4.18 ± 0.40 <sup>a</sup>	20.8 ± 0.40 <sup>a</sup>
9	NNK, 1% Myo-inositol + 200 ppm Atorvastatin	30	93	3.5 ± 0.43 <sup>c</sup>	0.64 ± 0.08 <sup>c</sup>	21.0 ± 0.47 <sup>a</sup>

\*Note: The mice were given two weekly doses of NNK (100 and 75 mg/kg body weight, i.p.) or saline. One week before the first dose of NNK, the mice were treated with EGCG (0.4% in the diet),  $\gamma$ -TmT (0.3% in the diet), EGCG (0.2% in the diet) plus  $\gamma$ -TmT (0.15% in the diet), myo-inositol (2% in drinking fluid), EGCG (0.2% in the diet) plus myo-inositol (1% in drinking fluid), atorvastatin (400 ppm in the diet), or myo-inositol (1% in drinking fluid) plus atorvastatin (200 ppm in the diet) for 20 weeks until the end of the experiment. Under a dissecting microscope, visible tumors > 0.1 mm in diameter in the lungs were scored. Tumor volume (mm<sup>3</sup>) were measured using the formula  $V = 4/3 \pi r^3$ , where  $V$  is tumor volume and  $r$  is the radius of the tumor determined by the mean values of the longest and shortest diameters. Total tumor volume/mouse was calculated as the sum of the tumor volume of all tumors in one animal. Values shown in the table are means ± SE. Different superscripts indicate statistical significance by one-way ANOVA followed by Turkey's post-hoc test ( $P < 0.05$ ).

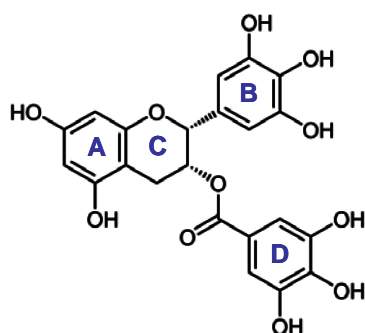
**Table 3:** Inhibition of NNK-induced lung tumorigenesis by EGCG,  $\gamma$ -TmT and myo-inositol treatment, alone or in combination \*

Group	Treatment	Total number of mice	Tumor incidence (%)	Total number of tumors/mouse	Total tumor volume/mouse (mm <sup>3</sup> )	Body weight (g)
1	Saline Control	10	0	0	0	21.7 ± 0.92
2	NNK Control	30	100	22.0 ± 1.54 <sup>a</sup>	4.72 ± 0.37 <sup>a</sup>	21.7 ± 0.81
3	NNK, 0.4% EGCG	30	100	17.9 ± 0.90 <sup>b</sup>	2.84 ± 0.28 <sup>b</sup>	22.8 ± 0.59
4	NNK, 0.3% $\gamma$ -TmT	29	100	18.9 ± 1.37 <sup>b</sup>	3.34 ± 0.31 <sup>b</sup>	22.2 ± 0.53
5	NNK, 0.2% EGCG + 0.15% $\gamma$ -TmT	30	100	17.3 ± 1.02 <sup>b</sup>	2.95 ± 0.29 <sup>b</sup>	20.9 ± 0.69
6	NNK, 0.25% Myo-inositol	30	93	7.1 ± 1.02 <sup>c</sup>	0.93 ± 0.15 <sup>c</sup>	21.1 ± 0.67
7	NNK, 0.5% Myo-inositol	30	87	5.9 ± 0.93 <sup>c</sup>	0.81 ± 0.10 <sup>c</sup>	22.8 ± 0.69
8	NNK, 1% Myo-inositol	30	93	4.0 ± 0.65 <sup>c</sup>	0.64 ± 0.12 <sup>c</sup>	20.7 ± 0.52
9	NNK, 0.2% EGCG + 0.25% Myo-inositol	30	93	6.7 ± 1.03 <sup>c</sup>	0.89 ± 0.09 <sup>c</sup>	22.6 ± 0.46
10	NNK, 0.2% EGCG + 0.5% Myo-inositol	30	90	6.5 ± 0.94 <sup>c</sup>	0.86 ± 0.11 <sup>c</sup>	21.3 ± 0.67

\*Note: The mice were given two weekly doses of NNK (100 and 75 mg/kg body weight, i.p.) or saline. One week before the first dose of NNK, the mice were treated with EGCG (0.4% in the diet),  $\gamma$ -TmT (0.3% in the diet), EGCG (0.2% in the diet) plus  $\gamma$ -TmT (0.15% in the diet), myo-inositol (0.25%, 0.5% or 1% in drinking fluid), or EGCG (0.2% in the diet) plus myo-inositol (0.25% or 0.5% in drinking fluid) for 20 weeks until the end of the experiment. Under a dissecting microscope, visible tumors > 0.1 mm in diameter in the lungs were scored. Tumor volume (mm<sup>3</sup>) was measured using the formula  $V = 4/3 \pi r^3$ , where  $V$  is tumor volume and  $r$  is the radius of the tumor determined by the mean values of the longest and shortest diameters. Total tumor volume/mouse was calculated as the sum of the tumor volume of all tumors in one animal. Values shown in the table are means ± SE. Different superscripts indicate statistical significance by one-way ANOVA followed by Turkey's post-hoc test ( $P < 0.05$ ).

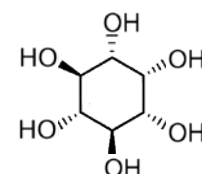
# Chemical Structures

**A**



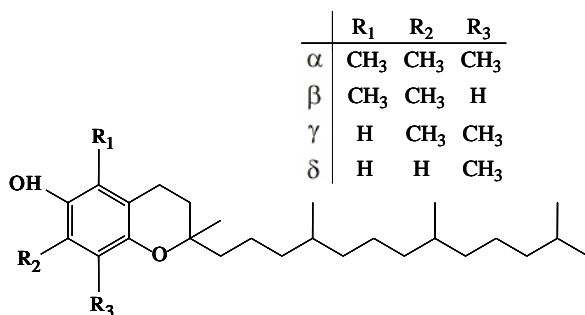
(-)-Epigallocatechin-3-gallate (EGCG)

**C**



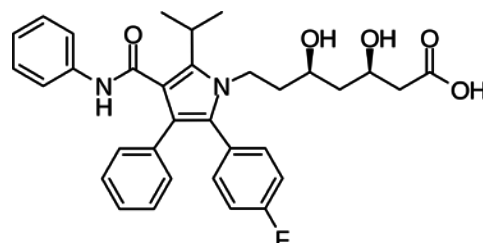
Myo-inositol

**B**



Tocopherols

**D**



Atorvastatin

**Figure 1.** Chemical structures of EGCG (A), tocopherols (B), myo-inositol (C) and atorvastatin (D).

## Experimental Designs

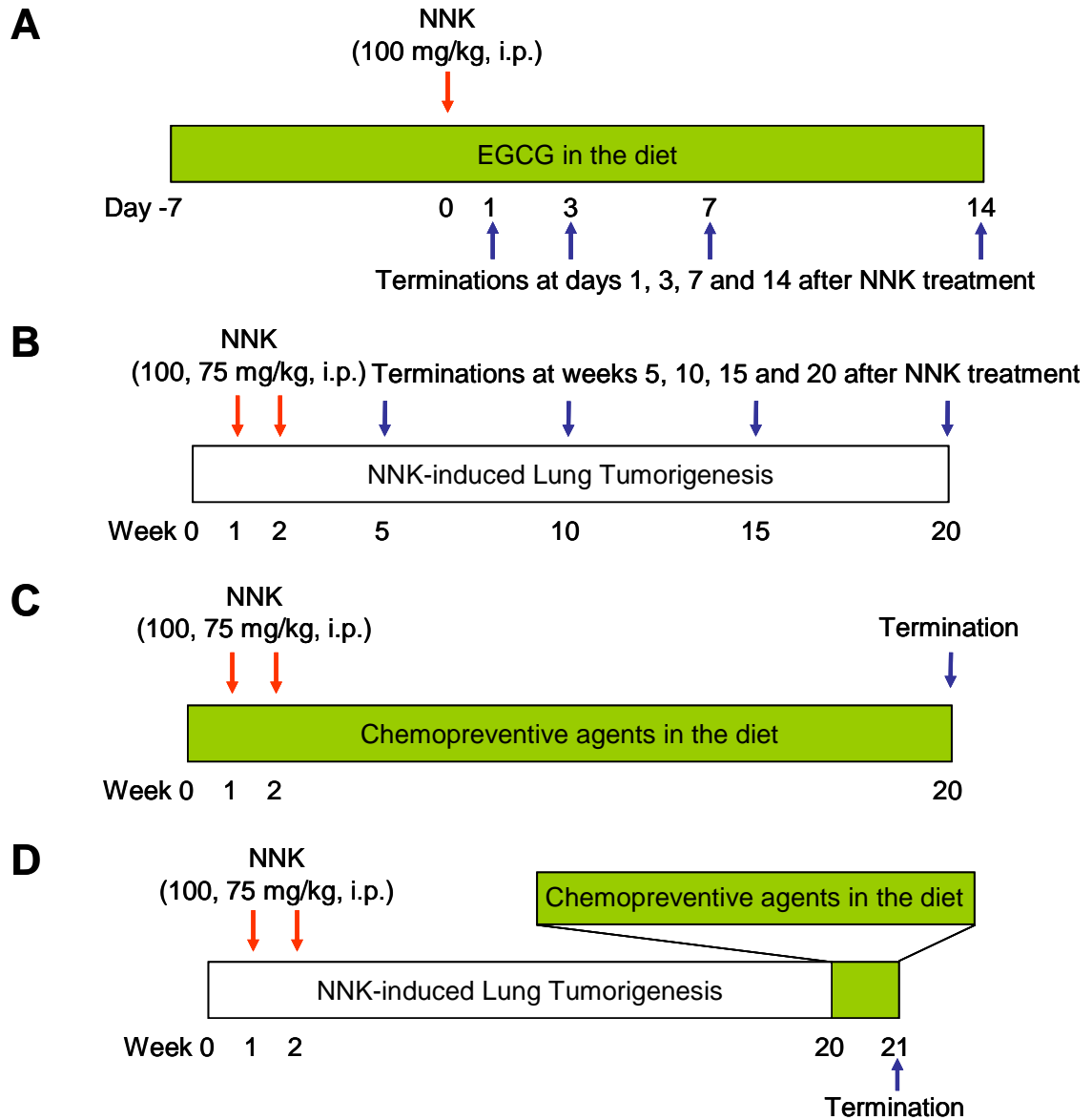


**Figure 2.** Experimental designs. (A and B) Molecular alterations in lung tissues of A/J mice following NNK administration and the inhibitory effect of EGCG (A), and during the progression of NNK-induced lung tumorigenesis (B). (C) Inhibition of NNK-induced lung tumorigenesis by EGCG,  $\gamma$ -TmT, myo-inositol and atorvastatin, alone or in combination. (D) Effects of short-term EGCG and  $\gamma$ -TmT treatment in NNK-induced lung tumors.

## DNMT1 Expression

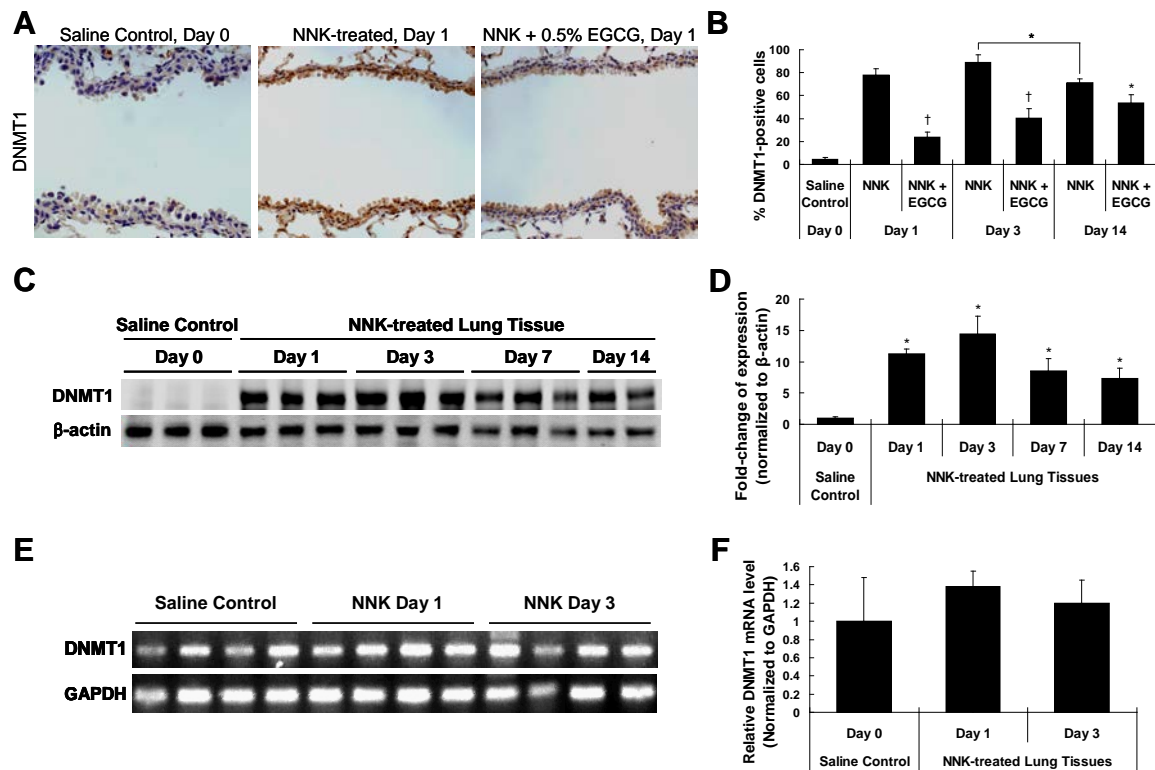


**Figure 3.** NNK-induced elevation of DNMT1 in lung tissues of NNK-treated mice and the inhibitory effect of EGCG. (A) Representative immunohistochemistry microphotographs for DNMT1 staining in lung tissues from day 0 saline control group, day 1 NNK-treated group and day 1 NNK + 0.5% EGCG group. (B) Quantification of DNMT1-positive cells in bronchial epithelial cells of saline-, NNK-treated or NNK + EGCG-treated mice at days 0, 1, 3 and 14. (C) Representative Western blot of protein levels of DNMT1 in lung tissues of saline- or NNK-treated mice at days 0, 1, 3, 7 and 14 after NNK treatment. (D) Quantification of Western blot results. (E) mRNA level of DNMT1 in lung tissues of saline- or NNK-treated mice at days 0, 1 and 3 after NNK treatment by qPCR. (F) Quantification of qPCR results. Values shown in the bar graphs are means  $\pm$  SD ( $n=25$  (5 slides  $\times$  5 fields) for immunohistochemistry,  $n=3$  for Western blot analysis and  $n=4$  for qPCR); \* ( $P < 0.05$ ) and † ( $P < 0.01$ ) indicate statistical significance by Student's *t*-test for NNK + 0.5% EGCG treatment groups as compared to same day NNK treatment groups, or between day 3 and day 14 NNK treatment groups.

## p-AKT Expression

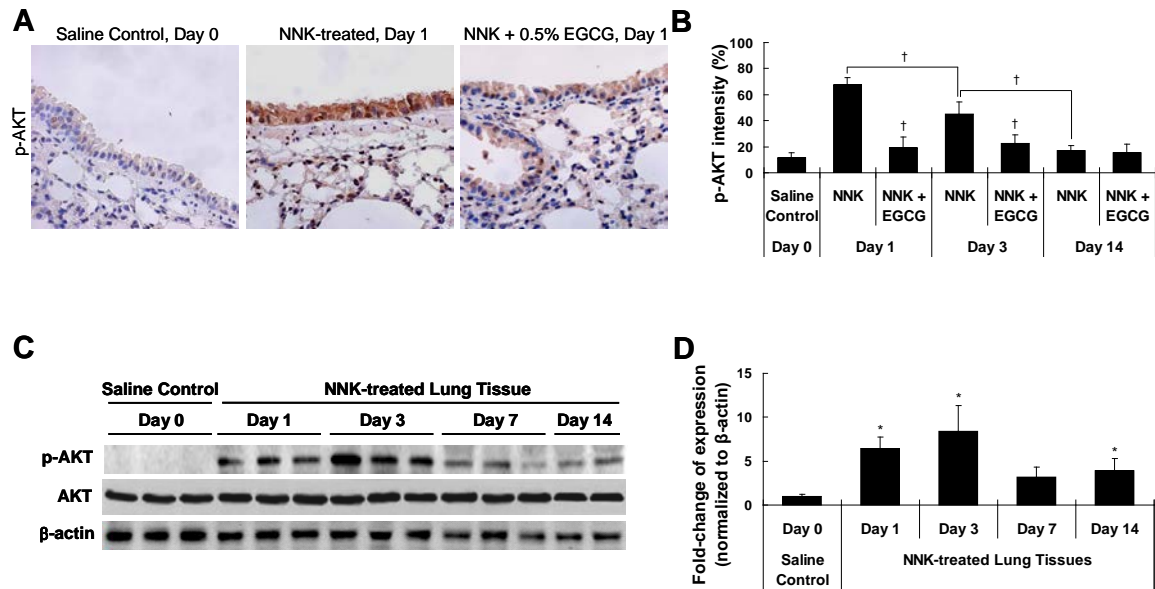


**Figure 4.** NNK-induced elevation of p-AKT in lung tissues of NNK-treated mice and the inhibitory effect of EGCG. (A) Representative immunohistochemistry microphotographs for p-AKT staining in lung tissues from day 0 saline control group, day 1 NNK-treated group and day 1 NNK + 0.5% EGCG group. (B) Quantification of p-AKT staining intensity in bronchial epithelial cells of saline-, NNK-treated or NNK + EGCG-treated mice at days 0, 1, 3 and 14. (C) Representative Western blot of protein levels of p-AKT in lung tissues of saline- or NNK-treated mice at days 0, 1, 3, 7 and 14 after NNK treatment. (D) Quantification of Western blot results. Values shown in the bar graphs are means  $\pm$  SD ( $n=25$  (5 slides  $\times$  5 fields) for immunohistochemistry and  $n=3$  for Western blot analysis); \* ( $P < 0.05$ ) and † ( $P < 0.01$ ) indicate statistical significance by Student's *t*-test for NNK + 0.5% EGCG treatment groups as compared to same day NNK treatment groups, or between day 3 NNK treatment group and day 1 or day 14 NNK treatment groups.

## $\gamma$ -H2AX, O<sup>6</sup>-methylguanine and Cleaved Caspase-3 Expression

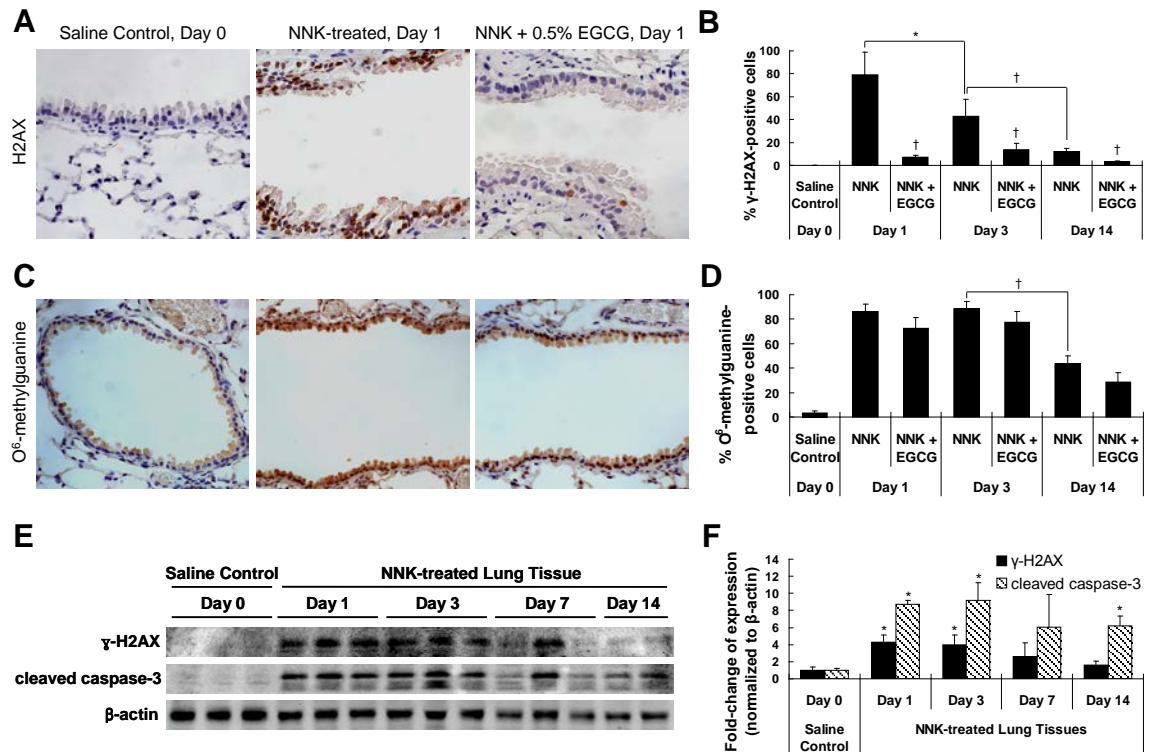


**Figure 5.** NNK-induced elevation of  $\gamma$ -H2AX and O<sup>6</sup>-methylguanine in lung tissues of NNK-treated mice and the inhibitory effect of EGCG. (A and C) Representative immunohistochemistry microphotographs for  $\gamma$ -H2AX (A) and O<sup>6</sup>-methylguanine (C) staining in lung tissues from day 0 saline control group, day 1 NNK-treated group and day 1 NNK + 0.5% EGCG group. (B and D) Quantification of  $\gamma$ -H2AX-positive (B) and O<sup>6</sup>-methylguanine-positive (D) cells in bronchial epithelial cells of saline-, NNK-treated or NNK + EGCG-treated mice at days 0, 1, 3 and 14. (E) Representative Western blot of protein levels of  $\gamma$ -H2AX and cleaved caspase-3 in lung tissues of saline- or NNK-treated mice at days 0, 1, 3, 7 and 14 after NNK treatment. (F) Quantification of Western blot results. Values shown in the bar graphs are means  $\pm$  SD ( $n=25$  (5 slides  $\times$  5 fields) for immunohistochemistry and  $n=3$  for Western blot analysis); \* ( $P < 0.05$ ) and † ( $P < 0.01$ ) indicate statistical significance by Student's *t*-test for NNK + 0.5% EGCG treatment groups as compared to same day NNK treatment groups, or between day 3 NNK treatment group and day 1 or day 14 NNK treatment groups.

## DNMT1 Expression during the Progression of NNK-induced Lung Tumorigenesis

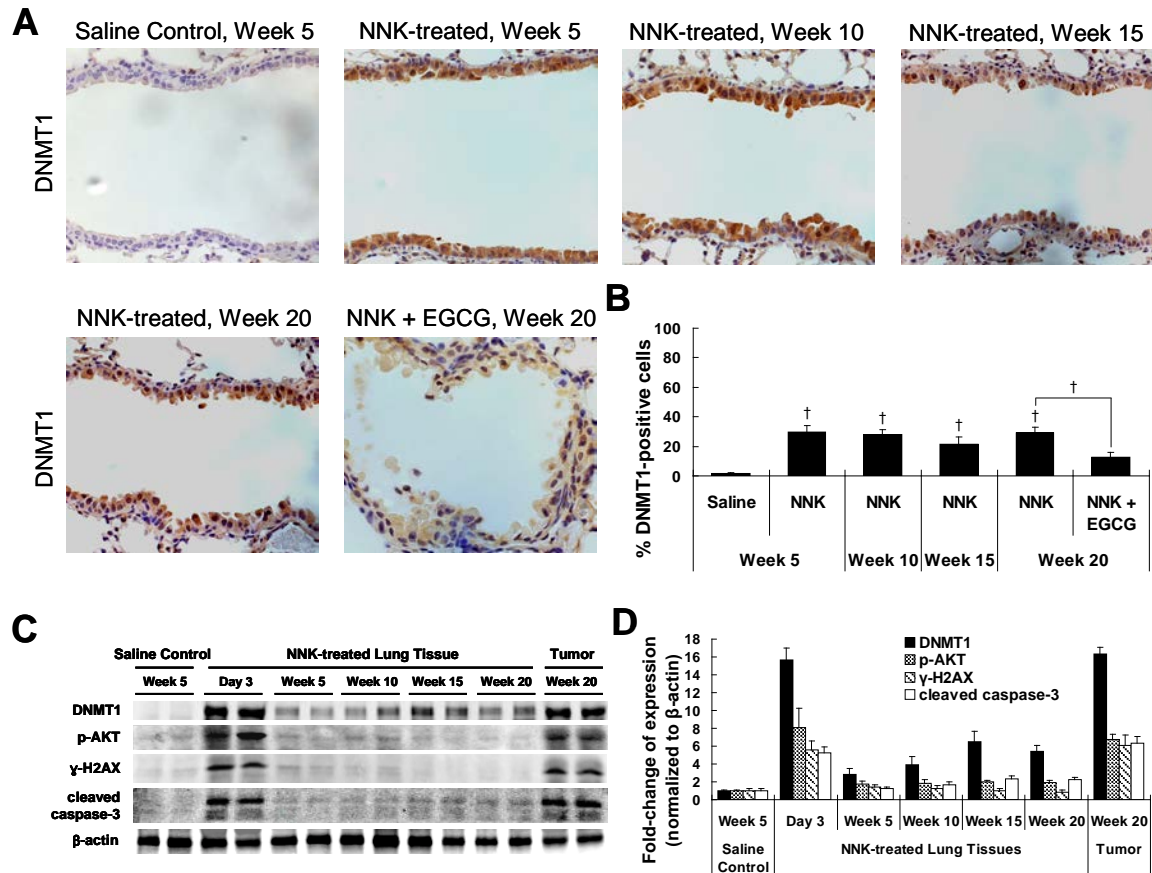


**Figure 6.** Increased DNMT1 expression during the progression of NNK-induced lung tumorigenesis and the inhibitory effect of EGCG. (A) Representative immunohistochemistry microphotographs for DNMT1 staining in lung tissues from saline control mice at week 5, NNK-treated mice at weeks 5, 10, 15 and 20, and mice from NNK + 0.5% EGCG group at week 20. (B) Quantification of DNMT1-positive cells in bronchial epithelial cells. (C) Representative Western blot of protein levels of DNMT1, p-AKT,  $\gamma$ -H2AX and cleaved caspase-3 in lung tissues of saline- or NNK-treated mice at day 3, weeks 5, 10, 15 and 20, or NNK-induced lung tumors at week 20. (D) Quantification of Western blot results. Values shown in the bar graphs are means  $\pm$  SD ( $n=25$  (5 slides  $\times$  5 fields) for immunohistochemistry,  $n=2$  for Western blot analysis); † ( $P < 0.01$ ) indicates statistical significance by Student's  $t$ -test for weeks 5-20 NNK treatment groups as compared to week 5 saline control group, or for week 20 NNK + 0.5% EGCG treatment group as compared to the same week NNK treatment group.

### DNMT1 Expression in Cell Culture

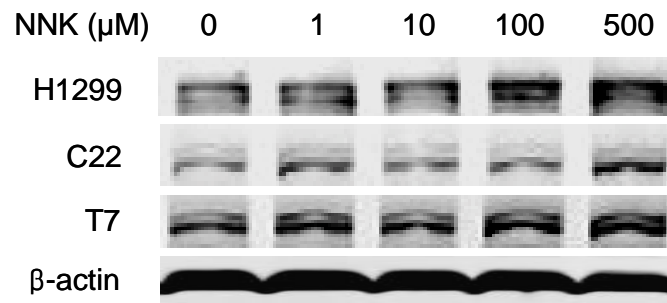


**Figure 7.** NNK-induced elevation of DNMT1 in H1299, C22 and T7 cells. Western blot analysis was performed on human non-small-cell lung cancer-derived cell line H1299, conditionally immortalized mouse clara cell line C22 and immortal differentiated mouse type II alveolar cell line T7 after treatment with NNK (1, 10, 100 and 500  $\mu\text{M}$ ) for 24 h.  $\beta$ -actin was used as an equal loading control.

## Gene-specific and Global DNA Methylation

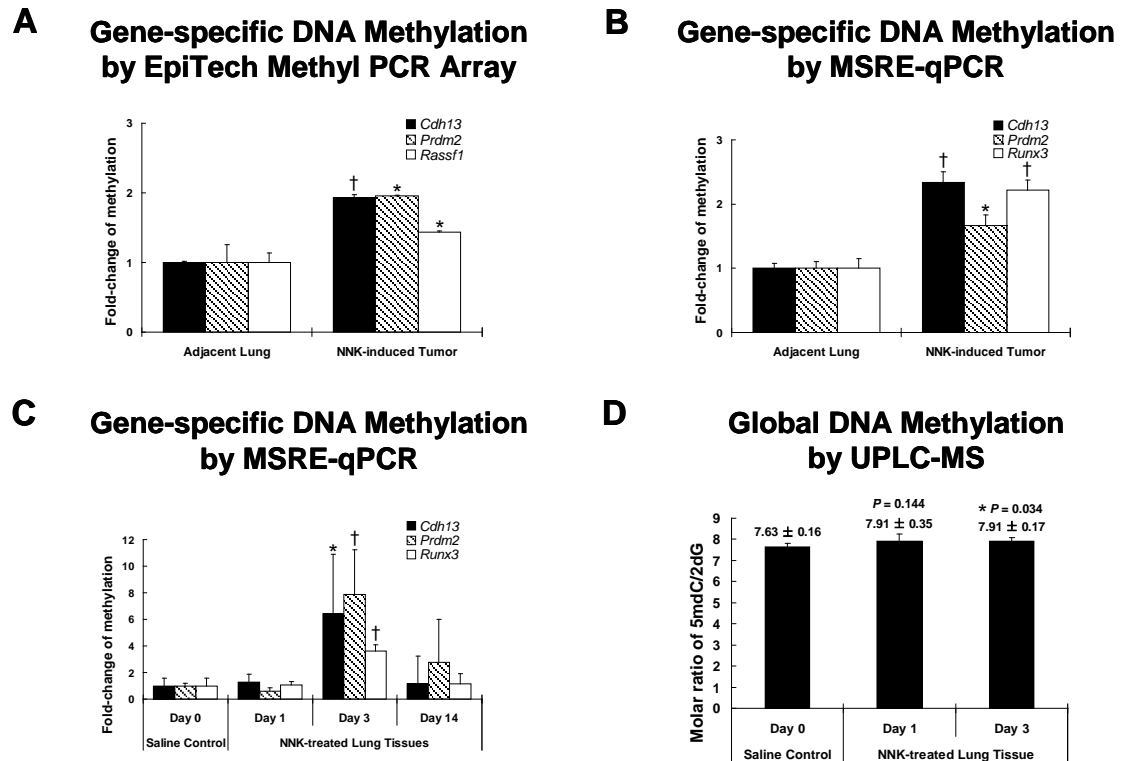


**Figure 8.** Increased gene-specific promoter hypermethylation and global DNA methylation in NNK-induced lung tumors and lung tissues of NNK-treated mice. (A and B) The fold-change of methylation of promoter regions of tumor suppressor genes in NNK-induced lung tumors and the adjacent lung tissues by EpiTect Methyl PCR array (*Cdh13*, *Prdm2* and *Rassf1*) (A) and Methylation-Sensitive, Restriction Enzyme-based quantitative PCR (*Cdh13*, *Prdm2* and *Runx3*) (B). (C) Fold-change of methylation of promoter regions of *Cdh13*, *Prdm2* and *Runx3* in lung tissues treated with saline or NNK at days 0, 1, 3 and 14. (D) The molar ratio of 5mC/2dG in lung tissues treated with saline or NNK at days 0, 1 and 3. Values shown in the bar graphs are means ± SD (n=4, 2 mice × 2 repeat). \* ( $P < 0.05$ ) and † ( $P < 0.01$ ) indicate statistical significance by Student's *t*-test for NNK-induced lung tumors as compared to the adjacent lung tissues or day 3 NNK treatment group as compared to day 0 saline control group.

# COX-2 Expression

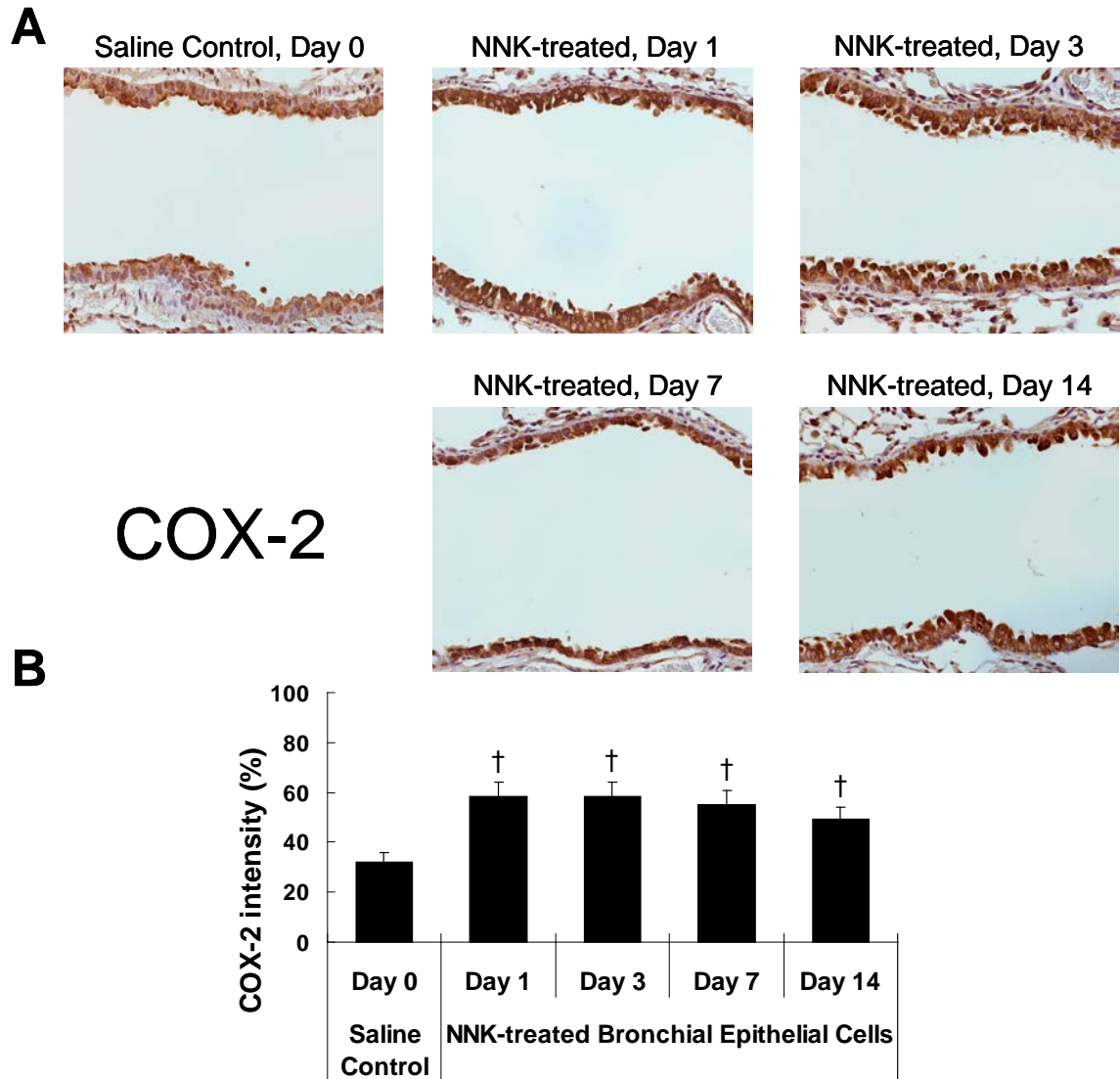


**Figure 9.** NNK-induced elevation of COX-2 in bronchial epithelial cells of NNK-treated mice. (A) Representative immunohistochemistry microphotographs for COX-2 staining in lung tissues from day 0 saline control mice, and days 1, 3, 7 and 14 NNK-treated mice. (B) Quantification of COX-2 staining intensity in bronchial epithelial cells of saline- or NNK-treated mice at days 0, 1, 3 and 14. Values shown in the bar graphs are means  $\pm$  SD (n=50, 5 slides  $\times$  10 fields); † ( $P < 0.01$ ) indicates statistical significance by Student's *t*-test for days 1, 3, 7 and 14 NNK treatment groups as compared to day 0 saline control group.

# SOD Expression

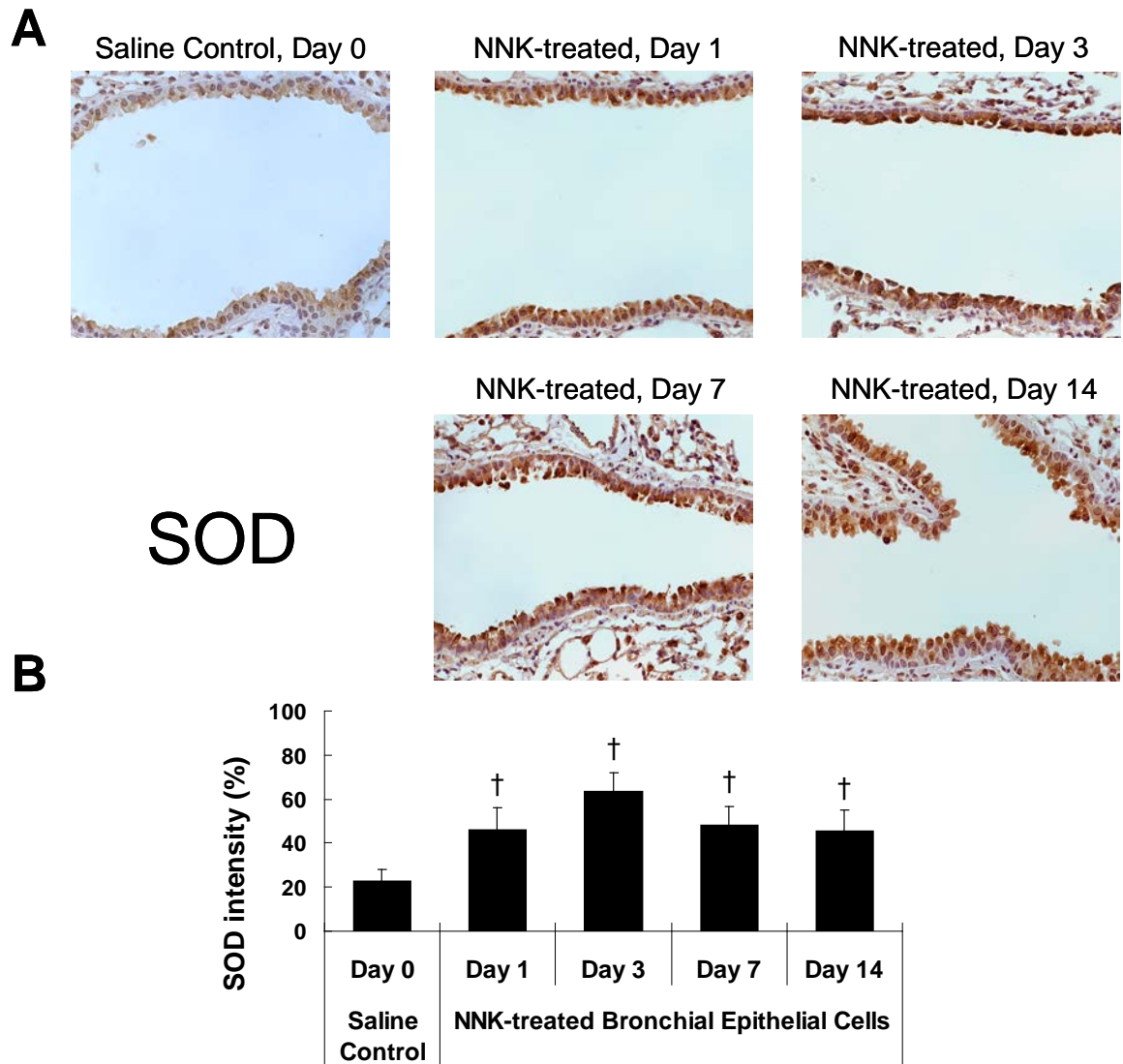


**Figure 10.** NNK-induced elevation of SOD in bronchial epithelial cells of NNK-treated mice. (A) Representative immunohistochemistry microphotographs for SOD staining in lung tissues from day 0 saline control mice, and days 1, 3, 7 and 14 NNK-treated mice. (B) Quantification of SOD staining intensity in bronchial epithelial cells of saline- or NNK-treated mice at days 0, 1, 3 and 14. Values shown in the bar graphs are means  $\pm$  SD (n=50, 5 slides  $\times$  10 fields); † ( $P < 0.01$ ) indicates statistical significance by Student's *t*-test for days 1, 3, 7 and 14 NNK treatment groups as compared to day 0 saline control group.

# Catalase Expression

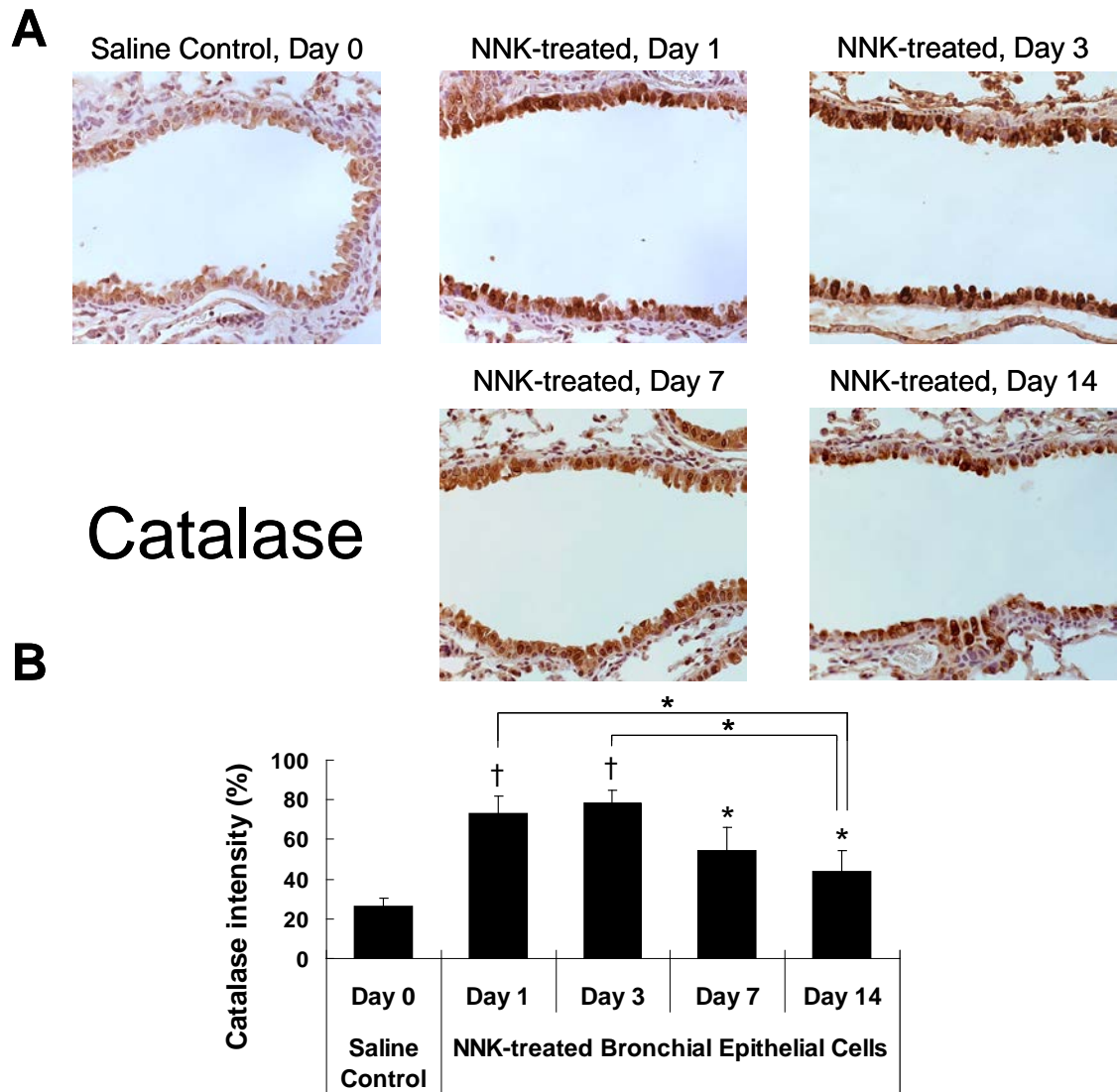


**Figure 11.** NNK-induced elevation of catalase in bronchial epithelial cells of NNK-treated mice. (A) Representative immunohistochemistry microphotographs for catalase staining in lung tissues from day 0 saline control mice, and days 1, 3, 7 and 14 NNK-treated mice. (B) Quantification of catalase staining intensity in bronchial epithelial cells of saline- or NNK-treated mice at days 0, 1, 3 and 14. Values shown in the bar graphs are means  $\pm$  SD (n=50, 5 slides  $\times$  10 fields); \* ( $P < 0.05$ ) and † ( $P < 0.01$ ) indicate statistical significance by Student's *t*-test for days 1, 3, 7 and 14 NNK treatment groups as compared to day 0 saline control group, or between day 14 NNK treatment group and day 1 or day 3 NNK treatment groups.

## Proposed Mechanism for EGCG Auto-oxidation

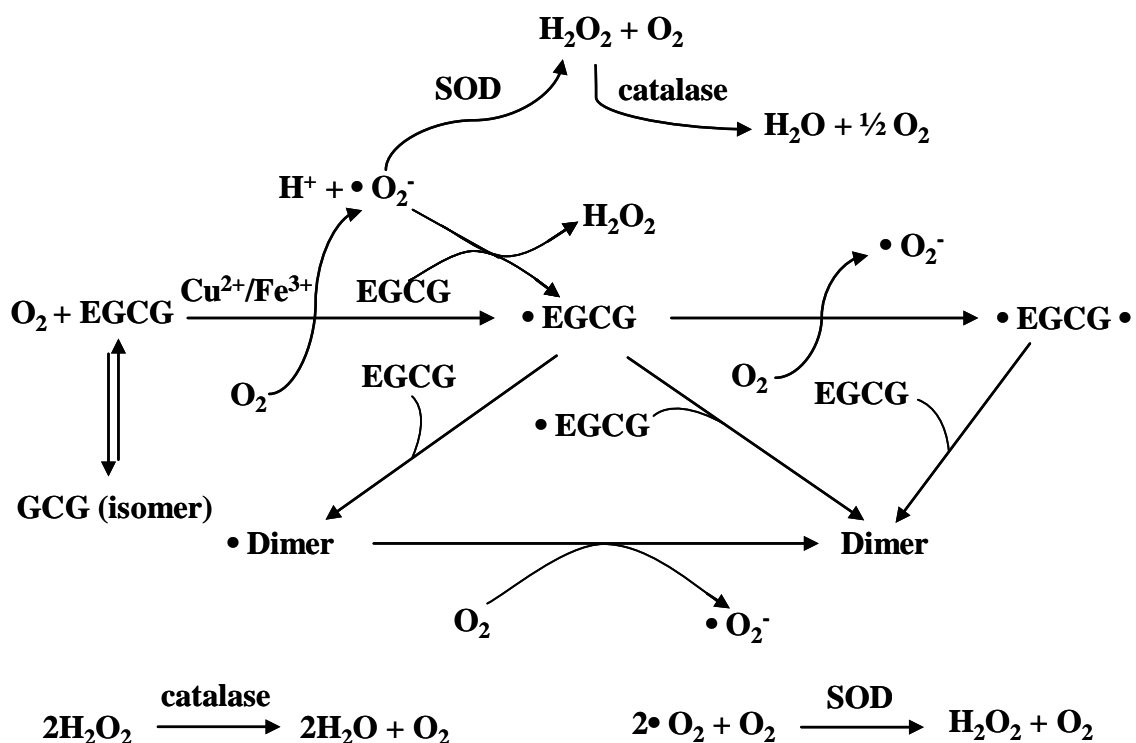


**Figure 12.** Proposed mechanism for EGCG auto-oxidation. Under neutral or slightly alkaline pH, EGCG is oxidized by oxygen to form superoxide radical ( $\bullet O_2^-$ ) and EGCG semiquinone radical ( $\bullet EGCG$ ) in a reaction possibly catalyzed by trace metal ions ( $Cu^{2+}$  and  $Fe^{3+}$ ). The  $\bullet O_2^-$  can further react with another EGCG to form  $\bullet EGCG$ . Two  $\bullet EGCG$  can collide and form an EGCG dimer.  $\bullet EGCG$  can also react with EGCG to form EGCG dimer radical, which may react with oxygen to generate EGCG dimer and  $\bullet O_2^-$ .  $\bullet EGCG$  may also be oxidized by oxygen to generate EGCG quinone ( $\bullet EGCG \bullet$ ) and  $\bullet O_2^-$ . The  $\bullet EGCG \bullet$  can react with another EGCG to form EGCG dimer.  $\bullet O_2^-$  generated by EGCG auto-oxidation can react with another EGCG to propagate the chain reaction. The addition of superoxide dismutase (SOD) to the culture medium can enhance the conversion of  $\bullet O_2^-$  to  $H_2O_2$  and inhibit the EGCG auto-oxidation. Adding catalase to the culture medium can catalyze the decomposition of  $H_2O_2$  thus reduce the reactive oxygen species (ROS) effect of EGCG (modified from Z. Hou *et al.* 2005 and C.S. Yang *et al.* 2007).

## Hydrogen Peroxide Formation by EGCG Auto-oxidation

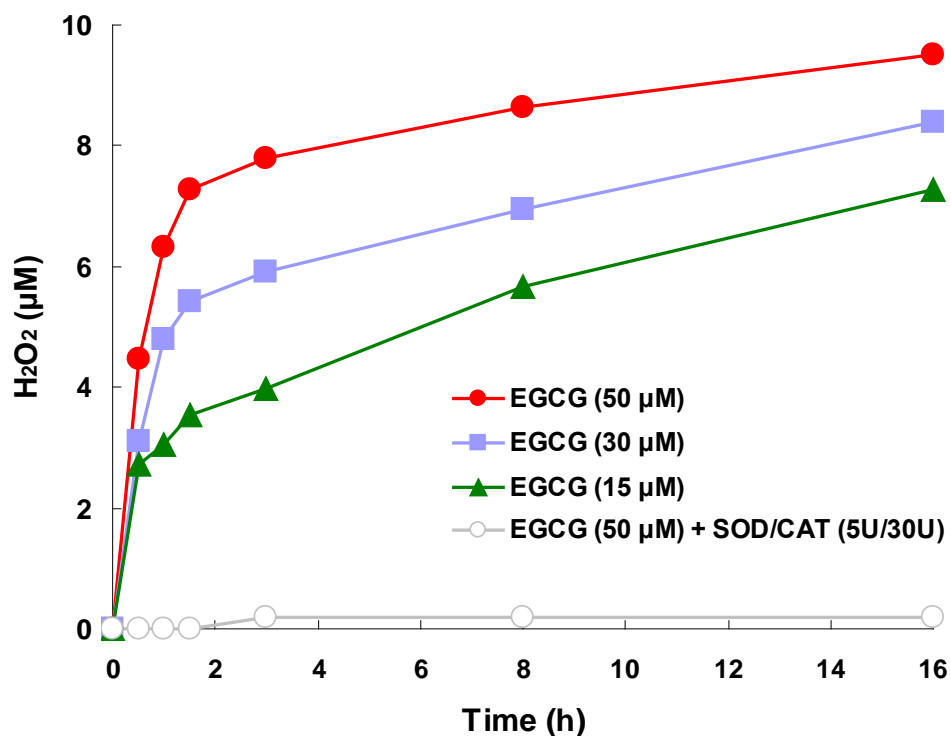


**Figure 13.** Hydrogen peroxide formation by EGCG auto-oxidation in RPMI-1640 culture medium. EGCG (15, 30, and 50 µM) was incubated in serum free RPMI-1640 medium without cells in the presence or absence of SOD (5 unit/mL) and catalase (30 unit/mL). At different time points (0, 0.5, 1.5, 3, 8 and 16 h), the hydrogen peroxide level in the incubated culture medium was measured by a colorimetric assay. Values shown are the means of duplicate incubations.

## Cell Growth Inhibition by EGCG $\pm$ SOD/catalase

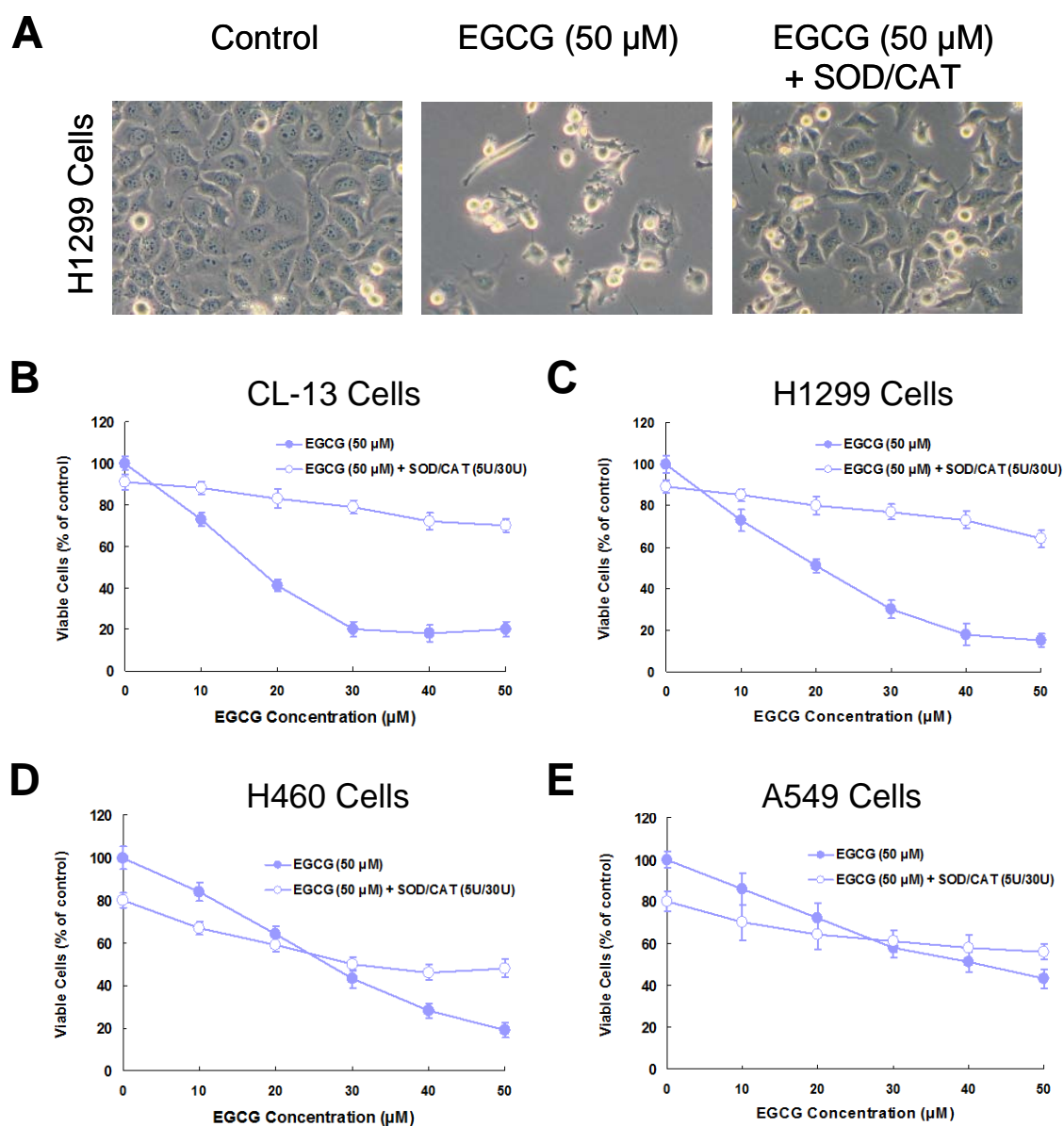


**Figure 14.** Cell growth inhibition by EGCG in the absence or presence of SOD and catalase. (A) Representative light photomicrographs of H1299 cells after treatment with EGCG (50  $\mu$ M) in the absence or presence of SOD (5 unit/mL) and catalase (30 unit/mL) for 24 h. (B-E) Cell growth inhibition by EGCG in CL-13 (B), H1299 (C), H460 (D) and A549 cells (E) after treatment with EGCG (50  $\mu$ M) in the absence or presence of SOD (5 unit/mL) and catalase (30 unit/mL) for 24 h.

## Cell Growth Inhibition by 2 h or 22 h EGCG $\pm$ SOD/catalase

**A**

Treatment Conditions of EGCG in the absence (solid) or presence (open) of SOD/CAT

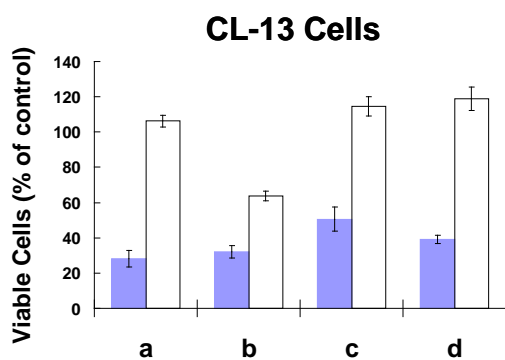
a. 24 h EGCG incubation in the absence (solid) or presence (open) of SOD/CAT

b. 2 h EGCG, 22 h fresh media in the absence (solid) or presence (open) of SOD/CAT

c. 2 h EGCG + SOD/CAT, 22 h fresh media in the absence (solid) or presence (open) of SOD/CAT

d. 2 h fresh media, 22 h EGCG conditional media (2h) in the absence (solid) or presence (open) of SOD/CAT

**B**



**C**

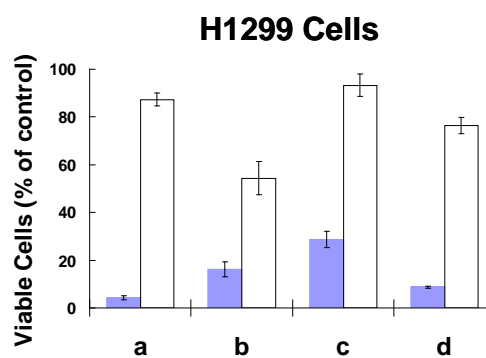


**Figure 15.** Cell growth inhibition by EGCG in the first 2 h or the following 22 h. (A) Treatment conditions of EGCG in the absence (solid) or presence (open) of SOD (5 unit/mL) and catalase (30 unit/mL). (B and C) Cell growth inhibition by EGCG in CL-13 (B) and H1299 cells (C) after treatment with EGCG (50  $\mu$ M) under different treatment conditions.

## Induction of Apoptosis and Pro-apoptotic Bcl-2 Family Proteins by EGCG

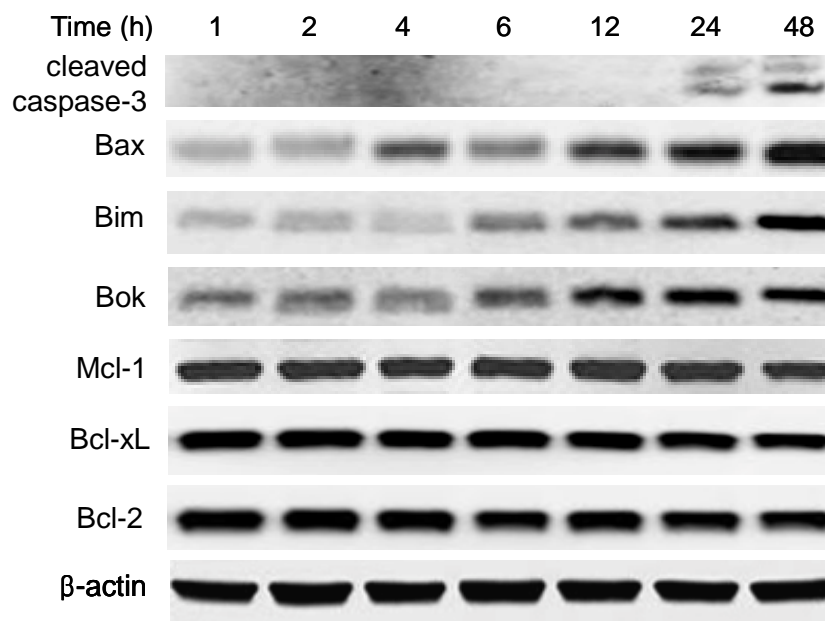


**Figure 16.** Induction of cleaved caspase-3 and changes in the levels of apoptosis-related Bcl-2 family proteins by EGCG in H1299 lung cancer cells. Western blot analysis was performed on H1299 cells after treatment with EGCG (40  $\mu$ M) in the presence of SOD (5 unit/mL) and catalase (30 unit/mL) for 1, 2, 4, 6, 12, 24 and 48 h.  $\beta$ -actin was used as an equal loading control.

## Induction of $\gamma$ -H2AX by EGCG $\pm$ SOD/catalase

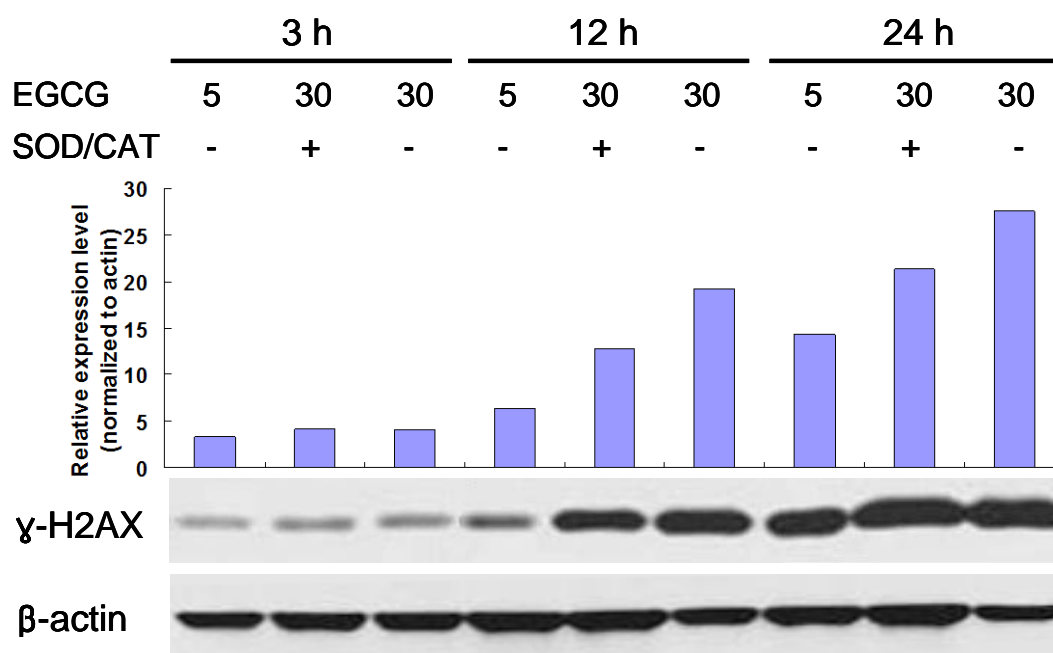


**Figure 17.** Induction of  $\gamma$ -H2AX by EGCG in CL-13 mouse lung cancer cells in the presence or absence of SOD and catalase. Western blot analysis was performed on CL-13 cells after treatment with 5  $\mu$ M of EGCG in the absence of SOD and catalase, or 30  $\mu$ M of EGCG in the presence or absence of SOD and catalase for 3, 12 and 24 h.  $\beta$ -actin was used as an equal loading control. Quantification of Western blot results was shown as relative expression level (normalized to  $\beta$ -actin).

## Short-term EGCG Treatment at the Tumor Stage

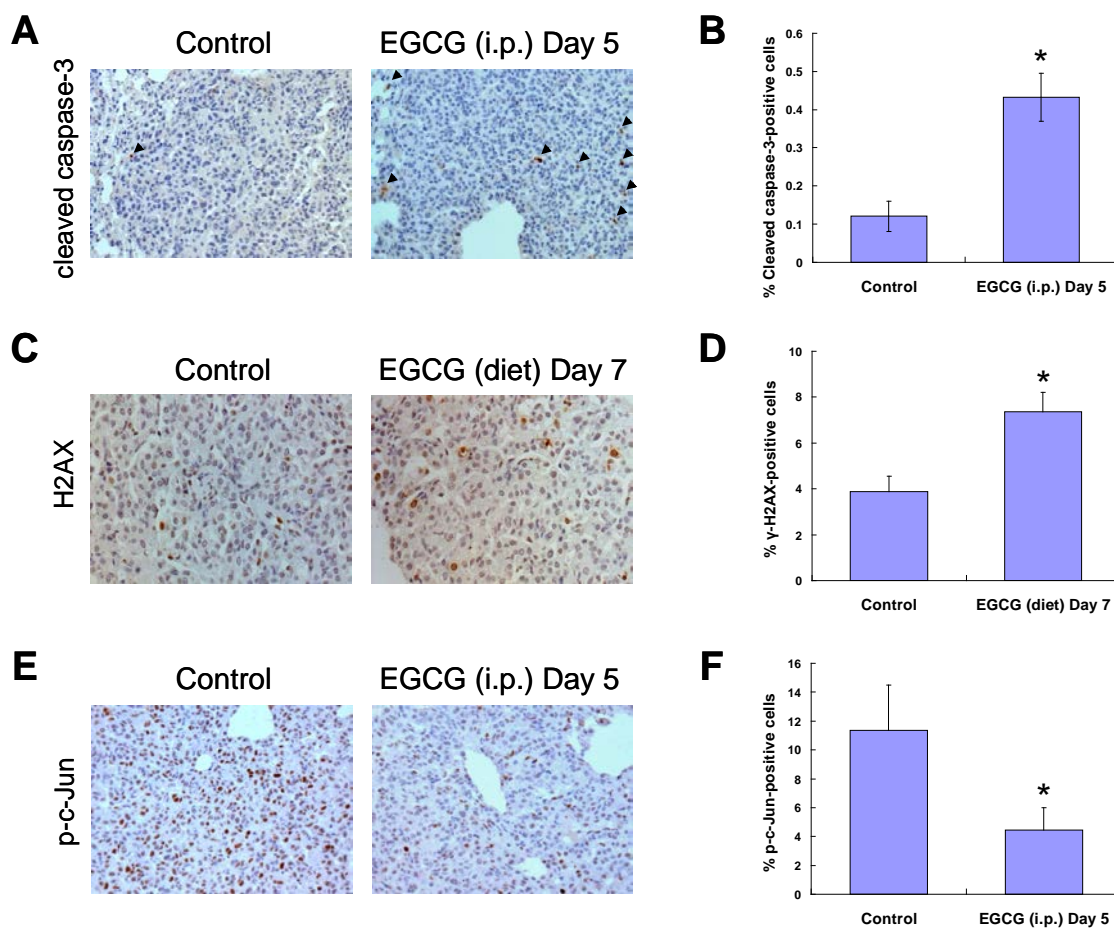


**Figure 18.** Effects of short-term EGCG treatment at the tumor stage on the levels of cleaved caspase-3,  $\gamma$ -H2AX and p-c-Jun in NNK-induced lung tumors. (A, C and E) Representative immunohistochemistry microphotographs for the levels of cleaved caspase-3 (A),  $\gamma$ -H2AX (C) and p-c-Jun (E) in NNK-induced lung tumors from NNK-treated control mice or EGCG-treated mice (0.4% in the diet for 7 days or 30mg/kg body weight by daily i.p. injection for 5 days). (B, D and F) Quantification of cleaved caspase-30-positive (B),  $\gamma$ -H2AX-positive (D), and p-c-Jun-positive (F) cells in NNK-induced lung tumors. Values shown in the bar graphs are means  $\pm$  SD (n=25, 5 slides  $\times$  5 fields); \* ( $P < 0.05$ ) indicates statistical significance by Student's *t*-test for lung tumors from EGCG-treated mice as compared to NNK-treated control mice.

## EGCG Interrupts the Support of Cancer Cells from Stromal Microenvironment (Myofibroblasts)

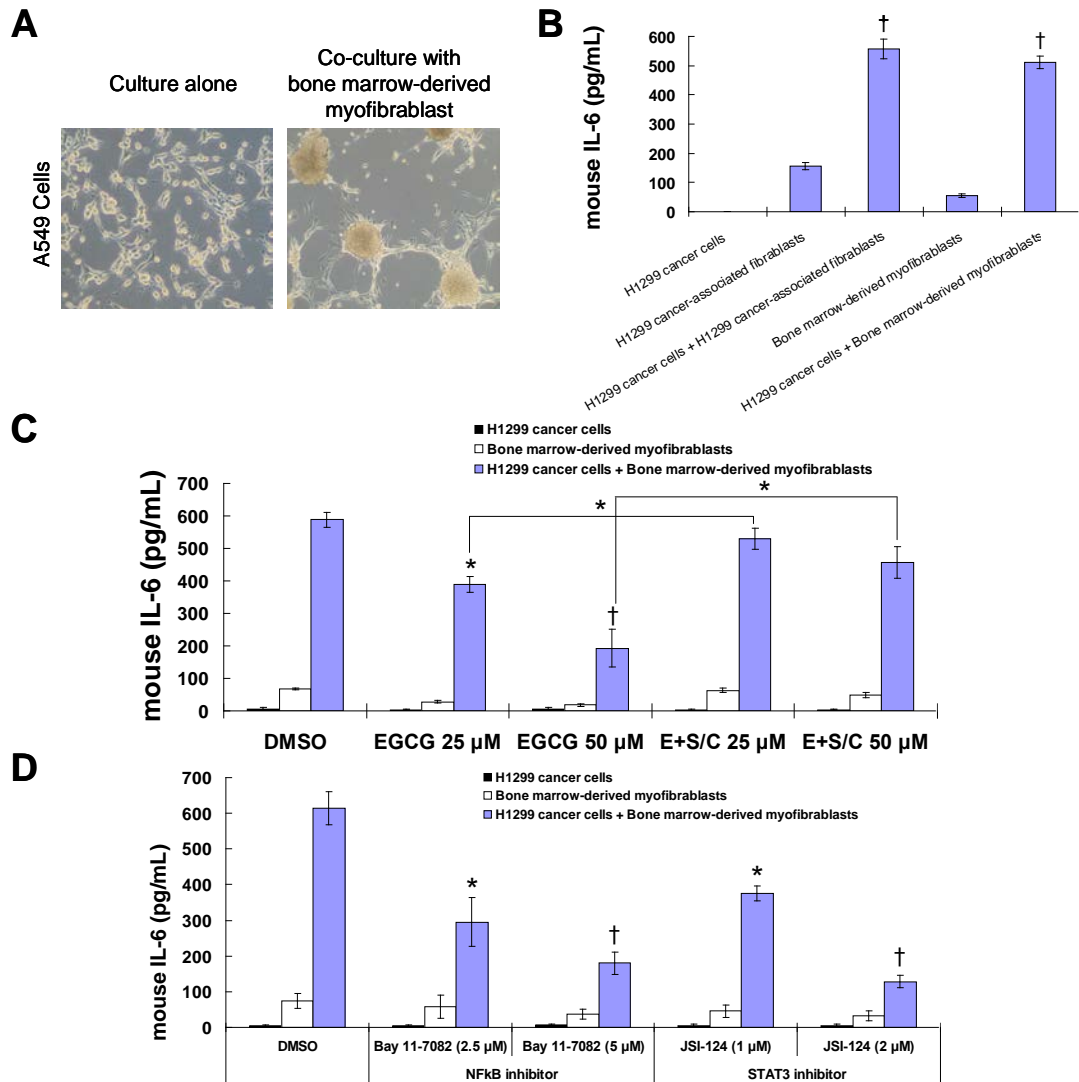


**Figure 19.** EGCG interrupts the support of cancer cells from stromal microenvironment (myofibroblasts). (A) Representative light photomicrographs of A549 human lung cancer cells after a 2-week period of culture, alone or co-cultured with bone marrow-derived myofibroblasts, in stem cell medium (RPMI-1640 medium supplemented with bFGF, EGF and 0.1% bovine serum albumin). (B) The secretion of mouse IL-6 by bone marrow-derived myofibroblasts or H1299 xenograft-derived cancer-associated fibroblasts, cultured alone or co-cultured with H1299 human lung cancer cells. (C and D) Inhibitory effects of EGCG (C) or NF $\kappa$ B and STAT3 inhibitors (D) on the secretion of mouse IL-6 by bone marrow-derived myofibroblasts, cultured alone or co-cultured with H1299 cancer cells.

## Body Weight of A/J mice

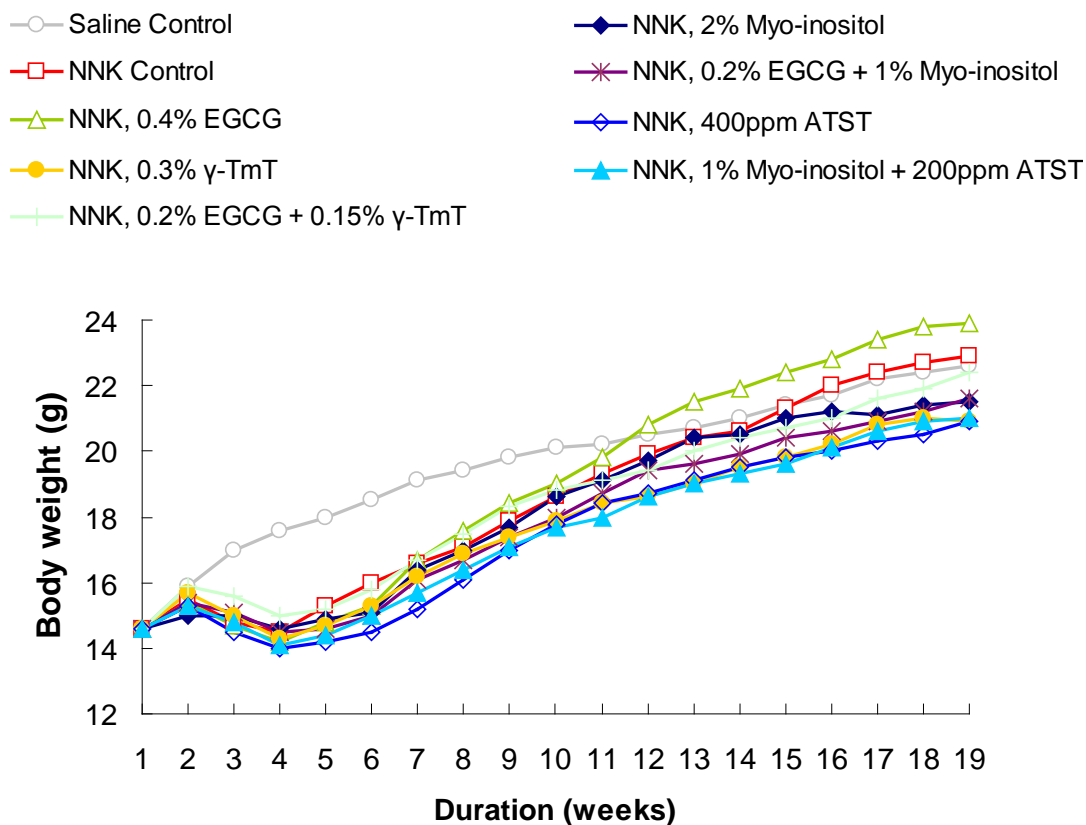


**Figure 20.** Body weight of A/J mice in the study of inhibition of NNK-induced lung tumorigenesis by EGCG,  $\gamma$ -TmT myo-inositol and atorvastatin, alone or in combination. The mice were given two weekly doses of NNK (100 and 75 mg/kg body weight, i.p.) or saline. One week before the first dose of NNK, the mice were treated with EGCG (0.4% in the diet),  $\gamma$ -TmT (0.3% in the diet), EGCG (0.2% in the diet) plus  $\gamma$ -TmT (0.15% in the diet), myo-inositol (2% in drinking fluid), EGCG (0.2% in the diet) plus myo-inositol (1% in drinking fluid), atorvastatin (400 ppm in the diet), or myo-inositol (1% in drinking fluid) plus atorvastatin (200 ppm in the diet) for 20 weeks until the end of the experiment. Body weight was measured weekly.

## Tumor Volume and Weight of CL-13 Allografts

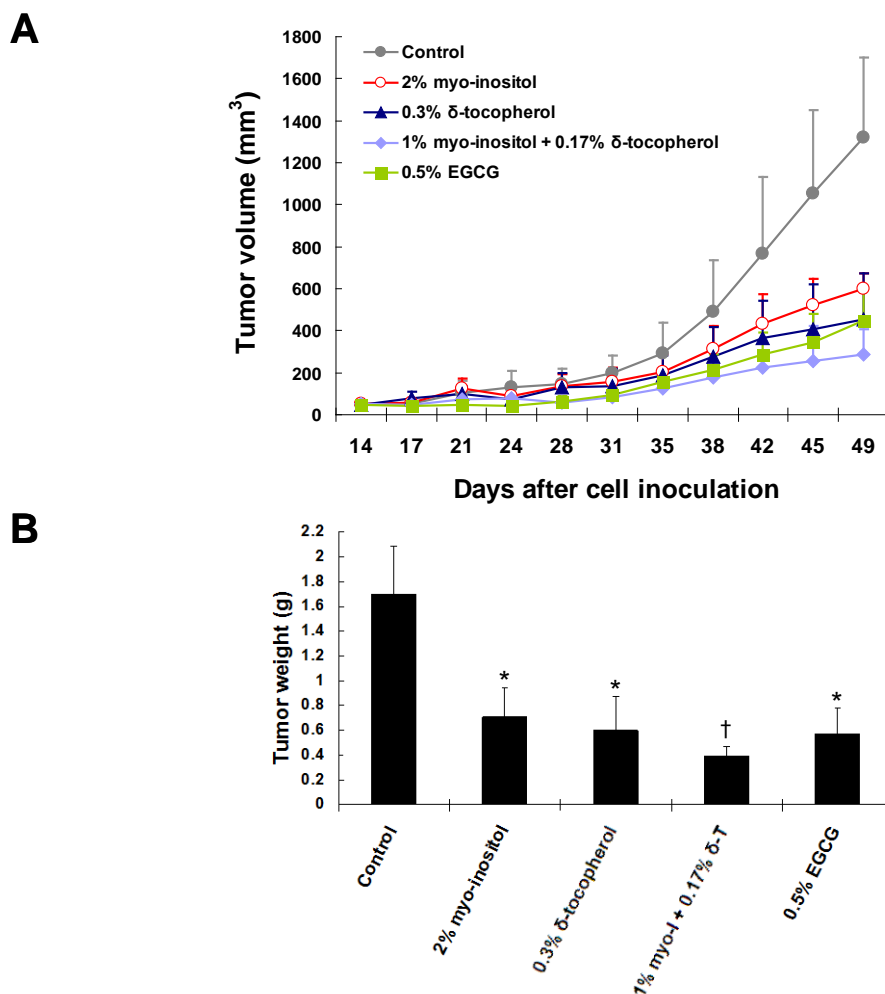


**Figure 21.** Inhibitory effects of EGCG,  $\delta$ -tocopherol and myo-inositol, alone or in combination, on the growth of CL-13 mouse lung cancer cell allografts. (A) Estimated tumor volume as a function of time. (B) Final tumor weight. Values are the mean  $\pm$  SE ( $n=24, 22, 38, 34$  and  $40$ , respectively, for control diet,  $0.5\%$  EGCG,  $0.3\%$   $\delta$ -tocopherol,  $2\%$  myo-inositol, and  $1\%$  myo-inositol plus  $0.17\%$   $\delta$ -tocopherol treatment groups); \* ( $P < 0.05$ ) and † ( $P < 0.01$ ) indicate statistical significance by Student's  $t$ -test for chemopreventive agent diet groups as compared to control diet group.

## Short-term $\gamma$ -TmT and EGCG Treatment at the Tumor Stage

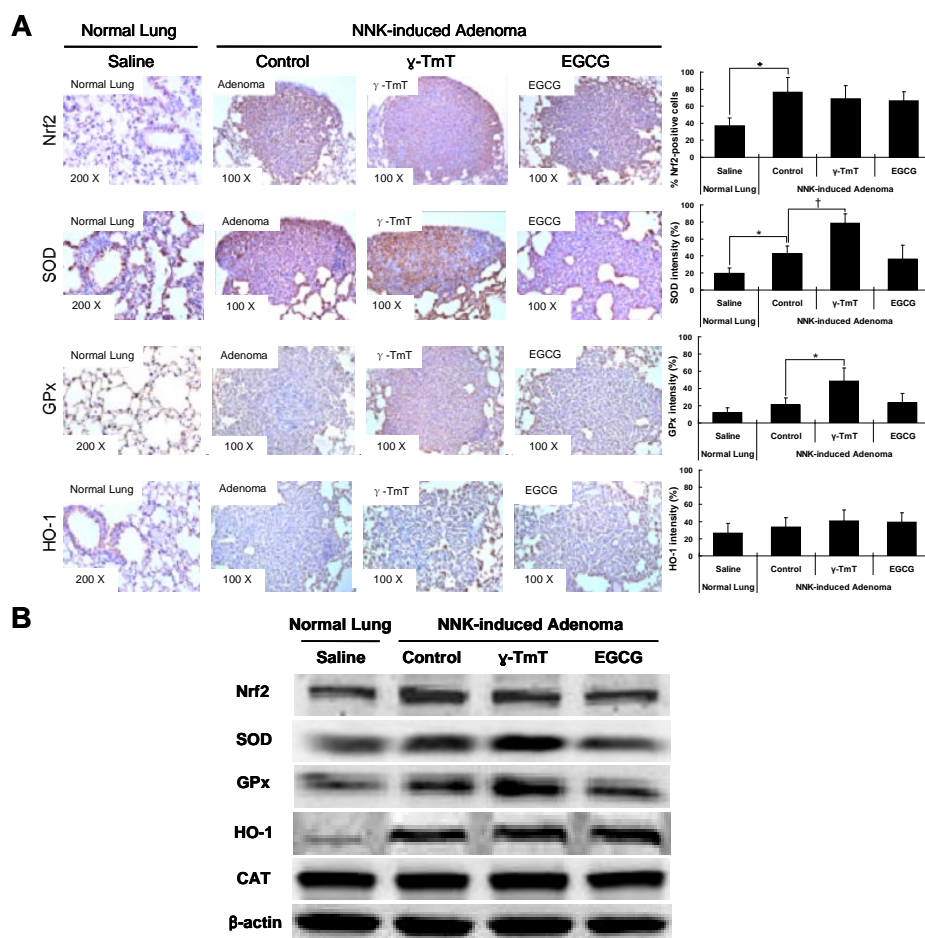


**Figure 22.** Effects of short-term  $\gamma$ -TmT and EGCG treatment at the tumor stage on the levels of Nrf2 and antioxidant enzymes in NNK-induced lung tumors. (A) Representative immunohistochemistry microphotographs for the levels of Nrf2, SOD, glutathione peroxidase and heme oxygenase-1 in saline-treated lung tissues or NNK-induced lung tumors treated with control diet or diet supplemented with 0.3%  $\gamma$ -TmT or 0.4% EGCG for 7 days at the tumor stage and the quantification of the immunohistochemistry results. (B) Western blot of protein levels of Nrf2, SOD, glutathione peroxidase, heme oxygenase-1 and catalase in saline-treated lung tissues or NNK-induced lung tumors treated with control diet or diet supplemented with 0.3%  $\gamma$ -TmT or 0.4% EGCG for 7 days at the tumor stage. Values shown in the bar graphs are means  $\pm$  SD ( $n=25$ , 5 slides  $\times$  5 fields); \* ( $P < 0.05$ ) and † ( $P < 0.01$ ) indicate statistical significance by Student's  $t$ -test for NNK-induced lung tumors treated with control diet as compared to saline-treated lung tissues, or between  $\gamma$ -TmT-treated tumors and control tumors.

## Inhibition of p-c-Jun by Myo-inositol

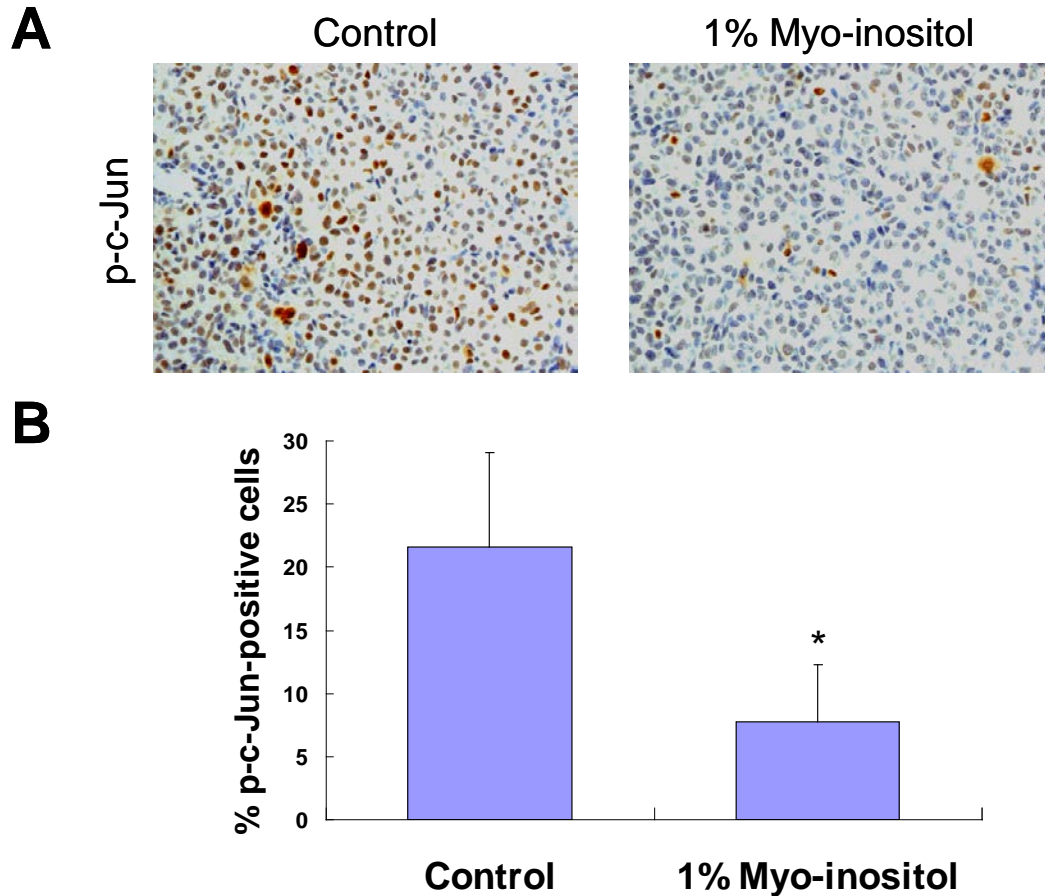


**Figure 23.** Effects of myo-inositol on the level of p-c-Jun in NNK-induced lung tumors. (A) Representative immunohistochemistry microphotographs for the level of p-c-Jun in NNK-induced lung tumors from NNK-treated control mice or NNK-treated mice fed 1% myo-inositol in drinking fluid starting one week before the first dose of NNK injection until the end of the 20-week experiment. (B) Quantification of p-c-Jun-positive cells in NNK-induced lung tumors from control mice or myo-inositol-treated mice. Values shown in the bar graphs are means  $\pm$  SD (n=25, 5 slides  $\times$  5 fields); \* ( $P < 0.05$ ) indicates statistical significance by Student's *t*-test for myo-inositol-treated lung tumors as compared to control lung tumors.

## Synergistic Inhibition by EGCG and Atorvastatin

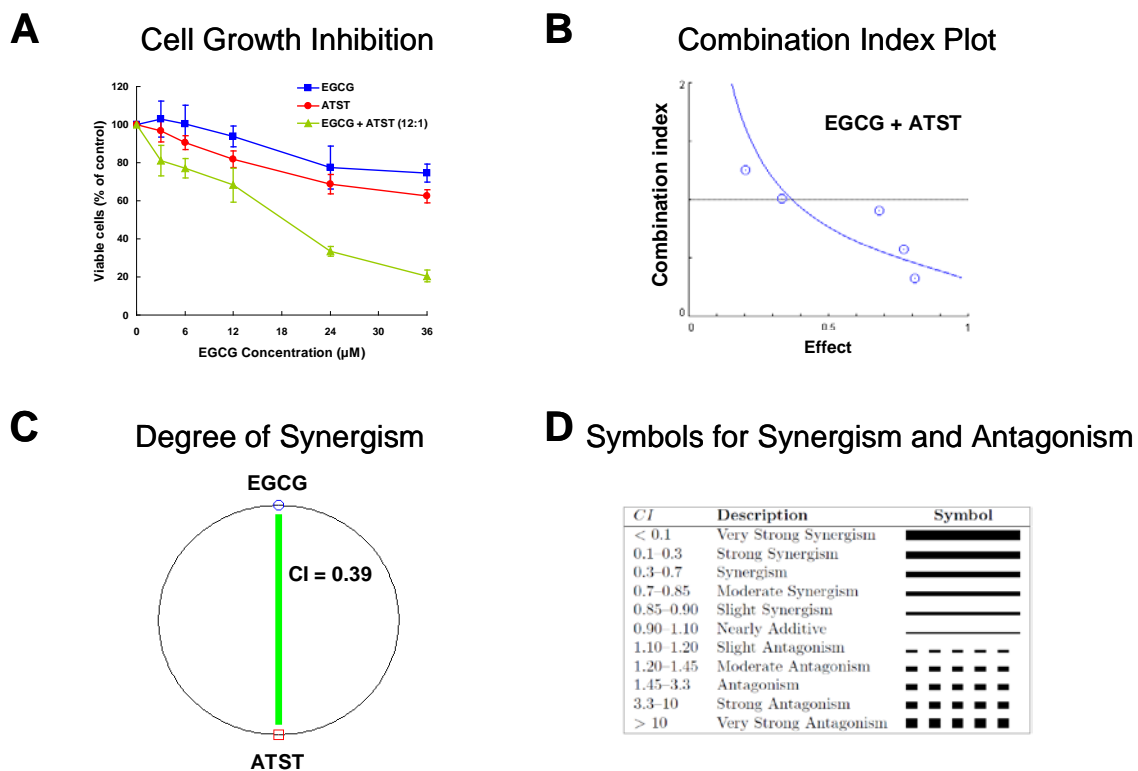


**Figure 24.** Effects of EGCG, atorvastatin, or their combination on the growth of CL-13 mouse lung cancer cells. (A) Growth inhibition curve of CL-13 cells (X axis, concentrations of EGCG; the concentrations of atorvastatin were 1/12 of EGCG, respectively) (B) Combination index plot of CL-13 cells. (C) Degree of synergism analyzed by the method of Chou and Talalay using CompuSyn program. (D) Symbols for synergism and antagonism. The cells were seeded (2000 cells/well) in 96-well plates with serum complete RPMI-1640 media; at 24 h after seeding, cells were treated with different concentrations of EGCG (3, 6, 12, 24 and 36 µM), atorvastatin (0.25, 0.5, 1, 2 and 3 µM), or their combination (12:1 ratio) in 200 µL of serum free RPMI-1640 media. After 48 h of treatments, growth inhibition was measured by MTT assay.

## Synergistic Inhibition by EGCG and Atorvastatin

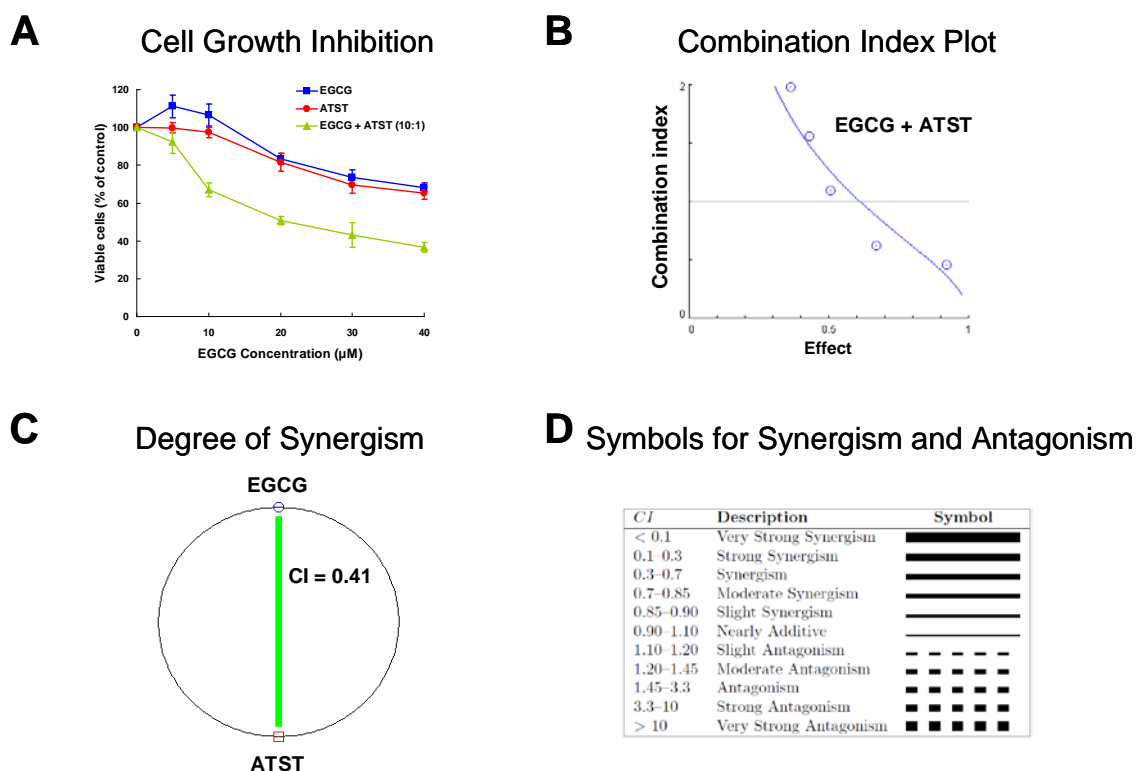


**Figure 25.** Effects of EGCG, atorvastatin, or their combination on the growth of H1299 human lung cancer cells. (A) Growth inhibition curve of H1299 cells (X axis, concentrations of EGCG; the concentrations of atorvastatin were 1/10 of EGCG, respectively) (B) Combination index plot of H1299 cells. (C) Degree of synergism analyzed by the method of Chou and Talalay using CompuSyn program. (D) Symbols for synergism and antagonism. The cells were seeded (1500 cells/well) in 96-well plates with serum complete RPMI-1640 media; at 24 h after seeding, cells were treated with different concentrations of EGCG (5, 10, 20, 30 and 40 µM), atorvastatin (0.5, 1, 2, 3 and 4 µM), or their combination (10:1 ratio) in 200 µL of serum free RPMI-1640 media. After 48 h of treatments, growth inhibition was measured by MTT assay.

## Apoptosis and Bcl-2 Family Proteins

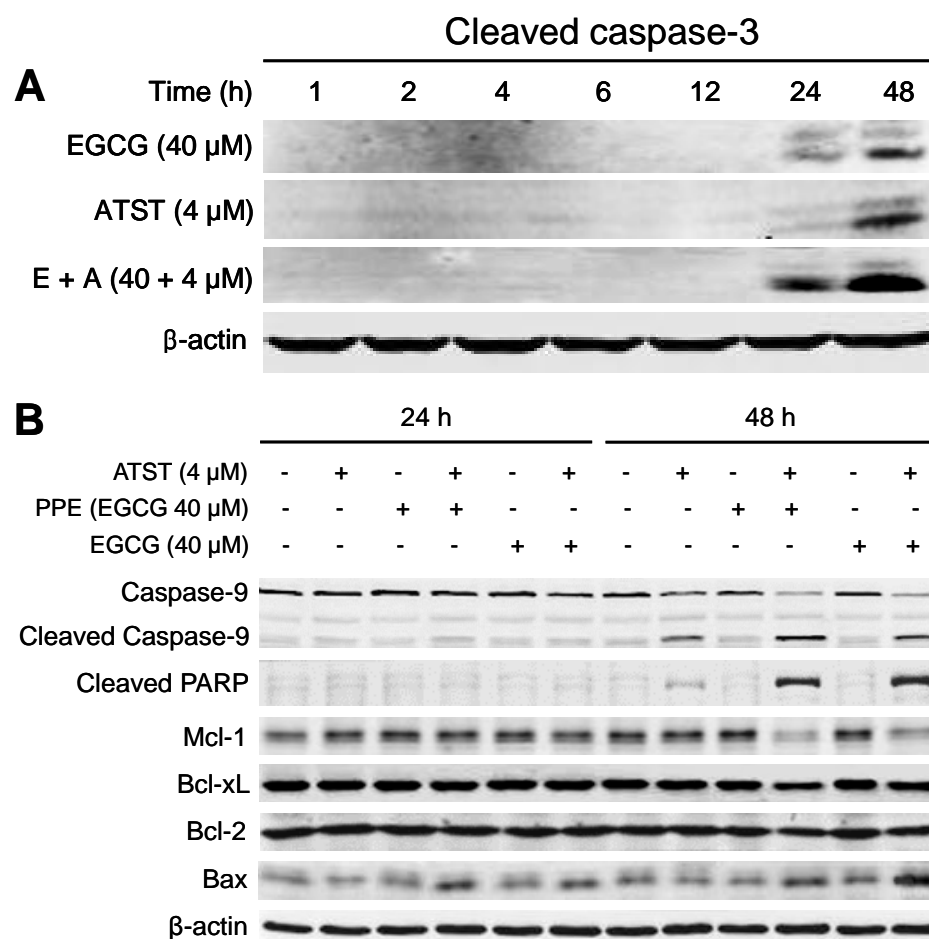


**Figure 26.** Induction of apoptosis and changes in the levels of apoptosis-related Bcl-2 family proteins by EGCG, atorvastatin, or their combination in H1299 lung cancer cells. Western blot analysis on H1299 cells was shown in (A) and (B). (A) Cells were treated with EGCG (40  $\mu$ M, in the presence of SOD and catalase), atorvastatin (4  $\mu$ M), or their combination in the presence of SOD and catalase for 1, 2, 4, 6, 12, 24 and 48 h. (B) Cells were treated with EGCG (40  $\mu$ M, in the presence of SOD and catalase), PPE (40  $\mu$ M EGCG equivalent, in the presence of SOD and catalase), atorvastatin (4  $\mu$ M), or their combination in the presence of SOD and catalase for 24 and 48 h.  $\beta$ -actin was used as an equal loading control for both experiments.

## Anti-apoptotic Bcl-2 Family Proteins

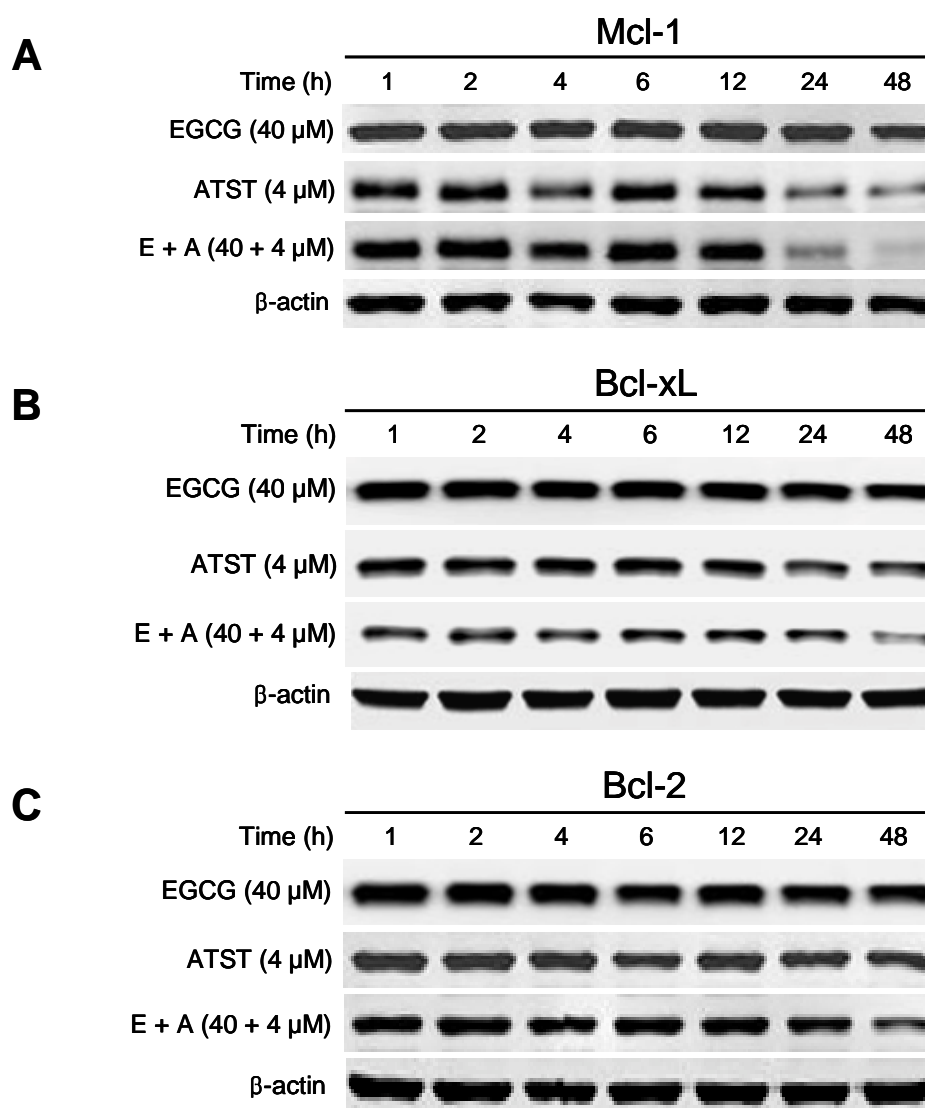


**Figure 27.** Down-regulation of anti-apoptotic Bcl-2 family proteins by EGCG, atorvastatin, or their combination in H1299 lung cancer cells. (A-C) The protein levels of Mcl-1 (A), Bcl-xL (B) and Bcl-2 (C) were determined by Western blot analysis. Cells were treated with EGCG (40  $\mu$ M, in the presence of SOD and catalase), atorvastatin (4  $\mu$ M), or their combination in the presence of SOD and catalase for 1, 2, 4, 6, 12, 24 and 48 h.  $\beta$ -actin was used as an equal loading control.

## Pro-apoptotic Bcl-2 Family Proteins

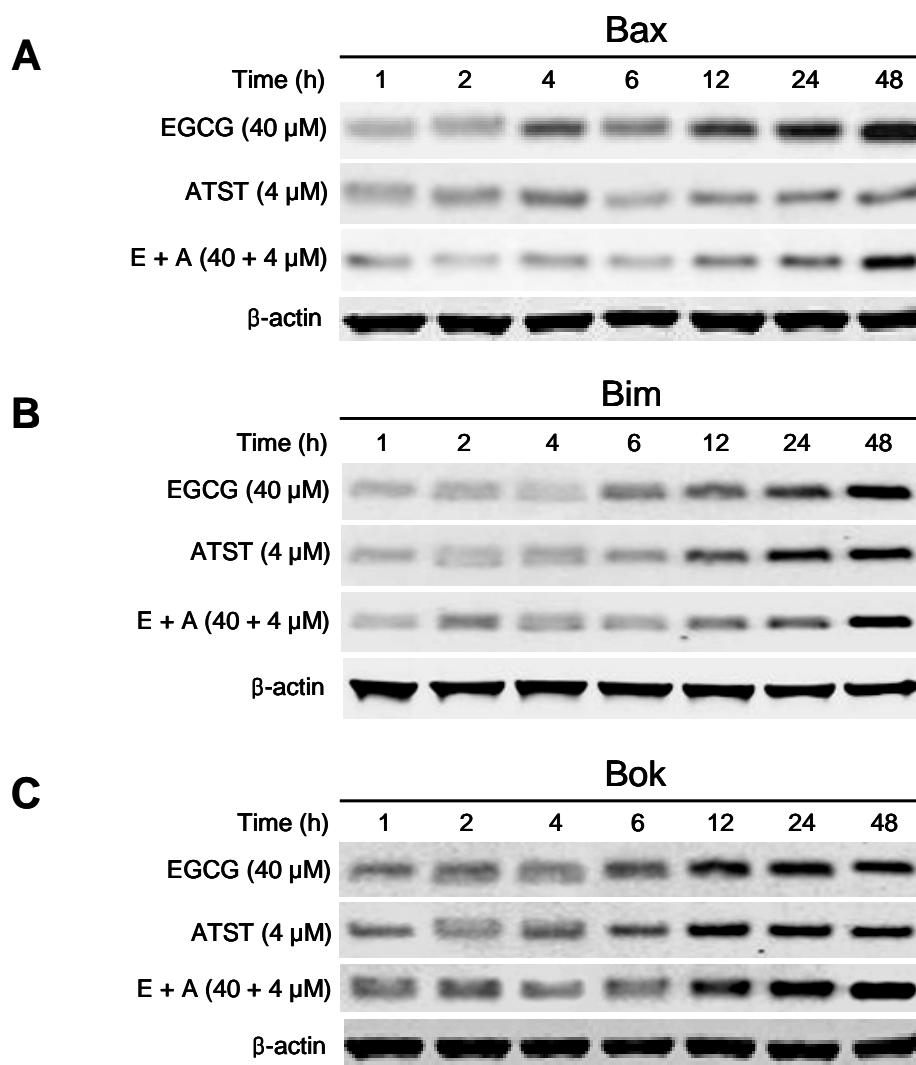


**Figure 28.** Induction of pro-apoptotic Bcl-2 family proteins by EGCG, atorvastatin, or their combination in H1299 lung cancer cells. (A-C) The protein levels of Bax (A), Bim (B) and Bok (C) were determined by Western blot analysis. Cells were treated with EGCG (40  $\mu$ M, in the presence of SOD and catalase), atorvastatin (4  $\mu$ M), or their combination in the presence of SOD and catalase for 1, 2, 4, 6, 12, 24 and 48 h.  $\beta$ -actin was used as an equal loading control.

## Inhibition of HMG-CoA Reductase by Atorvastatin

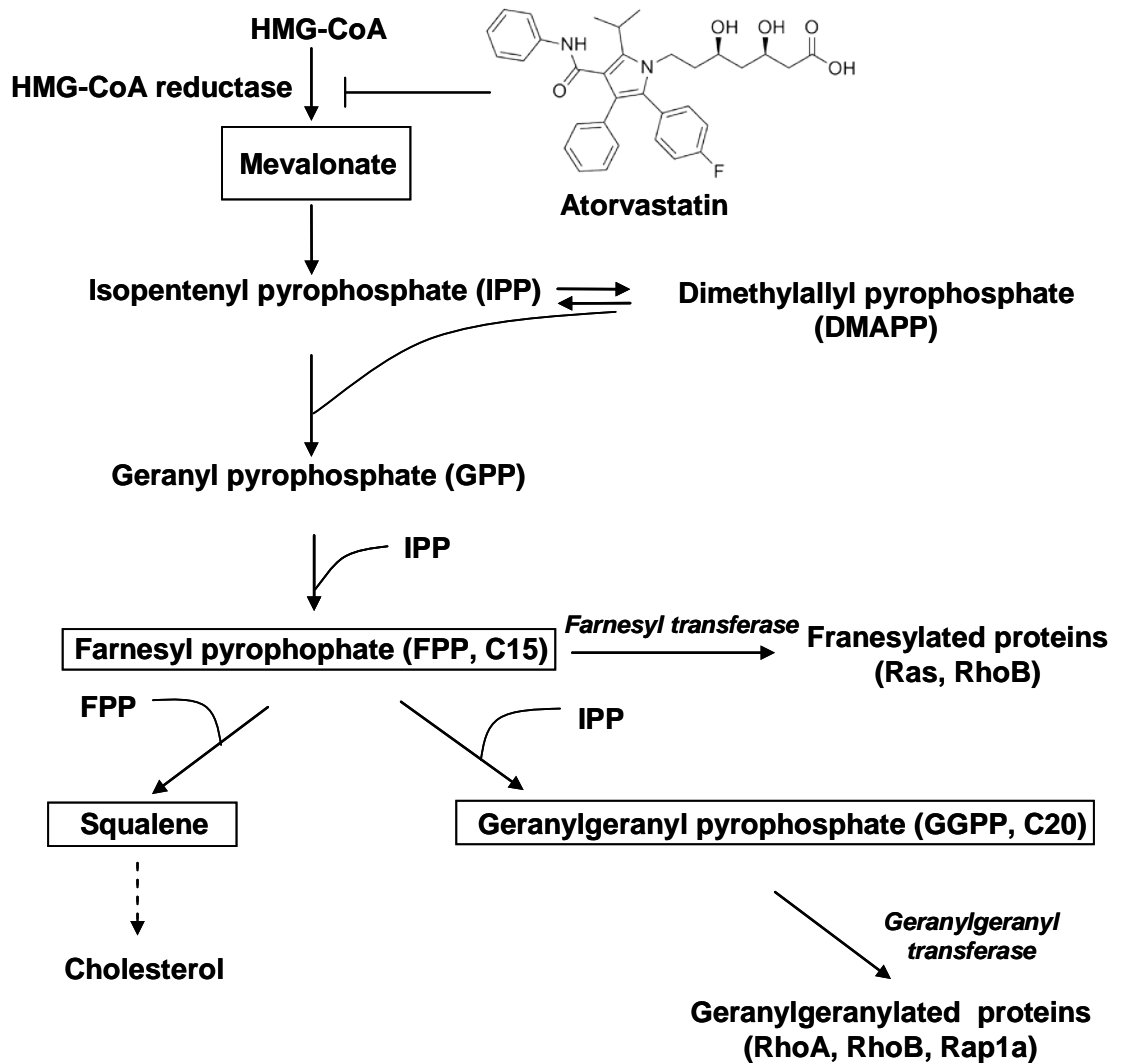


**Figure 29.** A diagram of the cholesterol synthesis pathway and the inhibition of HMG-CoA reductase by atorvastatin (Adopted from Z. Yang *et al.* 2009).

## Effects of Cholesterol Synthesis Intermediates on Atorvastatin-induced Cell Growth Inhibition

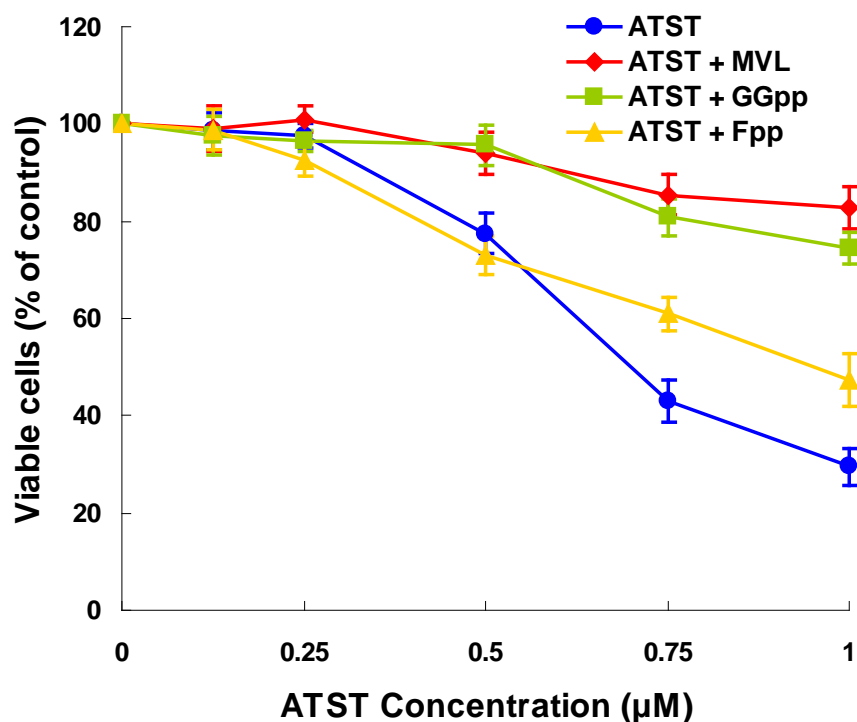


**Figure 30.** Effects of mevalonate, farnesyl pyrophosphate and geranylgeranyl pyrophosphate on the growth inhibition of CL-13 mouse lung cancer cells induced by atorvastatin. CL-13 cells were treated with different concentrations of atorvastatin (0.125, 0.25, 0.5, 0.75 and 1  $\mu\text{M}$ ) in the absence or presence of mevalonate (30  $\mu\text{M}$ ), farnesyl pyrophosphate (10  $\mu\text{M}$ ) or geranylgeranyl pyrophosphate (10  $\mu\text{M}$ ) for 48 h. Viable cells were measured by MTT assay.

## Synergistic Inhibition by $\gamma$ -TmT and Atorvastatin

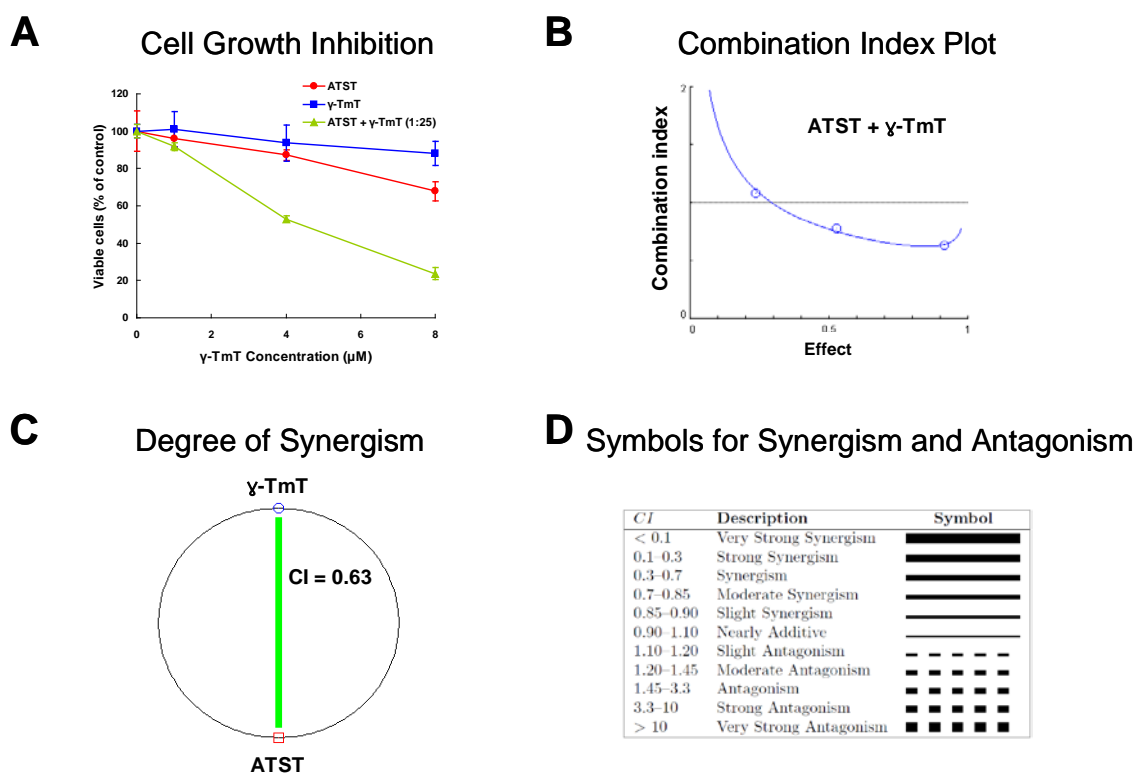


**Figure 31.** Effects of atorvastatin,  $\gamma$ -TmT, or their combination on the growth of CL-13 mouse lung cancer cells. (A) Growth inhibition curve of CL-13 cells (X axis, concentrations of  $\gamma$ -TmT; the concentrations of atorvastatin were 1/25 of  $\gamma$ -TmT, respectively) (B) Combination index plot of CL-13 cells. (C) Degree of synergism analyzed by the method of Chou and Talalay using CompuSyn program. (D) Symbols for synergism and antagonism. The cells were seeded (2000 cells/well) in 96-well plates with serum complete RPMI-1640 media; at 24 h after seeding, cells were treated with different concentrations of  $\gamma$ -TmT (1, 4 and 8  $\mu\text{M}$ ), atorvastatin (0.04, 0.16 and 0.32  $\mu\text{M}$ ), or their combination (25:1 ratio) in 200  $\mu\text{L}$  of serum free RPMI-1640 media. After 48 h of treatments, growth inhibition was measured by MTT assay.

## Cell Growth Inhibition by EGCG and Myo-inositol

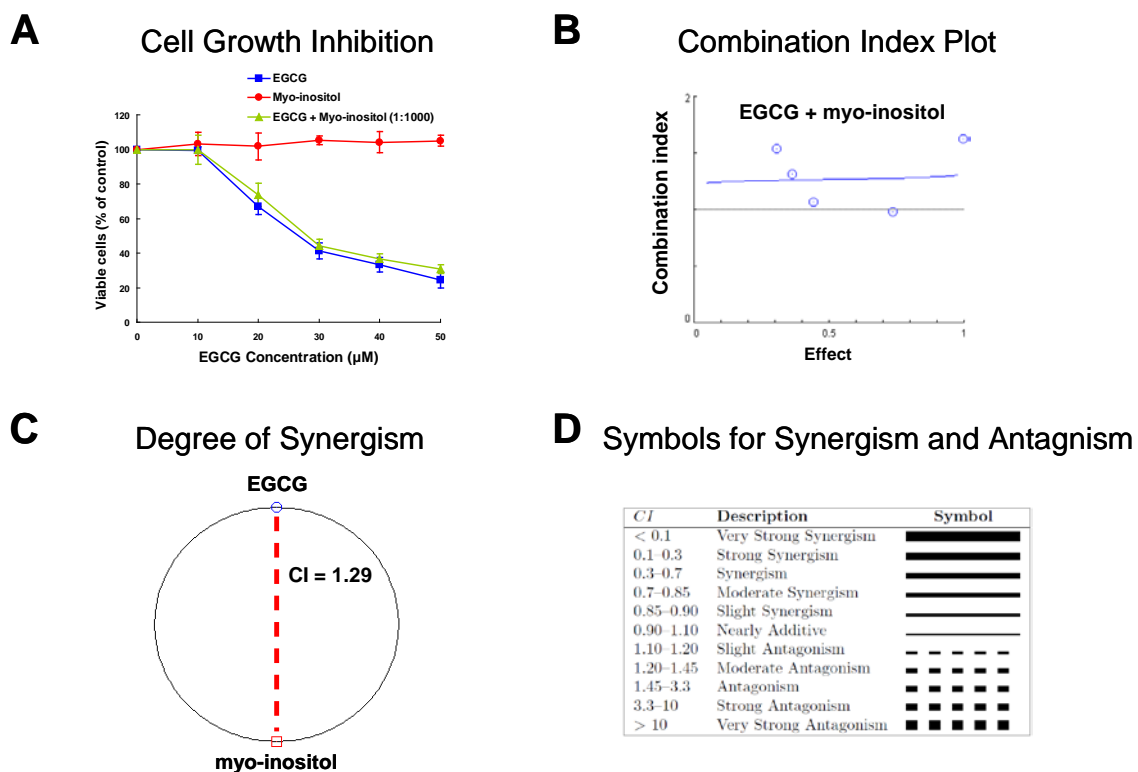


**Figure 32.** Effects of EGCG, myo-inositol, or their combination on the growth of CL-13 mouse lung cancer cells. (A) Growth inhibition curve of CL-13 cells (X axis, concentrations of EGCG; the concentrations of myo-inositol were 1000-fold of EGCG, respectively) (B) Combination index plot of CL-13 cells. (C) Degree of synergism analyzed by the method of Chou and Talalay using CompuSyn program. (D) Symbols for synergism and antagonism. The cells were seeded (2000 cells/well) in 96-well plates with serum complete RPMI-1640 media; at 24 h after seeding, cells were treated with different concentrations of EGCG (10, 20, 30, 40 and 50 µM), myo-inositol (10, 20, 30, 40 and 50 mM), or their combination (1:1000 ratio) in 200 µL of serum free RPMI-1640 media. After 48 h of treatments, growth inhibition was measured by MTT assay.

## Proposed Mechanism of NNK-induced Lung Tumorigenesis and the Inhibition by EGCG

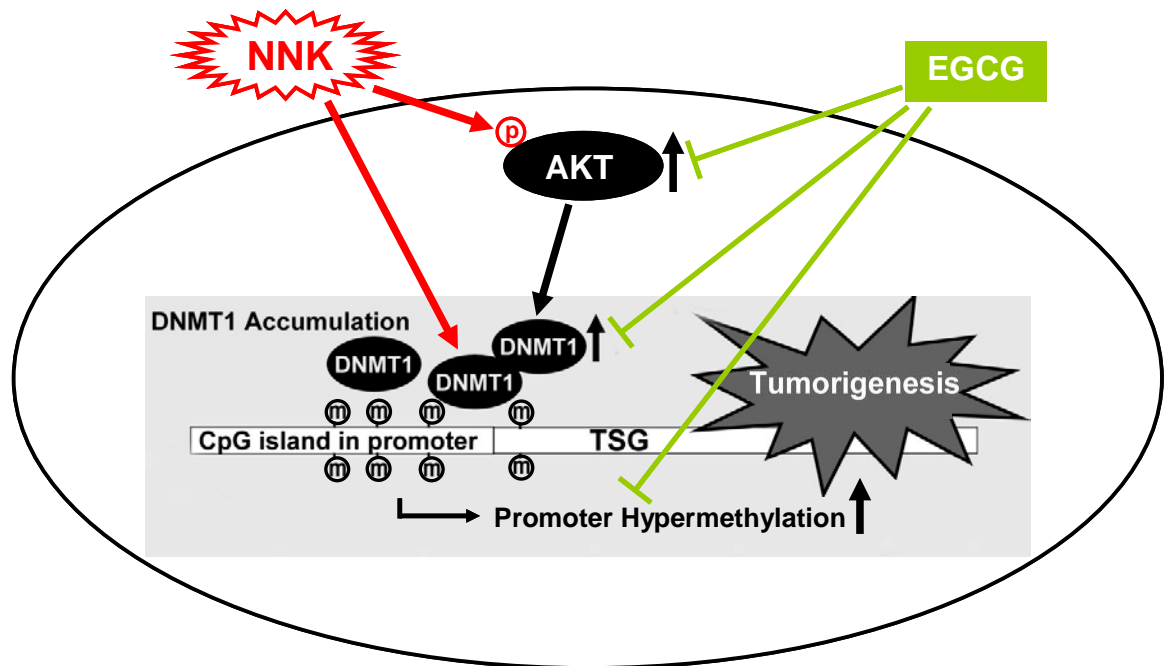


**Figure 33.** Proposed mechanism of NNK-induced lung tumorigenesis through DNMT1 elevation and tumor suppressor genes promoter hypermethylation and the possible inhibitory actions of EGCG.

## References

1. Siegel, R., D. Naishadham, and A. Jemal, *Cancer statistics, 2013*. CA: a cancer journal for clinicians, 2013. **63**(1): p. 11-30.
2. Jemal, A., et al., *Global cancer statistics*. CA: a cancer journal for clinicians, 2011.
3. Weinberg, R.A., *The biology of cancer*. Vol. 255. 2007: Garland Science New York.
4. Anand, P., et al., *Cancer is a preventable disease that requires major lifestyle changes*. Pharmaceutical research, 2008. **25**(9): p. 2097-2116.
5. Croce, C.M., *Oncogenes and cancer*. New England Journal of Medicine, 2008. **358**(5): p. 502-511.
6. Evan, G.I. and K.H. Vousden, *Proliferation, cell cycle and apoptosis in cancer*. Nature, 2001. **411**(6835): p. 342-348.
7. Henley, S.J., et al., *State-Specific Trends in Lung Cancer Incidence and Smoking*. Morbidity and mortality weekly report, 2011. **60**(36): p. 1243-1247.
8. Sekido, Y., K.M. Fong, and J.D. Minna, *Progress in understanding the molecular pathogenesis of human lung cancer*. Biochimica et Biophysica Acta (BBA)-Reviews on Cancer, 1998. **1378**(1): p. F21-F59.
9. Stewart, B.W., P. Kleihues, and I.A.f.R.o. Cancer, *World cancer report*. Vol. 194. 2003: IARC press Lyon.
10. Wood, A.J.J., A. Spira, and D.S. Ettinger, *Multidisciplinary management of lung cancer*. New England Journal of Medicine, 2004. **350**(4): p. 379-392.
11. Berger, D., et al., *Harrison's Principles of Internal Medicine*. 1987.
12. Hamilton, W., et al., *What are the clinical features of lung cancer before the diagnosis is made? A population based case-control study*. Thorax, 2005. **60**(12): p. 1059.
13. Sher, T., G.K. Dy, and A.A. Adjei. *Small cell lung cancer*. 2008. Mayo Clinic.
14. Travis, W.D., *Pathology and genetics of tumours of the lung, pleura, thymus and heart* 2004: Iarc.
15. Travis, W.D., *Pathology of lung cancer*. Clinics in chest medicine, 2002. **23**(1): p. 65-81.
16. Jackman, D.M. and B.E. Johnson, *Small-cell lung cancer*. The Lancet, 2005. **366**(9494): p. 1385-1396.
17. Chute, J.P., et al., *Twenty years of phase III trials for patients with extensive-stage small-cell lung cancer: perceptible progress*. Journal of clinical oncology, 1999. **17**(6): p. 1794-1794.
18. Corvalan, A. and I.I. Wistuba, *Molecular Pathology of Lung Cancer*. Lung Cancer, 2010: p. 1-25.
19. Boffetta, P. and F. Nyberg, *Contribution of environmental factors to cancer risk*. British medical bulletin, 2003. **68**(1): p. 71-94.
20. Lam, W., N. White, and M. Chan-Yeung, *Lung cancer epidemiology and risk factors in Asia and Africa State of the Art*. The International Journal of Tuberculosis and Lung Disease, 2004. **8**(9): p. 1045-1057.
21. Thun, M.J., et al., *Lung cancer occurrence in never-smokers: an analysis of 13 cohorts and 22 cancer registry studies*. PLoS medicine, 2008. **5**(9): p. e185.
22. Mačingová, Z. and S. Filip, *CANCER STEM CELLS—NEW APPROACH TO CANCEROGENESIS AND TREATMENT*. Acta Medica (Hradec Kralove), 2008. **51**(3): p. 139-144.
23. SPIRO, S.G., et al., *Lung cancer: progress in diagnosis, staging and therapy*. Respirology, 2010. **15**(1): p. 44-50.
24. Braithwaite, K.L. and P.H. Rabbitts. *Multi-step evolution of lung cancer*. 1999. Elsevier.
25. Biesalski, H.K., et al., *European Consensus Statement on Lung Cancer: risk factors and prevention*. Lung Cancer Panel. CA: a cancer journal for clinicians, 1998. **48**(3): p. 167-176.
26. Hecht, S.S., *Tobacco smoke carcinogens and lung cancer*. Journal of the National Cancer Institute, 1999. **91**(14): p. 1194-1210.
27. Catelinois, O., et al., *Lung cancer attributable to indoor radon exposure in france: impact of the risk models and uncertainty analysis*. Environmental health perspectives, 2006. **114**(9): p. 1361.
28. O'REILLY, K.M.A., et al., *Asbestos-related lung disease*. Chest, 2007. **100**: p. 2.
29. Leroux, C., et al., *Jaagsiekte Sheep Retrovirus (JSRV): from virus to lung cancer in sheep*. Veterinary research, 2007. **38**(2): p. 211-228.
30. Palmarini, M. and H. Fan, *Retrovirus-induced ovine pulmonary adenocarcinoma, an animal model for lung cancer*. Journal of the National Cancer Institute, 2001. **93**(21): p. 1603-1614.

31. Pope, C.A., et al., *Lung cancer, cardiopulmonary mortality, and long-term exposure to fine particulate air pollution*. JAMA: the journal of the American Medical Association, 2002. **287**(9): p. 1132.
32. Krewski, D., et al., *Mortality and long-term exposure to ambient air pollution: ongoing analyses based on the American Cancer Society cohort*. Journal of Toxicology and Environmental Health, Part A, 2005. **68**(13-14): p. 1093-1109.
33. Subramanian, J. and R. Govindan, *Lung cancer in never smokers: a review*. Journal of clinical oncology, 2007. **25**(5): p. 561-570.
34. D'Addario, G. and E. Felip, *Non-small-cell lung cancer: ESMO clinical recommendations for diagnosis, treatment and follow-up*. Ann Oncol, 2008. **19**(suppl 2).
35. Gorlova, O.Y., et al., *Aggregation of cancer among relatives of never - smoking lung cancer patients*. International Journal of Cancer, 2007. **121**(1): p. 111-118.
36. Hackshaw, A.K., M.R. Law, and N.J. Wald, *The accumulated evidence on lung cancer and environmental tobacco smoke*. Bmj, 1997. **315**(7114): p. 980-988.
37. Bartsch, H., et al., *Genetic polymorphism of CYP genes, alone or in combination, as a risk modifier of tobacco-related cancers*. Cancer Epidemiology Biomarkers & Prevention, 2000. **9**(1): p. 3-28.
38. Hecht, S.S., *Tobacco carcinogens, their biomarkers and tobacco-induced cancer*. Nature Reviews Cancer, 2003. **3**(10): p. 733-744.
39. Organization, W.H., *Tobacco free initiative [website]*, 2010.
40. Ruano-Ravina, A., A. Figueiras, and J. Barros-Dios, *Lung cancer and related risk factors: an update of the literature*. Public Health, 2003. **117**(3): p. 149-156.
41. Soria, J.C., et al., *Chemoprevention of lung cancer*. The lancet oncology, 2003. **4**(11): p. 659-669.
42. Wei, Q. and M.R. Spitz, *The role of DNA repair capacity in susceptibility to lung cancer: a review*. Cancer and Metastasis Reviews, 1997. **16**(3): p. 295-307.
43. Matakidou, A., T. Eisen, and R. Houlston, *Systematic review of the relationship between family history and lung cancer risk*. British journal of cancer, 2005. **93**(7): p. 825-833.
44. Schwartz, A.G., *Genetic Predisposition to Lung Cancer\**. Chest, 2004. **125**(5 suppl): p. 86S-89S.
45. You, M., et al., *Fine mapping of chromosome 6q23-25 region in familial lung cancer families reveals RGS17 as a likely candidate gene*. Clinical cancer research, 2009. **15**(8): p. 2666-2674.
46. Riely, G.J., J. Marks, and W. Pao, *KRAS mutations in non-small cell lung cancer*. Proceedings of the American Thoracic Society, 2009. **6**(2): p. 201-205.
47. Johnson, L., et al., *Somatic activation of the K-ras oncogene causes early onset lung cancer in mice*. Nature, 2001. **410**(6832): p. 1111-1116.
48. Stehelin, D., et al., *DNA related to the transforming gene (s) of avian sarcoma viruses is present in normal avian DNA*. 1976.
49. Futreal, P.A., et al., *A census of human cancer genes*. Nature Reviews Cancer, 2004. **4**(3): p. 177-183.
50. Devereux, T.R. and S.A. Belinsky, *Role of ras protooncogene activation in the formation of spontaneous and nitrosamine-induced lung tumors in the resistant C3H mouse*. Carcinogenesis, 1991. **12**(2): p. 299.
51. Shields, P., *Molecular epidemiology of lung cancer*. Annals of oncology, 1999. **10**(suppl 5): p. S7.
52. Fisher, G.H., et al., *Induction and apoptotic regression of lung adenocarcinomas by regulation of a K-Ras transgene in the presence and absence of tumor suppressor genes*. Genes & development, 2001. **15**(24): p. 3249-3262.
53. Jackson, E.L., et al., *Analysis of lung tumor initiation and progression using conditional expression of oncogenic K-ras*. Genes & development, 2001. **15**(24): p. 3243-3248.
54. Lee, W.H., et al., *The retinoblastoma susceptibility gene encodes a nuclear phosphoprotein associated with DNA binding activity*. 1987.
55. Fung, Y., et al., *Structural evidence for the authenticity of the human retinoblastoma gene*. Science, 1987. **236**(4809): p. 1657-1661.
56. Hanahan, D. and R.A. Weinberg, *The hallmarks of cancer*. cell, 2000. **100**(1): p. 57-70.
57. Burkhart, D.L. and J. Sage, *Cellular mechanisms of tumour suppression by the retinoblastoma gene*. Nature Reviews Cancer, 2008. **8**(9): p. 671-682.
58. Bourdon, J.C., *p53 and its isoforms in cancer*. British journal of cancer, 2007. **97**(3): p. 277-282.
59. Bennett, W.P., et al., *Molecular epidemiology of human cancer risk: gene-environment interactions and p53 mutation spectrum in human lung cancer*. The Journal of pathology, 1999. **187**(1): p. 8-18.

60. Whibley, C., P.D.P. Pharoah, and M. Hollstein, *p53 polymorphisms: cancer implications*. Nature Reviews Cancer, 2009. **9**(2): p. 95-107.
61. Rocco, J.W. and D. Sidransky, *p16 (MTS-1/CDKN2/INK4a) in cancer progression*. Experimental cell research, 2001. **264**(1): p. 42-55.
62. Cairns, P., et al., *Frequency of homozygous deletion at p16/CDKN2 in primary human tumours*. Nature genetics, 1995. **11**(2): p. 210-212.
63. Belinsky, S.A., et al., *Aberrant methylation of p16INK4a is an early event in lung cancer and a potential biomarker for early diagnosis*. Proceedings of the National Academy of Sciences, 1998. **95**(20): p. 11891.
64. Panani, A.D. and C. Roussos, *Cytogenetic and molecular aspects of lung cancer*. Cancer letters, 2006. **239**(1): p. 1-9.
65. Massion, P.P. and D.P. Carbone, *The molecular basis of lung cancer: molecular abnormalities and therapeutic implications*. Respiratory Research, 2003. **4**(1): p. 12.
66. Beranek, D.T., C.C. Weis, and D.H. Swenson, *A comprehensive quantitative analysis of methylated and ethylated DNA using high pressure liquid chromatography*. Carcinogenesis, 1980. **1**(7): p. 595-606.
67. Shmookler, R.R.J. and S. Goldstein, *Loss of reiterated DNA sequences during serial passage of human diploid fibroblasts*. cell, 1980. **21**(3): p. 739.
68. Lapeyre, J.N., M.S. Walker, and F.F. Becker, *DNA methylation and methylase levels in normal and malignant mouse hepatic tissues*. Carcinogenesis, 1981. **2**(9): p. 873-878.
69. Ehrlich, M., *DNA methylation in cancer: too much, but also too little*. Oncogene, 2002. **21**(35): p. 5400.
70. Jones, P.A. and S.M. Taylor, *Cellular differentiation, cytidine analogs and DNA methylation*. cell, 1980. **20**(1): p. 85.
71. Shen, C. and T. Maniatis, *Tissue-specific DNA methylation in a cluster of rabbit beta-like globin genes*. Proceedings of the National Academy of Sciences, 1980. **77**(11): p. 6634.
72. McGhee, J.D. and G.D. Ginder, *Specific DNA methylation sites in the vicinity of the chicken  $\beta$ -globin genes*. 1979.
73. Shiraishi, M. and T. Sekiya, *Change in methylation status of DNA of remaining allele in human lung cancers with loss of heterozygosity on chromosomes 3p and 13q*. Cancer Science, 1989. **80**(10): p. 924-927.
74. Costello, J.F., et al., *Aberrant CpG-island methylation has non-random and tumour-type-specific patterns*. Nature genetics, 2000. **24**(2): p. 132-138.
75. Merlo, A., et al., *5' CpG island methylation is associated with transcriptional silencing of the tumour suppressor p16/CDKN2/MTS1 in human cancers*. Nature medicine, 1995. **1**(7): p. 686-692.
76. Ahuja, N., et al., *Association between CpG island methylation and microsatellite instability in colorectal cancer*. Cancer Research, 1997. **57**(16): p. 3370.
77. Zöchbauer-Müller, S., et al., *5' CpG island methylation of the FHIT gene is correlated with loss of gene expression in lung and breast cancer*. Cancer Research, 2001. **61**(9): p. 3581.
78. Bestor, T.H., *Activation of mammalian DNA methyltransferase by cleavage of a Zn binding regulatory domain*. The EMBO journal, 1992. **11**(7): p. 2611.
79. Li, E., T.H. Bestor, and R. Jaenisch, *Targeted mutation of the DNA methyltransferase gene results in embryonic lethality*. cell, 1992. **69**(6): p. 915.
80. Fatemi, M., et al., *Dnmt3a and Dnmt1 functionally cooperate during de novo methylation of DNA*. European Journal of Biochemistry, 2002. **269**(20): p. 4981-4984.
81. Miyake, T., et al., *Expression of DNA Methyltransferase (DNMT) 1, 3a and 3b Proteins in Human Hepatocellular Carcinoma*. Yonago Acta medica, 2010. **53**(1): p. 1-7.
82. Qu, Y., et al., *Overexpression of DNA methyltransferases 1, 3a, and 3b significantly correlates with retinoblastoma tumorigenesis*. American journal of clinical pathology, 2010. **134**(5): p. 826-834.
83. Rahman, M.M., et al., *DNA methyltransferases 1, 3a, and 3b overexpression and clinical significance in gastroenteropancreatic neuroendocrine tumors*. Human pathology, 2010. **41**(8): p. 1069-1078.
84. Lin, R.K., et al., *The tobacco-specific carcinogen NNK induces DNA methyltransferase 1 accumulation and tumor suppressor gene hypermethylation in mice and lung cancer patients*. The Journal of clinical investigation, 2010. **120**(2): p. 521.

85. Patra, S.K., et al., *DNA methyltransferase and demethylase in human prostate cancer*. Molecular carcinogenesis, 2002. **33**(3): p. 163-171.
86. Girault, I., et al., *Expression analysis of DNA methyltransferases 1, 3A, and 3B in sporadic breast carcinomas*. Clinical cancer research, 2003. **9**(12): p. 4415-4422.
87. Etoh, T., et al., *Increased DNA methyltransferase 1 (DNMT1) protein expression correlates significantly with poorer tumor differentiation and frequent DNA hypermethylation of multiple CpG islands in gastric cancers*. The American journal of pathology, 2004. **164**(2): p. 689-699.
88. Okano, M., et al., *DNA methyltransferases Dnmt3a and Dnmt3b are essential for de novo methylation and mammalian development*. cell, 1999. **99**(3): p. 247-257.
89. Clark, S.J. and J. Melki, *DNA methylation and gene silencing in cancer: which is the guilty party?* Oncogene, 2002. **21**(35): p. 5380.
90. Rountree, M.R., K.E. Bachman, and S.B. Baylin, *DNMT1 binds HDAC2 and a new co-repressor, DMAP1, to form a complex at replication foci*. Nature genetics, 2000. **25**(3): p. 269-277.
91. Robertson, K.D., et al., *DNMT1 forms a complex with Rb, E2F1 and HDAC1 and represses transcription from E2F-responsive promoters*. Nature genetics, 2000. **25**(3): p. 338-342.
92. Stoner, G.D., *Introduction to mouse lung tumorigenesis*. Experimental lung research, 1998. **24**(4): p. 375.
93. Shimkin, M.B. and G.D. Stoner, *Lung tumors in mice: application to carcinogenesis bioassay*. Adv. Cancer Res, 1975. **21**(1): p. 58.
94. Jones, P.A. and P.W. Laird, *Cancer-epigenetics comes of age*. Nature genetics, 1999. **21**(2): p. 163-167.
95. Ehrlich, M., *DNA hypomethylation in cancer cells*. Epigenomics, 2009. **1**(2): p. 239-259.
96. Yanagawa, N., et al., *Demethylation of the synuclein  $\gamma$  gene CpG island in primary gastric cancers and gastric cancer cell lines*. Clinical cancer research, 2004. **10**(7): p. 2447-2451.
97. Wang, Q., et al., *Hypomethylation of WNT5A, CRIP1 and S100P in prostate cancer*. Oncogene, 2007. **26**(45): p. 6560-6565.
98. Shao, C., et al., *Integrated, genome-wide screening for hypomethylated oncogenes in salivary gland adenoid cystic carcinoma*. Clinical cancer research, 2011. **17**(13): p. 4320.
99. Belinsky, S.A., *Gene-promoter hypermethylation as a biomarker in lung cancer*. Nature Reviews Cancer, 2004. **4**(9): p. 707-717.
100. Belinsky, S.A., *Silencing of genes by promoter hypermethylation: key event in rodent and human lung cancer*. Carcinogenesis, 2005. **26**(9): p. 1481-1487.
101. Taby, R. and J.P.J. Issa, *Cancer epigenetics*. CA: a cancer journal for clinicians, 2010. **60**(6): p. 376-392.
102. Baylin, S.B., et al., *DNA methylation patterns of the calcitonin gene in human lung cancers and lymphomas*. Cancer Research, 1986. **46**(6): p. 2917.
103. Sakai, T., et al., *Allele-specific hypermethylation of the retinoblastoma tumor-suppressor gene*. American journal of human genetics, 1991. **48**(5): p. 880.
104. Greger, V., et al., *Epigenetic changes may contribute to the formation and spontaneous regression of retinoblastoma*. Human genetics, 1989. **83**(2): p. 155-158.
105. Slavotinek, A.M., et al., *Methylation of the CDH1 promoter as the second genetic hit in hereditary diffuse gastric cancer*. Nature genetics, 2000. **26**: p. 17.
106. Herman, J.G., et al., *Inactivation of the CDKN2/p16/MTS1 gene is frequently associated with aberrant DNA methylation in all common human cancers*. Cancer Research, 1995. **55**(20): p. 4525.
107. Dammann, R., et al., *Epigenetic inactivation of a RAS association domain family protein from the lung tumour suppressor locus 3p21. 3*. Nature genetics, 2000. **25**(3): p. 315-319.
108. Dammann, R., G. Yang, and G.P. Pfeifer, *Hypermethylation of the cpG island of Ras association domain family 1A (RASSF1A), a putative tumor suppressor gene from the 3p21. 3 locus, occurs in a large percentage of human breast cancers*. Cancer Research, 2001. **61**(7): p. 3105.
109. Hesson, L., et al., *Frequent epigenetic inactivation of RASSF1A and BLU genes located within the critical 3p21. 3 region in gliomas*. Oncogene, 2004. **23**(13): p. 2408-2419.
110. van Engeland, M., et al., *K-ras mutations and RASSF 1 A promoter methylation in colorectal cancer*. Oncogene, 2002. **21**(23): p. 3792-3795.
111. Morrissey, C., et al., *Epigenetic inactivation of the RASSF1A 3p21. 3 tumor suppressor gene in both clear cell and papillary renal cell carcinoma*. Cancer Research, 2001. **61**(19): p. 7277.

112. Vaissière, T., et al., *Quantitative analysis of DNA methylation profiles in lung cancer identifies aberrant DNA methylation of specific genes and its association with gender and cancer risk factors*. Cancer Research, 2009. **69**(1): p. 243.
113. Toyooka, K.O., et al., *Loss of expression and aberrant methylation of the CDH13 (H-cadherin) gene in breast and lung carcinomas*. Cancer Research, 2001. **61**(11): p. 4556.
114. Toyooka, S., et al., *Aberrant methylation of the CDH13 (H-cadherin) promoter region in colorectal cancers and adenomas*. Cancer Research, 2002. **62**(12): p. 3382.
115. Feng, Q., et al., *DNA methylation in tumor and matched normal tissues from non-small cell lung cancer patients*. Cancer Epidemiology Biomarkers & Prevention, 2008. **17**(3): p. 645-654.
116. Missaoui, N., et al., *Promoter hypermethylation of CDH13, DAPK1 and TWIST1 genes in precancerous and cancerous lesions of the uterine cervix*. Pathology-Research and Practice, 2011. **207**(1): p. 37-42.
117. Pehlivan, S., et al., *Gene methylation of SFRP2, P16, DAPK1, HIC1, and MGMT and KRAS mutations in sporadic colorectal cancer*. Cancer Genetics and Cytogenetics, 2010. **201**(2): p. 128-132.
118. Buckingham, L., et al., *PTEN, RASSF1 and DAPK site - specific hypermethylation and outcome in surgically treated stage I and II nonsmall cell lung cancer patients*. International Journal of Cancer, 2010. **126**(7): p. 1630-1639.
119. Lu, C., et al., *Prognostic factors in resected stage I non-small-cell lung cancer: A multivariate analysis of six molecular markers*. Journal of clinical oncology, 2004. **22**(22): p. 4575-4583.
120. Hecht, S.S., *Biochemistry, biology, and carcinogenicity of tobacco-specific N-nitrosamines*. Chemical research in toxicology, 1998. **11**(6): p. 559-603.
121. Tuveson, D.A. and T. Jacks, *Modeling human lung cancer in mice: similarities and shortcomings*. Oncogene, 1999. **18**(38): p. 5318.
122. Meuwissen, R. and A. Berns, *Mouse models for human lung cancer*. Genes & development, 2005. **19**(6): p. 643-664.
123. You, M., et al., *SHORT COMMUNICATION: K-ras mutations in benzotrichloride-induced lung tumors of A/J mice*. Carcinogenesis, 1993. **14**(6): p. 1247-1249.
124. Herzog, C.R., et al., *Cdkn2a encodes functional variation of p16INK4a but not p14ARF, which confers selection in mouse lung tumorigenesis*. Molecular carcinogenesis, 1999. **25**(2): p. 92-98.
125. Devereux, T.R. and S.A. Belinsky, *Role of ras protooncogene activation in the formation of spontaneous and nitrosamine-induced lung tumors in the resistant C3H mouse*. Carcinogenesis, 1991. **12**(2): p. 299-303.
126. Nikitin, A.Y., et al., *Classification of proliferative pulmonary lesions of the mouse recommendations of the mouse models of human cancers consortium*. Cancer Research, 2004. **64**(7): p. 2307-2316.
127. Thaete, L.G. and A.M. Malkinson, *Cells of origin of primary pulmonary neoplasms in mice: morphologic and histochemical studies*. Experimental lung research, 1991. **17**(2): p. 219-228.
128. Belinsky, S.A., et al., *Role of Clara cells and type II cells in the development of pulmonary tumors in rats and mice following exposure to a tobacco-specific nitrosamine*. Experimental lung research, 1991. **17**(2): p. 263-278.
129. Belinsky, S.A., et al., *Role of the Alveolar Type II Cell in the Development and Progression of Pulmonary Tumors Induced by 4-(Methylnitrosamino)-(3-pyridyl)-1-butanone in the A/J Mouse*. Cancer Research, 1992. **52**(11): p. 3164.
130. Thaete, L. and A. Malkinson, *Differential staining of normal and neoplastic mouse lung epithelia by succinate dehydrogenase histochemistry*. Cancer letters, 1990. **52**(3): p. 219-227.
131. Lu, G., et al., *Inhibition of adenoma progression to adenocarcinoma in a 4-(methylnitrosamino)-1-(3-pyridyl)-1-butanone-induced lung tumorigenesis model in A/J mice by tea polyphenols and caffeine*. Cancer Research, 2006. **66**(23): p. 11494.
132. Li, G.X., et al., *Pro-oxidative activities and dose-response relationship of (-)-epigallocatechin-3-gallate in the inhibition of lung cancer cell growth: a comparative study in vivo and in vitro*. Carcinogenesis, 2010. **31**(5): p. 902.
133. Lu, G., et al., *Synergistic inhibition of lung tumorigenesis by a combination of green tea polyphenols and atorvastatin*. Clinical cancer research, 2008. **14**(15): p. 4981-4988.
134. Yang, C.S., et al., *Cancer prevention by tea: animal studies, molecular mechanisms and human relevance*. Nature Reviews Cancer, 2009. **9**(6): p. 429-439.

135. Lambert, J.D., et al., *Inhibition of carcinogenesis by polyphenols: evidence from laboratory investigations*. The American journal of clinical nutrition, 2005. **81**(1): p. 284S-291S.
136. Dutt, A. and K.-K. Wong, *Mouse models of lung cancer*. Clinical cancer research, 2006. **12**(14): p. 4396s-4402s.
137. Pulling, L.C., et al., *Aberrant promoter hypermethylation of the death-associated protein kinase gene is early and frequent in murine lung tumors induced by cigarette smoke and tobacco carcinogens*. Cancer Research, 2004. **64**(11): p. 3844.
138. Pulling, L.C., D.M. Klinge, and S.A. Belinsky, *p16INK4a and beta-catenin alterations in rat liver tumors induced by NNK*. Carcinogenesis, 2001. **22**(3): p. 461-466.
139. Vuilleminot, B.R., J.A. Hutt, and S.A. Belinsky, *Gene promoter hypermethylation in mouse lung tumors*. Molecular cancer research, 2006. **4**(4): p. 267.
140. Hutt, J.A., et al., *Life-span inhalation exposure to mainstream cigarette smoke induces lung cancer in B6C3F1 mice through genetic and epigenetic pathways*. Carcinogenesis, 2005. **26**(11): p. 1999-2009.
141. Belinsky, S.A., et al., *Increased cytosine DNA-methyltransferase activity is target-cell-specific and an early event in lung cancer*. Proceedings of the National Academy of Sciences, 1996. **93**(9): p. 4045.
142. Pesek, M., et al., *Clinical Significance of Hypermethylation Status in NSCLC: Evaluation of a 30-Gene Panel in Patients with Advanced Disease*. Anticancer research, 2011. **31**(12): p. 4647-4652.
143. Zhang, B., et al., *Cigarette Smoking and p16INK4a Gene Promoter Hypermethylation in Non-Small Cell Lung Carcinoma Patients: A Meta-Analysis*. PloS one, 2011. **6**(12): p. e28882.
144. Piperi, C., et al., *Epigenetic effects of lung cancer predisposing factors impact on clinical diagnosis and prognosis*. Journal of Cellular and Molecular Medicine, 2008. **12**(5a): p. 1495-1501.
145. Balentine, D.A., S.A. Wiseman, and L.C. Bouwens, *The chemistry of tea flavonoids*. Critical Reviews in Food Science & Nutrition, 1997. **37**(8): p. 693-704.
146. Yang, C.S., P. Maliakal, and X. Meng, *Inhibition of Carcinogenesis by Tea*. Annual Review of Pharmacology and Toxicology, 2002. **42**(1): p. 25-54.
147. Higdon, J.V. and B. Frei, *Tea catechins and polyphenols: health effects, metabolism, and antioxidant functions*. 2003.
148. Yang, C.S., P. Maliakal, and X. Meng, *Inhibition of Carcinogenesis by Tea\**. Annual Review of Pharmacology and Toxicology, 2002. **42**(1): p. 25-54.
149. Siddiqui, I.A., et al., *Antioxidants of the beverage tea in promotion of human health*. Antioxidants and Redox Signaling, 2004. **6**(3): p. 571-582.
150. Grove, K.A. and J.D. Lambert, *Laboratory, epidemiological, and human intervention studies show that tea (Camellia sinensis) may be useful in the prevention of obesity*. The Journal of nutrition, 2010. **140**(3): p. 446-453.
151. Landau, J.M., et al., *Inhibition of spontaneous formation of lung tumors and rhabdomyosarcomas in A/J mice by black and green tea*. Carcinogenesis, 1998. **19**(3): p. 501-507.
152. Sazuka, M., et al., *Inhibitory effects of green tea infusion on in vitro invasion and in vivo metastasis of mouse lung carcinoma cells*. Cancer letters, 1995. **98**(1): p. 27-31.
153. Wang, Z.Y., et al., *Inhibition of N-nitrosodiethylamine-and 4-(methylnitrosamino)-1-(3-pyridyl)-1-butanone-induced tumorigenesis in A/J mice by green tea and black tea*. Cancer Research, 1992. **52**(7): p. 1943-1947.
154. Xu, Y., et al., *Inhibition of tobacco-specific nitrosamine-induced lung tumorigenesis in A/J mice by green tea and its major polyphenol as antioxidants*. Cancer Research, 1992. **52**(14): p. 3875-3879.
155. Ju, J., et al., *Inhibition of intestinal tumorigenesis in Apcmin/+ mice by (-)-epigallocatechin-3-gallate, the major catechin in green tea*. Cancer Research, 2005. **65**(22): p. 10623-10631.
156. Yuan, J.-M., C. Sun, and L.M. Butler, *Tea and cancer prevention: epidemiological studies*. Pharmacological Research, 2011. **64**(2): p. 123-135.
157. Sturgeon, J.L., M. Williams, and G. Van Servellen, *Efficacy of green tea in the prevention of cancers*. Nursing & health sciences, 2009. **11**(4): p. 436-446.
158. Boehm, K., et al., *Green tea for the prevention of cancer*. 2009.

159. Valcic, S., et al., *Antioxidant chemistry of green tea catechins. Identification of products of the reaction of (-)-epigallocatechin gallate with peroxy radicals*. Chemical research in toxicology, 1999. **12**(4): p. 382-386.
160. Sang, S., et al., *Theadibenzotropolone A, a new type pigment from enzymatic oxidation of (-)-epicatechin and (-)-epigallocatechin gallate and characterized from black tea using LC/MS/MS*. Tetrahedron letters, 2002. **43**(40): p. 7129-7133.
161. Yang, C.S., et al., *Bioavailability issues in studying the health effects of plant polyphenolic compounds*. Molecular nutrition & food research, 2008. **52**(S1): p. S139-S151.
162. Yang, C.S., et al., *Tea and cancer prevention: molecular mechanisms and human relevance*. Toxicology and applied pharmacology, 2007. **224**(3): p. 265-273.
163. Hou, Z., et al., *Mechanism of Action of (-)-Epigallocatechin-3-Gallate: Auto-oxidation-Dependent Inactivation of Epidermal Growth Factor Receptor and Direct Effects on Growth Inhibition in Human Esophageal Cancer KYSE 150 Cells*. Cancer Research, 2005. **65**(17): p. 8049-8056.
164. Hong, J., et al., *Stability, cellular uptake, biotransformation, and efflux of tea polyphenol (-)-epigallocatechin-3-gallate in HT-29 human colon adenocarcinoma cells*. Cancer Research, 2002. **62**(24): p. 7241-7246.
165. Hou, Z., et al., *Effects of tea polyphenols on signal transduction pathways related to cancer chemoprevention*. Mutation Research/Fundamental and Molecular Mechanisms of Mutagenesis, 2004. **555**(1): p. 3-19.
166. Chow, H.-H.S. and I.A. Hakim, *Pharmacokinetic and chemoprevention studies on tea in humans*. Pharmacological Research, 2011. **64**(2): p. 105-112.
167. Fang, M.Z., et al., *Tea polyphenol (-)-epigallocatechin-3-gallate inhibits DNA methyltransferase and reactivates methylation-silenced genes in cancer cell lines*. Cancer Research, 2003. **63**(22): p. 7563-7570.
168. Urusova, D.V., et al., *Epigallocatechin-gallate suppresses tumorigenesis by directly targeting Pin1*. Cancer Prevention Research, 2011. **4**(9): p. 1366-1377.
169. Constantinou, C., A. Papas, and A.I. Constantinou, *Vitamin E and cancer: an insight into the anticancer activities of vitamin E isomers and analogs*. International Journal of Cancer, 2008. **123**(4): p. 739-752.
170. Traber, M.G., *Vitamin E regulatory mechanisms*. Annu. Rev. Nutr., 2007. **27**: p. 347-362.
171. Shils, M.E., *Modern nutrition in health and disease* 2006: Lippincott Williams & Wilkins.
172. Eitenmiller, R.R. and J. Lee, *Vitamin E: food chemistry, composition, and analysis*. Vol. 137. 2004: CRC Press.
173. Burton, G., et al. *Vitamin E as an antioxidant in vitro and in vivo*. in *Biology of Vitamin E. Ciba Foundation Symposium*. 1983.
174. Traber, M.G. and J. Atkinson, *Vitamin E, antioxidant and nothing more*. Free Radical Biology and Medicine, 2007. **43**(1): p. 4-15.
175. Burton, G.W. and M.G. Traber, *Vitamin E: antioxidant activity, biokinetics, and bioavailability*. Annual review of nutrition, 1990. **10**(1): p. 357-382.
176. Burton, G.W. and K.U. Ingold, *Vitamin E as an in Vitro and in Vivo Antioxidant*. Annals of the New York Academy of Sciences, 1989. **570**(1): p. 7-22.
177. Lee, I.-M., et al., *Vitamin E in the primary prevention of cardiovascular disease and cancer*. JAMA: the journal of the American Medical Association, 2005. **294**(1): p. 56-65.
178. Salonen, R.M., et al., *Six-year effect of combined vitamin C and E supplementation on atherosclerotic progression The antioxidant supplementation in atherosclerosis prevention (ASAP) study*. Circulation, 2003. **107**(7): p. 947-953.
179. Fang, J.C., et al., *Effect of vitamins C and E on progression of transplant-associated arteriosclerosis: a randomised trial*. Lancet, 2002. **359**(9312): p. 1108-1113.
180. Zandi, P.P., et al., *Reduced risk of Alzheimer disease in users of antioxidant vitamin supplements: the Cache County Study*. Archives of neurology, 2004. **61**(1): p. 82.
181. Ascherio, A., et al., *Vitamin E intake and risk of amyotrophic lateral sclerosis*. Annals of neurology, 2005. **57**(1): p. 104-110.
182. Wagner, K.-H., A. Kamal-Eldin, and I. Elmadfa, *Gamma-tocopherol—an underestimated vitamin?* Annals of nutrition and metabolism, 2004. **48**(3): p. 169-188.
183. Itoh, K., J. Mimura, and M. Yamamoto, *Discovery of the negative regulator of Nrf2, Keap1: a historical overview*. Antioxidants & redox signaling, 2010. **13**(11): p. 1665-1678.

184. Kwak, M.-K. and T.W. Kensler, *Targeting NRF2 signaling for cancer chemoprevention*. Toxicology and applied pharmacology, 2010. **244**(1): p. 66-76.
185. Jaiswal, A.K., *Nrf2 signaling in coordinated activation of antioxidant gene expression*. Free Radical Biology and Medicine, 2004. **36**(10): p. 1199-1207.
186. Kline, K., et al., *Vitamin E and breast cancer prevention: current status and future potential*. Journal of mammary gland biology and neoplasia, 2003. **8**(1): p. 91-102.
187. Kline, K., et al., *Vitamin E and cancer*. Vitamins & Hormones, 2007. **76**: p. 435-461.
188. STONE, W.L., et al., *Tocopherols and the treatment of colon cancer*. Annals of the New York Academy of Sciences, 2004. **1031**(1): p. 223-233.
189. Dietrich, M., et al., *Does  $\gamma$ -tocopherol play a role in the primary prevention of heart disease and cancer? A review*. Journal of the American College of Nutrition, 2006. **25**(4): p. 292-299.
190. Lu, G., et al., *A  $\gamma$ -tocopherol-rich mixture of tocopherols inhibits chemically induced lung tumorigenesis in A/J mice and xenograft tumor growth*. Carcinogenesis, 2010. **31**(4): p. 687-694.
191. Ju, J., et al., *Cancer-preventive activities of tocopherols and tocotrienols*. Carcinogenesis, 2010. **31**(4): p. 533-542.
192. Lippman, S.M., et al., *Effect of selenium and vitamin E on risk of prostate cancer and other cancers*. JAMA: the journal of the American Medical Association, 2009. **301**(1): p. 39-51.
193. Gaziano, J.M., et al., *Vitamins E and C in the Prevention of Prostate and Total Cancer in Men*. JAMA: the journal of the American Medical Association, 2009. **301**(1): p. 52-62.
194. Hensley, K., et al., *New perspectives on vitamin E:  $\gamma$ -tocopherol and carboxyethylhydroxychroman metabolites in biology and medicine*. Free Radical Biology and Medicine, 2004. **36**(1): p. 1-15.
195. Campbell, S., et al., *Development of gamma (g)-tocopherol as a colorectal cancer chemopreventive agent*. Critical Reviews in Oncology Hematology, 2003. **47**(3): p. 249-260.
196. Reiter, E., Q. Jiang, and S. Christen, *Anti-inflammatory properties of  $\alpha$ - and  $\gamma$ -tocopherol*. Molecular aspects of medicine, 2007. **28**(5): p. 668-691.
197. Barve, A., et al.,  *$\gamma$  - Tocopherol - enriched mixed tocopherol diet inhibits prostate carcinogenesis in TRAMP mice*. International Journal of Cancer, 2009. **124**(7): p. 1693-1699.
198. Yang, C.S., et al., *Inhibition of inflammation and carcinogenesis in the lung and colon by tocopherols*. Annals of the New York Academy of Sciences, 2010. **1203**(1): p. 29-34.
199. Newmark, H.L., M.-T. Huang, and B.S. Reddy, *Mixed tocopherols inhibit azoxymethane-induced aberrant crypt foci in rats*. Nutrition and cancer, 2006. **56**(1): p. 82-85.
200. Suh, N., et al., *Mixed tocopherols inhibit N-methyl-N-nitrosourea-induced mammary tumor growth in rats*. Nutrition and cancer, 2007. **59**(1): p. 76-81.
201. Lee, H.J., et al., *Mixed tocopherols prevent mammary tumorigenesis by inhibiting estrogen action and activating PPAR- $\gamma$* . Clinical cancer research, 2009. **15**(12): p. 4242-4249.
202. Taylor, P.R., et al., *Prospective study of serum vitamin E levels and esophageal and gastric cancers*. Journal of the National Cancer Institute, 2003. **95**(18): p. 1414-1416.
203. Greenwald, P., C. Clifford, and J. Milner, *Diet and cancer prevention*. European Journal of Cancer, 2001. **37**(8): p. 948-965.
204. Knekt, P., et al., *Vitamin E and cancer prevention*. The American journal of clinical nutrition, 1991. **53**(1): p. 283S-286S.
205. Comstock, G.W., et al., *The risk of developing lung cancer associated with antioxidants in the blood: ascorbic acid, carotenoids, alpha-tocopherol, selenium, and total peroxy radical absorbing capacity*. Cancer Epidemiology Biomarkers & Prevention, 1997. **6**(11): p. 907-916.
206. Menkes, M.S., et al., *Serum beta-carotene, vitamins A and E, selenium, and the risk of lung cancer*. The New England journal of medicine, 1986. **315**(20): p. 1250-1254.
207. Ratnasinghe, D., et al., *Serum tocopherols, selenium and lung cancer risk among tin miners in China*. Cancer Causes & Control, 2000. **11**(2): p. 129-135.
208. Goodman, G.E., et al., *The Association between Lung and Prostate Cancer Risk, and Serum Micronutrients Results and Lessons Learned from  $\beta$ -Carotene and Retinol Efficacy Trial*. Cancer Epidemiology Biomarkers & Prevention, 2003. **12**(6): p. 518-526.
209. Woodson, K., et al., *Association between alcohol and lung cancer in the alpha-tocopherol, beta-carotene cancer prevention study in Finland*. Cancer Causes & Control, 1999. **10**(3): p. 219-226.
210. Yong, L.-C., et al., *Intake of vitamins E, C, and A and risk of lung cancer the NHANES I epidemiologic followup study*. American journal of epidemiology, 1997. **146**(3): p. 231-243.

211. Shibata, A., et al., *Intake of vegetables, fruits, beta-carotene, vitamin C and vitamin supplements and cancer incidence among the elderly: a prospective study*. British journal of cancer, 1992. **66**(4): p. 673.
212. Michell, R.H., *Inositol derivatives: evolution and functions*. Nature Reviews Molecular Cell Biology, 2008. **9**(2): p. 151-161.
213. Lam, S., et al., *A phase I study of myo-inositol for lung cancer chemoprevention*. Cancer Epidemiology Biomarkers & Prevention, 2006. **15**(8): p. 1526-1531.
214. Zhang, Z., et al., *A germ-line p53 mutation accelerates pulmonary tumorigenesis: p53-independent efficacy of chemopreventive agents green tea or dexamethasone/myo-inositol and chemotherapeutic agents taxol or adriamycin*. Cancer Research, 2000. **60**(4): p. 901-907.
215. Wattenberg, L.W. and R.D. Estensen, *Chemopreventive effects of myo-inositol and dexamethasone on benzo [a] pyrene and 4-(methylnitrosoamino)-1-(3-pyridyl)-1-butanone-induced pulmonary carcinogenesis in female A/J mice*. Cancer Research, 1996. **56**(22): p. 5132-5135.
216. Wattenberg, L., et al., *Chemoprevention of pulmonary carcinogenesis by brief exposures to aerosolized budesonide or beclomethasone dipropionate and by the combination of aerosolized budesonide and dietary myo-inositol*. Carcinogenesis, 2000. **21**(2): p. 179-182.
217. Estensen, R.D. and L.W. Wattenberg, *Studies of chemopreventive effects of myo-inositol on benzo (a) pyrene-induced neoplasia of the lung and forestomach of female A/J mice*. Carcinogenesis, 1993. **14**(9): p. 1975-1977.
218. Hecht, S.S., et al., *Evaluation of butylated hydroxyanisole, myo-inositol, curcumin, esculetin, resveratrol and lycopene as inhibitors of benzo [a] pyrene plus 4-(methylnitrosamino)-1-(3-pyridyl)-1-butanone-induced lung tumorigenesis in A/J mice*. Cancer letters, 1999. **137**(2): p. 123-130.
219. Hecht, S.S., et al., *Dose-response study of myo-inositol as an inhibitor of lung tumorigenesis induced in A/J mice by benzo [a] pyrene and 4-(methylnitrosamino)-1-(3-pyridyl)-1-butanone*. Cancer letters, 2001. **167**(1): p. 1-6.
220. Hecht, S.S., et al., *Inhibition of lung tumorigenesis in A/J mice by N-acetyl-S-(N-2-phenethylthiocarbamoyl)-L-cysteine and myo-inositol, individually and in combination*. Carcinogenesis, 2002. **23**(9): p. 1455-1461.
221. Kassie, F., et al., *Combinations of N-Acetyl-S-(N-2-Phenethylthiocarbamoyl)-L-Cysteine and myo-Inositol Inhibit Tobacco Carcinogen-Induced Lung Adenocarcinoma in Mice*. Cancer Prevention Research, 2008. **1**(4): p. 285-297.
222. Levine, J., *Controlled trials of inositol in psychiatry*. European neuropsychopharmacology, 1997. **7**(2): p. 147-155.
223. Elizur, A., O. Kofman, and R. Belmaker, *Double-blind, controlled trial of inositol treatment of depression*. Am J Psychiatry, 1995. **152**: p. 792-794.
224. Benjamin, J., et al., *Double-blind, placebo-controlled, crossover trial of inositol treatment for panic disorder*. American Journal of Psychiatry, 1995. **152**(7): p. 1084-1086.
225. Palatnik, A., et al., *Double-blind, controlled, crossover trial of inositol versus fluvoxamine for the treatment of panic disorder*. Journal of clinical psychopharmacology, 2001. **21**(3): p. 335-339.
226. Gelber, D., J. Levine, and R. Belmaker, *Effect of inositol on bulimia nervosa and binge eating*. International Journal of Eating Disorders, 2001. **29**(3): p. 345-348.
227. Fux, M., et al., *Inositol treatment of obsessive-compulsive disorder*. American Journal of Psychiatry, 1996. **153**(9): p. 1219-1221.
228. Han, W., et al., *The chemopreventive agent myoinositol inhibits Akt and extracellular signal-regulated kinase in bronchial lesions from heavy smokers*. Cancer Prevention Research, 2009. **2**(4): p. 370-376.
229. Huang, C., et al., *Inositol hexaphosphate inhibits cell transformation and activator protein 1 activation by targeting phosphatidylinositol-3' kinase*. Cancer Research, 1997. **57**(14): p. 2873-2878.
230. Piccolo, E., et al., *Inositol pentakisphosphate promotes apoptosis through the PI 3-K/Akt pathway*. Oncogene, 2004. **23**(9): p. 1754-1765.
231. Jyonouchi, H., et al., *Effects of anti-7, 8-dihydroxy-9, 10-epoxy-7, 8, 9, 10-tetrahydrobenzo [a] pyrene on human small airway epithelial cells and the protective effects of myo-inositol*. Carcinogenesis, 1999. **20**(1): p. 139-145.

232. Yorek, M.A., et al., *Normalization of hyperosmotic-induced inositol uptake by renal and endothelial cells is regulated by NF- $\kappa$ B*. American Journal of Physiology-Cell Physiology, 2000. **278**(5): p. C1011-C1018.
233. Tobert, J.A., *Lovastatin and beyond: the history of the HMG-CoA reductase inhibitors*. Nature Reviews Drug Discovery, 2003. **2**(7): p. 517-526.
234. Graaf, M.R., et al., *Effects of statins and farnesyltransferase inhibitors on the development and progression of cancer*. Cancer treatment reviews, 2004. **30**(7): p. 609-642.
235. Blais, L., A. Desgagné, and J. LeLorier, *3-Hydroxy-3-methylglutaryl coenzyme A reductase inhibitors and the risk of cancer: a nested case-control study*. Archives of internal medicine, 2000. **160**(15): p. 2363.
236. Kusama, T., et al., *3-hydroxy-3-methylglutaryl-coenzyme a reductase inhibitors reduce human pancreatic cancer cell invasion and metastasis*. Gastroenterology, 2002. **122**(2): p. 308-317.
237. Yang, Z., et al., *Synergistic actions of atorvastatin with  $\gamma$ -tocotrienol and celecoxib against human colon cancer HT29 and HCT116 cells*. International Journal of Cancer, 2010. **126**(4): p. 852-863.
238. Holstein, S.A., et al., *Isoprenoid pyrophosphate analogues regulate expression of Ras-related proteins*. Biochemistry, 2003. **42**(15): p. 4384-4391.
239. Wong, W., et al., *HMG-CoA reductase inhibitors and the malignant cell: the statin family of drugs as triggers of tumor-specific apoptosis*. Leukemia: official journal of the Leukemia Society of America, Leukemia Research Fund, UK, 2002. **16**(4): p. 508.
240. Kensler, T.W., N. Wakabayashi, and S. Biswal, *Cell survival responses to environmental stresses via the Keap1-Nrf2-ARE pathway*. Annu. Rev. Pharmacol. Toxicol., 2007. **47**: p. 89-116.
241. Osburn, W.O. and T.W. Kensler, *Nrf2 signaling: an adaptive response pathway for protection against environmental toxic insults*. Mutation Research/Reviews in Mutation Research, 2008. **659**(1): p. 31-39.
242. Itoh, K., et al., *Transcription factor Nrf2 regulates inflammation by mediating the effect of 15-deoxy- $\Delta$ 12, 14-prostaglandin J2*. Molecular and cellular biology, 2004. **24**(1): p. 36-45.
243. Chan, K.K., A.M. Oza, and L.L. Siu, *The statins as anticancer agents*. Clinical cancer research, 2003. **9**(1): p. 10-19.
244. Boudreau, D.M., O. Yu, and J. Johnson, *Statin use and cancer risk: a comprehensive review*. Expert opinion on drug safety, 2010. **9**(4): p. 603-621.
245. Denoyelle, C., et al., *Cerivastatin, an inhibitor of HMG-CoA reductase, inhibits the signaling pathways involved in the invasiveness and metastatic properties of highly invasive breast cancer cell lines: an in vitro study*. Carcinogenesis, 2001. **22**(8): p. 1139-1148.
246. Wong, W.W.-L., et al., *Cerivastatin triggers tumor-specific apoptosis with higher efficacy than lovastatin*. Clinical cancer research, 2001. **7**(7): p. 2067-2075.
247. Graaf, M.R., et al., *The risk of cancer in users of statins*. Journal of clinical oncology, 2004. **22**(12): p. 2388-2394.
248. Coogan, P.F., L. Rosenberg, and B.L. Strom, *Statin use and the risk of 10 cancers*. Epidemiology, 2007. **18**(2): p. 213-219.
249. Kaye, J. and H. Jick, *Statin use and cancer risk in the General Practice Research Database*. British journal of cancer, 2004. **90**(3): p. 635-637.
250. Khurana, V., et al., *Statins Reduce the Risk of Lung Cancer in Humans A Large Case-Control Study of US Veterans*. CHEST Journal, 2007. **131**(5): p. 1282-1288.
251. Setoguchi, S., et al., *Statins and the risk of lung, breast, and colorectal cancer in the elderly*. Circulation, 2007. **115**(1): p. 27-33.
252. Friis, S., et al., *Cancer risk among statin users: A population - based cohort study*. International Journal of Cancer, 2005. **114**(4): p. 643-647.
253. Haukka, J., et al., *Incidence of cancer and statin usage—record linkage study*. International Journal of Cancer, 2010. **126**(1): p. 279-284.
254. Farwell, W.R., et al., *The association between statins and cancer incidence in a veterans population*. Journal of the National Cancer Institute, 2008. **100**(2): p. 134-139.
255. Lu, G., et al., *A  $\gamma$ -tocopherol-rich mixture of tocopherols inhibits chemically induced lung tumorigenesis in A/J mice and xenograft tumor growth*. Carcinogenesis, 2010. **31**(4): p. 687-694.
256. Liao, J., et al., *Inhibition of lung carcinogenesis and effects on angiogenesis and apoptosis in A/J mice by oral administration of green tea*. Nutrition and cancer, 2004. **48**(1): p. 44-53.

257. Kassie, F., et al., *Inhibition of lung carcinogenesis and critical cancer-related signaling pathways by N-acetyl-S-(N-2-phenethylthiocarbamoyl)-l-cysteine, indole-3-carbinol and myo-inositol, alone and in combination*. *Carcinogenesis*, 2010. **31**(9): p. 1634-1641.
258. Greenblatt, M., et al., *Mutations in the p53 tumor suppressor gene: clues to cancer etiology and molecular pathogenesis*. *Cancer Research*, 1994. **54**(18): p. 4855-4878.
259. Hua, D., et al., *Quantitative methylation analysis of multiple genes using methylation-sensitive restriction enzyme-based quantitative PCR for the detection of hepatocellular carcinoma*. *Experimental and molecular pathology*, 2011. **91**(1): p. 455-460.
260. Oakes, C.C., et al., *Research Paper Evaluation of a Quantitative DNA Methylation Analysis Technique Using Methylation-Sensitive/Dependent Restriction Enzymes and Real-Time PCR*. *Epigenetics*, 2006. **1**(3): p. 146-152.
261. Yang, I., et al., *Fused-core silica column ultra-performance liquid chromatography-ion trap tandem mass spectrometry for determination of global DNA methylation status*. *Analytical biochemistry*, 2011. **409**(1): p. 138-143.
262. Quante, M., et al., *Bone marrow-derived myofibroblasts contribute to the mesenchymal stem cell niche and promote tumor growth*. *Cancer cell*, 2011. **19**(2): p. 257-272.
263. Takaiishi, S., et al., *Identification of gastric cancer stem cells using the cell surface marker CD44*. *Stem cells*, 2009. **27**(5): p. 1006-1020.
264. Chou, T.-C. and P. Talalay, *Quantitative analysis of dose-effect relationships: the combined effects of multiple drugs or enzyme inhibitors*. *Advances in enzyme regulation*, 1984. **22**: p. 27-55.
265. Yang, G.-y., et al., *Characterization of early pulmonary hyperproliferation and tumor progression and their inhibition by black tea in a 4-(methylnitrosamino)-1-(3-pyridyl)-1-butanone-induced lung tumorigenesis model with A/J mice*. *Cancer Research*, 1997. **57**(10): p. 1889-1894.
266. Sun, L., et al., *Phosphatidylinositol 3-kinase/protein kinase B pathway stabilizes DNA methyltransferase I protein and maintains DNA methylation*. *Cellular signalling*, 2007. **19**(11): p. 2255-2263.
267. Peterson, L.A. and S.S. Hecht, *O6-methylguanine is a critical determinant of 4-(methylnitrosamino)-1-(3-pyridyl)-1-butanone tumorigenesis in A/J mouse lung*. *Cancer Research*, 1991. **51**(20): p. 5557-5564.
268. Khuri, F.R., et al., *Cyclooxygenase-2 overexpression is a marker of poor prognosis in stage I non-small cell lung cancer*. *Clinical cancer research*, 2001. **7**(4): p. 861-867.
269. Zhang, H. and X.-F. Sun, *Overexpression of cyclooxygenase-2 correlates with advanced stages of colorectal cancer*. *The American journal of gastroenterology*, 2002. **97**(4): p. 1037-1041.
270. Hwang, D., et al., *Expression of cyclooxygenase-1 and cyclooxygenase-2 in human breast cancer*. *Journal of the National Cancer Institute*, 1998. **90**(6): p. 455-460.
271. Joo, Y.-E., et al., *Cyclooxygenase-2 overexpression correlates with vascular endothelial growth factor expression and tumor angiogenesis in gastric cancer*. *Journal of clinical gastroenterology*, 2003. **37**(1): p. 28-33.
272. Hou, Z., et al., *Mechanism of Action of (-)-Epigallocatechin-3-Gallate: Auto-oxidation-Dependent Inactivation of Epidermal Growth Factor Receptor and Direct Effects on Growth Inhibition in Human Esophageal Cancer KYSE 150 Cells*. *Cancer Research*, 2005. **65**(17): p. 8049.
273. Yang, G.Y., et al., *Effect of black and green tea polyphenols on c-jun phosphorylation and H2O2 production in transformed and non-transformed human bronchial cell lines: possible mechanisms of cell growth inhibition and apoptosis induction*. *Carcinogenesis*, 2000. **21**(11): p. 2035-2039.
274. Mochizuki, M., et al., *Kinetic analysis and mechanistic aspects of autoxidation of catechins*. *Biochimica et Biophysica Acta (BBA)-General Subjects*, 2002. **1569**(1-3): p. 35-44.
275. NAKAYAMA, T., Y. ENOKI, and K. HASHIMOTO, *Hydrogen peroxide formation during catechin oxidation is inhibited by superoxide dismutase*. *Food Science and Technology International*, Tokyo, 1995. **1**(1): p. 65-69.
276. Yang, G., et al., *Characterization of early pulmonary hyperproliferation and tumor progression and their inhibition by black tea in a 4-(methylnitrosamino)-1-(3-pyridyl)-1-butanone-induced lung tumorigenesis model with A/J mice*. *Cancer Research*, 1997. **57**(10): p. 1889.
277. Li, W. and A.N. Kong, *Molecular mechanisms of Nrf2 - mediated antioxidant response*. *Molecular carcinogenesis*, 2009. **48**(2): p. 91-104.
278. Traber, M.G., *Vitamin E*. In *Present knowledge in nutrition*. ILSI Press, 2006: p. 211-219.

279. Barve, A., et al., *N*. 2009. *Gamma-tocopherol-enriched mixed tocopherol diet inhibits prostate carcinogenesis in TRAMP mice*. *Int J Cancer*. **124**: p. 1693-1699.
280. Jiad, L. and J. Liue,  *$\alpha$ -Tocopherol is an effective Phase II enzyme inducer: protective effects on acrolein-induced oxidative stress and mitochondrial dysfunction in human retinal pigment epithelial cells* ☆. *Journal of Nutritional Biochemistry*, 2010. **21**: p. 1222-1231.
281. Li, G., et al., *The antioxidant and anti-inflammatory activities of tocopherols are independent of Nrf2 in mice*. *Free Radical Biology and Medicine*, 2012. **52**(7): p. 1151-1158.
282. Xiao, H., et al., *Combination of atorvastatin and celecoxib synergistically induces cell cycle arrest and apoptosis in colon cancer cells*. *International Journal of Cancer*, 2008. **122**(9): p. 2115-2124.
283. Tsurutani, J., et al., *Tobacco components stimulate Akt-dependent proliferation and NF $\kappa$ B-dependent survival in lung cancer cells*. *Carcinogenesis*, 2005. **26**(7): p. 1182-1195.
284. West, K.A., et al., *Rapid Akt activation by nicotine and a tobacco carcinogen modulates the phenotype of normal human airway epithelial cells*. *Journal of Clinical Investigation*, 2003. **111**(1): p. 81-90.
285. Gustafson, A.M., et al., *Airway PI3K pathway activation is an early and reversible event in lung cancer development*. *Science translational medicine*, 2010. **2**(26): p. 26ra25-26ra25.
286. Agoston, A.T., et al., *Retinoblastoma pathway dysregulation causes DNA methyltransferase 1 overexpression in cancer via MAD2-mediated inhibition of the anaphase-promoting complex*. *The American journal of pathology*, 2007. **170**(5): p. 1585.
287. Sato, M., et al., *The H-cadherin (CDH13) gene is inactivated in human lung cancer*. *Human genetics*, 1998. **103**(1): p. 96-101.
288. Tsou, J.A., et al., *Identification of a panel of sensitive and specific DNA methylation markers for lung adenocarcinoma*. *Mol Cancer*, 2007. **6**(70): p. 17.
289. Toyooka, K.O., et al., *Loss of expression and aberrant methylation of the CDH13 (H-cadherin) gene in breast and lung carcinomas*. *Cancer Research*, 2001. **61**(11): p. 4556-4560.
290. Maruyama, R., et al., *Hypermethylation of FHIT as a prognostic marker in nonsmall cell lung carcinoma*. *Cancer*, 2004. **100**(7): p. 1472-1477.
291. Toyooka, S., et al., *Smoke exposure, histologic type and geography - related differences in the methylation profiles of non - small cell lung cancer*. *International Journal of Cancer*, 2003. **103**(2): p. 153-160.
292. Ulivi, P., et al., *p16INK4A and CDH13 hypermethylation in tumor and serum of non - small cell lung cancer patients*. *Journal of cellular physiology*, 2006. **206**(3): p. 611-615.
293. Zhong, Y., et al., *Loss of H-cadherin protein expression in human non-small cell lung cancer is associated with tumorigenicity*. *Clinical cancer research*, 2001. **7**(6): p. 1683-1687.
294. Blanco, D., et al., *Molecular analysis of a multistep lung cancer model induced by chronic inflammation reveals epigenetic regulation of p16 and activation of the DNA damage response pathway*. *Neoplasia (New York, NY)*, 2007. **9**(10): p. 840.
295. Huang, S., G. Shao, and L. Liu, *The PR domain of the Rb-binding zinc finger protein RIZ1 is a protein binding interface and is related to the SET domain functioning in chromatin-mediated gene expression*. *Journal of Biological Chemistry*, 1998. **273**(26): p. 15933-15939.
296. Kim, K.-C. and S. Huang, *Histone methyltransferases in tumor suppression*. *Cancer biology & therapy*, 2003. **2**(5): p. 491-499.
297. Steele-Perkins, G., et al., *Tumor formation and inactivation of RIZ1, an Rb-binding member of a nuclear protein-methyltransferase superfamily*. *Genes & development*, 2001. **15**(17): p. 2250-2262.
298. Lal, G., et al., *RIZ1 is epigenetically inactivated by promoter hypermethylation in thyroid carcinoma*. *Cancer*, 2006. **107**(12): p. 2752-2759.
299. Du, Y., et al., *Hypermethylation in human cancers of the RIZ1 tumor suppressor gene, a member of a histone/protein methyltransferase superfamily*. *Cancer Research*, 2001. **61**(22): p. 8094-8099.
300. Hasegawa, Y., et al., *DNA methylation of the RIZ1 gene is associated with nuclear accumulation of p53 in prostate cancer*. *Cancer Science*, 2007. **98**(1): p. 32-36.
301. Oshimo, Y., et al., *Frequent epigenetic inactivation of RIZ1 by promoter hypermethylation in human gastric carcinoma*. *International Journal of Cancer*, 2004. **110**(2): p. 212-218.

302. He, L., et al., *RIZ1, but not the alternative RIZ2 product of the same gene, is underexpressed in breast cancer, and forced RIZ1 expression causes G2-M cell cycle arrest and/or apoptosis*. Cancer Research, 1998. **58**(19): p. 4238-4244.
303. Dammann, R., et al., *Epigenetic inactivation of a RAS association domain family protein from the lung tumour suppressor locus 3p21. 3*. Nature genetics, 2000. **25**(3): p. 315-319.
304. Tomizawa, Y., et al., *Clinicopathological significance of epigenetic inactivation of RASSF1A at 3p21. 3 in stage I lung adenocarcinoma*. Clinical cancer research, 2002. **8**(7): p. 2362-2368.
305. Pfeifer, G.P., et al., *Methylation of the RASSF1A gene in human cancers*. Biological chemistry, 2002. **383**(6): p. 907-914.
306. Kim, D.-H., et al., *Hypermethylation of RASSF1A promoter is associated with the age at starting smoking and a poor prognosis in primary non-small cell lung cancer*. Cancer Research, 2003. **63**(13): p. 3743-3746.
307. Niklinska, W., et al., *Prognostic significance of DAPK and RASSF1A promoter hypermethylation in non-small cell lung cancer (NSCLC)*. Folia Histochemica et Cytobiologica, 2009. **47**(2): p. 275-280.
308. Agathangelou, A., et al., *Identification of novel gene expression targets for the Ras association domain family 1 (RASSF1A) tumor suppressor gene in non-small cell lung cancer and neuroblastoma*. Cancer Research, 2003. **63**(17): p. 5344-5351.
309. Chow, L.S., et al., *Identification of RASSF1A modulated genes in nasopharyngeal carcinoma*. Oncogene, 2005. **25**(2): p. 310-316.
310. Tan, K.O., et al., *MAP-1, a novel proapoptotic protein containing a BH3-like motif that associates with Bax through its Bcl-2 homology domains*. Journal of Biological Chemistry, 2001. **276**(4): p. 2802-2807.
311. Ito, Y. and K. Miyazono, *RUNX transcription factors as key targets of TGF- $\beta$  superfamily signaling*. Current opinion in genetics & development, 2003. **13**(1): p. 43-47.
312. Li, Q.-L., et al., *Causal relationship between the loss of RUNX3 expression and gastric cancer*. cell, 2002. **109**(1): p. 113.
313. Vuilleminot, B.R., J.A. Hutt, and S.A. Belinsky, *Gene promoter hypermethylation in mouse lung tumors*. Molecular cancer research, 2006. **4**(4): p. 267-273.
314. Jamaluddin, M.S., X. Yang, and H. Wang, *Hyperhomocysteinemia, DNA methylation and vascular disease*. Clinical Chemical Laboratory Medicine, 2008. **45**(12): p. 1660-1666.
315. Costa, E., et al., *Reviewing the role of DNA (cytosine-5) methyltransferase overexpression in the cortical GABAergic dysfunction associated with psychosis vulnerability*. Epigenetics, 2007. **2**(1): p. 29-36.
316. Kanai, Y., *Alterations of DNA methylation and clinicopathological diversity of human cancers*. Pathology international, 2008. **58**(9): p. 544-558.
317. Egger, G., et al., *Epigenetics in human disease and prospects for epigenetic therapy*. Nature, 2004. **429**(6990): p. 457-463.
318. Abdolmaleky, H.M., et al., *Methylomics in psychiatry: modulation of gene-environment interactions may be through DNA methylation*. American Journal of Medical Genetics Part B: Neuropsychiatric Genetics, 2004. **127**(1): p. 51-59.
319. Wang, J., et al., *The tobacco-specific carcinogen NNK induces DNA methyltransferase 1 accumulation in laryngeal carcinoma*. Oral Oncology, 2012. **48**(6): p. 541-546.
320. Lin, R.K., et al., *Alteration of DNA methyltransferases contributes to 5' CpG methylation and poor prognosis in lung cancer*. Lung Cancer, 2007. **55**(2): p. 205-213.
321. Kwon, Y.M., et al., *Different susceptibility of increased DNMT1 expression by exposure to tobacco smoke according to histology in primary non-small cell lung cancer*. Journal of cancer research and clinical oncology, 2007. **133**(4): p. 219-226.
322. Smith, T.J., G.D. Stoner, and C.S. Yang, *Activation of 4-(methylnitrosamino)-1-(3-pyridyl)-1-butanone (NNK) in human lung microsomes by cytochromes P450, lipoxygenase, and hydroperoxides*. Cancer Research, 1995. **55**(23): p. 5566-5573.
323. Albino, A., et al., *Report Induction of H2AX Phosphorylation in Pulmonary Cells by Tobacco Smoke*. Cell Cycle, 2004. **3**(8): p. 1062-1068.
324. Le Gac, G., et al., *DNA damage-induced down-regulation of human Cdc25C and Cdc2 is mediated by cooperation between p53 and maintenance DNA (cytosine-5) methyltransferase 1*. Journal of Biological Chemistry, 2006. **281**(34): p. 24161-24170.

325. Mortusewicz, O., et al., *Recruitment of DNA methyltransferase I to DNA repair sites*. Proceedings of the National Academy of Sciences of the United States of America, 2005. **102**(25): p. 8905.
326. Lee, W.J., J.Y. Shim, and B.T. Zhu, *Mechanisms for the inhibition of DNA methyltransferases by tea catechins and bioflavonoids*. Molecular pharmacology, 2005. **68**(4): p. 1018-1030.
327. Fang, M., D. Chen, and C.S. Yang, *Dietary polyphenols may affect DNA methylation*. The Journal of nutrition, 2007. **137**(1): p. 223S.
328. Fang, M.Z., et al., *Tea polyphenol (-)-epigallocatechin-3-gallate inhibits DNA methyltransferase and reactivates methylation-silenced genes in cancer cell lines*. Cancer research, 2003. **63**(22): p. 7563.
329. Wodrich, W. and M. Volm, *Overexpression of oncoproteins in non-small cell lung carcinomas of smokers*. Carcinogenesis, 1993. **14**(6): p. 1121-1124.
330. Szabo, E., et al., *Altered cJUN expression: an early event in human lung carcinogenesis*. Cancer Research, 1996. **56**(2): p. 305-315.
331. Barthelman, M., et al., *(-)-Epigallocatechin-3-gallate inhibition of ultraviolet B-induced AP-1 activity*. Carcinogenesis, 1998. **19**(12): p. 2201-2204.
332. Chung, J.Y., et al., *Inhibition of Activator Protein 1 Activity and Cell Growth by Purified Green Tea and Black Tea Polyphenols in H-ras-transformed Cells Structure-Activity Relationship and Mechanisms Involved*. Cancer Research, 1999. **59**(18): p. 4610-4617.
333. Dong, Z., et al., *Inhibition of tumor promoter-induced activator protein 1 activation and cell transformation by tea polyphenols, (-)-epigallocatechin gallate, and theaflavins*. Cancer Research, 1997. **57**(19): p. 4414-4419.
334. Chung, J.Y., et al., *Mechanisms of inhibition of the Ras-MAP kinase signaling pathway in 30.7 b Ras 12 cells by tea polyphenols (-)-epigallocatechin-3-gallate and theaflavin-3, 3' -digallate*. The FASEB Journal, 2001. **15**(11): p. 2022-2024.
335. Bigey, P., et al., *Transcriptional regulation of the human DNA Methyltransferase (DNMT1) gene*. Gene, 2000. **242**(1): p. 407-418.
336. Lu, H., X. Meng, and C.S. Yang, *Enzymology of methylation of tea catechins and inhibition of catechol-O-methyltransferase by (-)-epigallocatechin gallate*. Drug metabolism and disposition, 2003. **31**(5): p. 572-579.
337. Lambert, J.D., et al., *Synthesis and biological activity of the tea catechin metabolites, M4 and M6 and their methoxy-derivatives*. Bioorganic & medicinal chemistry letters, 2005. **15**(4): p. 873-876.
338. Grivennikov, S.I. and M. Karin, *Inflammatory cytokines in cancer: tumour necrosis factor and interleukin 6 take the stage*. Annals of the Rheumatic Diseases, 2011. **70**(Suppl 1): p. i104-i108.
339. Halappanavar, S., et al., *Induction of the interleukin 6/signal transducer and activator of transcription pathway in the lungs of mice sub-chronically exposed to mainstream tobacco smoke*. BMC medical genomics, 2009. **2**(1): p. 56.
340. Chen, W., et al., *Low-dose gamma-irradiation inhibits IL-6 secretion from human lung fibroblasts that promotes bronchial epithelial cell transformation by cigarette-smoke carcinogen*. Carcinogenesis, 2012. **33**(7): p. 1368-1374.
341. Ernst, M., et al., *STAT3 and STAT1 mediate IL-11-dependent and inflammation-associated gastric tumorigenesis in gp130 receptor mutant mice*. J Clin Invest, 2008. **118**(5): p. 1727-38.
342. Judd, L.M., et al., *STAT3 activation regulates growth, inflammation, and vascularization in a mouse model of gastric tumorigenesis*. Gastroenterology, 2006. **131**(4): p. 1073-85.
343. Grivennikov, S., et al., *IL-6 and Stat3 are required for survival of intestinal epithelial cells and development of colitis-associated cancer*. Cancer Cell, 2009. **15**(2): p. 103-13.
344. Bollrath, J., et al., *gp130-mediated Stat3 activation in enterocytes regulates cell survival and cell-cycle progression during colitis-associated tumorigenesis*. Cancer Cell, 2009. **15**(2): p. 91-102.
345. Baek, H.J., et al., *Hepatocellular cancer arises from loss of transforming growth factor beta signaling adaptor protein embryonic liver fodrin through abnormal angiogenesis*. Hepatology, 2008. **48**(4): p. 1128-37.
346. Tang, Y., et al., *Progenitor/stem cells give rise to liver cancer due to aberrant TGF-beta and IL-6 signaling*. Proc Natl Acad Sci U S A, 2008. **105**(7): p. 2445-50.